SEPTEMBER 2023 M.Sc. in Biochemistry Science and Technology İKRAM ELMUSTAFA

REPUBLIC OF TÜRKİYE

GAZİANTEP UNIVERSITY

GRADUATE SCHOOL OF NATURAL & APPLIED SCIENCES

ANALYSIS OF THE COMPOSITION OF GANODERMA MUSHROOM EXTRACTS AND THEIR NOURISHING LIQUID SOAP PREPARATION

M.Sc. THESIS

IN

BIOCHEMISTRY SCIENCE AND TECHNOLOGY

BY

İkram ELMUSTAFA

SEPTEMBER 2023

ANALYSIS OF THE COMPOSITION OF GANODERMA MUSHROOM EXTRACTS AND THEIR NOURISHING LIQUID SOAP PREPARATION

M.Sc. Thesis
in
Biochemistry Science and Technology
Gaziantep University

Supervisor

Prof. Dr. Gülay ZENGİN

by
İkram ELMUSTAFA

September 2023

©2023 [Gaziantep University]

ANALYSIS OF THE COMPOSITION OF GANODERMA MUSHROOM EXTRACTS AND THEIR NOURISHING LIQUID SOAP PREPARATION

Submitted by **İkram ELMUSTAFA** in partial fulfillment of the requirements for the degree of Master of Science in **Biochemistry Science and Technology, Gaziantep University** is approved by,

Prof. Dr. Çiğdem AYKAÇ
Director of the Graduate School of Natural and Applied Sciences …….....

Prof. Dr. Abuzer ÇELEKLİ
Head of the Department of Biochemistry Science and Technology …….....

Prof. Dr. Gülay ZENGİN
Supervisor, Chemistry
Gaziantep University …….....

Exam Date: 15 September 2023

Examining Committee Members:

Prof. Dr. Gülay ZENGİN
Gaziantep University …….....

Assoc. Prof. Dr. Tuğba TAŞKIN TOK
Gaziantep University …….....

Prof. Dr. Mehmet ASLANOĞLU
Harran University …….....

I hereby declare that all information in this document has been obtained and presented in accordance with academic rules and ethical conduct. I also declare that, as required by these rules and conduct, I have fully cited and referenced all material and results that are not original to this work.

İkram ELMUSTAFA

ABSTRACT

ANALYSIS OF THE COMPOSITION OF GANODERMA MUSHROOM EXTRACTS AND THEIR NOURISHING LIQUID SOAP PREPARATION

ELMUSTAFA, İkram

M.Sc. in Biochemistry Science and Technology

Supervisor: Prof. Dr. Gülay ZENGİN

September 2023

109 pages

In this study, *Ganoderma lucidum* was extracted with Soxhlet and sonication techniques. Also, respective soaps were prepared and subjected to various tests like color, odor, and foaming, and analyses were performed *via* UV-Vis, FTIR, GC-MS, and PL spectroscopic methods. Antioxidant and antibacterial properties for both extracts and extract-made soaps were examined. FTIR spectroscopical study confirmed the chemical structure consistency of the *ganoderma* samples, where squalene and ethyl linoleate, were the prominent compounds in the GC-MS analyses. Notably, these extracts had antioxidant activity percentages of 92.01 ±1.04% and 93.32 ±1.05%, respectively for both *gaonderma* extract *via* Soxhlet and sonicator techniques. However, for the soaps, the antioxidant potential diminished, presumably due to reduced *ganoderma* concentration and other soap constituents. The antimicrobial activity of the *ganoderma*-infused soap was confirmed, particularly against *Staphylococcus aureus*, showing the soap with *ganoderma* to be more efficacious versus the soap without the extract. The photoluminescent properties of these extracts and the soap were significant. Furthermore, the observed photoluminescence agreed with Kasha's rule, with notable changes upon soap integration. These findings in regard to *Ganoderma lucidum*'s value in Eastern medicine for treatment and its modern use in organic soaps have been confirmed.

Keywords: *Ganoderma lucidum*, Extraction, Bioactive Compounds, Antibacterial Activity, Antioxidant Activity, Soap Preparation, Spectroscopical Analysis.

ÖZET

GANODERMA MANTAR EKSTRAKTLARININ BİLEŞİMİNİN VE BUNLARIN BESLEYİCİ SIVI SABUN HAZIRLANMASININ ANALİZİ

ELMUSTAFA, İkram

Yüksek Lisans Tezi, Biyokimya Bilimi ve Teknolojisi

Danışman: Prof. Dr. Gülay ZENGİN

Eylül 2023

109 sayfa

Bu çalışmada, *Ganoderma lucidum* Soxhlet ve sonikasyon teknikleri ile ekstrakte edildi. Ayrıca ilgili sabunlar hazırlandı ve renk, koku, köpürme gibi çeşitli testlere tabi tutuldular ve UV-Vis, FTIR, GC-MS ve PL spektroskopik yöntemler aracılığıyla analizler gerçekleştirildi. Hem ekstraktlar hem de ekstrakten üretilmiş sabunlar için antioksidan ve antibakteriyel özellikler incelendi. FTIR spektroskopik çalışması, *ganoderma* örneklerinin kimyasal yapı tutarlılığını doğruladı, burada yapılan GC-MS analizlerinde ise squalene ve etil linoleat molekülleri belirgin bileşiklerdi. Özellikle, bu ekstraktlar hem Soxhlet hem de sonikasyon teknikleri yoluyla elde edilen *gaonderma* ekstresi için sırasıyla %92,01 ± 1,04 ve %93,32 ± 1,05 antioksidan aktivite yüzdelerine sahipti. Bununla birlikte, sabunlar için, muhtemelen azalmış *ganoderma* konsantrasyonu ve diğer sabun bileşenleri nedeniyle antioksidan potansiyel azalmıştır. *Ganoderma* içeren sabunun antimikrobiyal aktivitesi, özellikle *Staphylococcus aureus*'a karşı doğrulandı, bu da *ganoderma* içeren sabunun *ganoderma* içermeyen sabuna göre daha etkili olduğunu gösterdi. Bu ekstraktların ve sabunun fotolüminesans özelliklerinin önemli derecede olduğu bulunmuştur. Ayrıca, gözlemlenen fotolüminesans, sabun entegrasyonu üzerine kayda değer değişikliklerle Kasha'nın kuralı ile uyumluydu. Bu bulgular *Ganoderma lucidum*'un doğu tıbbındaki tedavi değerini ve organik sabunlardaki modern kullanımını doğrulamıştır.

Anahtar Kelimeler: *Ganoderma lucidum*, Ekstraksiyon, Biyoaktif Bileşikler, Antibakteriyel Aktivite, Antioksidan Aktivite, Sabun Hazırlama, Spektroskopik Analiz

"Dedicated to my beloved family"

My mother Muna, my father Mohammed, my dear husband İbrahim and our precious daughter Aya.

ACKNOWLEDGEMENTS

I would like to extend my heartfelt gratitude to my supervisor Prof. Dr. Gülay ZENGİN, for her consistent guidance and support during my academic journey. Her dedication to my progress, coupled with her enduring patience and encouragement, has been invaluable to me.

Additionally, my deep gratitude goes to Prof. Dr. Hüseyin ZENGİN for his unwavering support and invaluable insights during my academic pursuits. I am so grateful for all of the classes and annotations he gave me which shaped my understanding as well as for every accomplishment towards this research and my professional life. Also I thank my thesis jury members Assoc. Prof. Dr. Tuğba TAŞKIN TOK and Prof. Dr. Mehmet ASLANOĞLU for their kind contributions in evaluating my thesis.

I would also thank my colleagues Mohmmad MOUAMER HAKKI, Anas ALTOUTANJI, and Müge ŞENGÜN from the Departments of Chemistry and Biochemistry Science and Technology for their assistance and encouragement while I am doing the studies.

I extend my appreciation to TÜBİTAK (Project No: 104M367) and Gaziantep University (Project No: FEF.11.07) for providing the essential chemicals, equipment, tools, and research lab facilities. My sincere thanks also go to the Turkish government for creating an environment conducive to my academic progress.

I wish to convey my deepest affection and heartfelt gratitude to mother Muna, father Mohammed, and my dear husband İbrahim for the everlasting love, encouragement, and supporting that they provided to me in my whole life.

TABLE OF CONTENTS

Page

ABSTRACT ..... **VI**

ÖZET ..... **V**

ACKNOWLEDGEMENTS ..... **VIII**

TABLE OF CONTENTS ..... **IX**

LIST OF TABLES ..... **XII**

LIST OF FIGURES ..... **XIV**

LIST OF ABBREVIATIONS ..... **XIX**

CHAPTER I INTRODUCTION **1**

1.1 Description and Definition of Mushroom in Biology 1

1.2 Mushroom Existence and Importance 1

1.3 *Ganoderma Lucidum* and Studies on Progress 2

1.4 Motivation of Study 4

CHAPTER II LITERATURE REVIEW **5**

2.1 *Ganoderma lucidum* History 5

2.2 *G. lucidum* Taxonomy and Strains 6

2.3 *G. lucidum's* Chemical Components 8

2.3.1 Polysaccharides and Peptidoglycans 9

2.3.2 Triterpenes 12

2.3.3 Ganoderic Acids 13

2.3.4 Other Components 15

2.4 The Bacteria 16

2.4.1 Bacteria Mutating 16

2.4.2 Antibacterial Propriety in *G. lucidum* 17

2.5 Oxidative Stress 19

2.5.1 Biological Effects of ROS 20

2.5.2 The Antioxidant Activity *in G. lucidum* 21

CHAPTER III MATERIALS AND METHODS 23

3.1 Materials and Methods Used Overview 23
3.2 Chemicals/Reagents List 23
3.3 *Ganoderma lucidum* Samples Collection and Identification 23
3.4 *Ganoderma lucidum* Samples Preparation 24
3.5 Devices Used in the Extraction 24
3.5.1 Soxhlet Apparatus 24
3.5.2 Sonication 25
3.5.3 Extraction of *G. lucidum* Using Soxhlet Apparatus 26
3.5.4 Extraction of *G. lucidum* Using Sonicator 27
3.6 Soap Preparation 29
3.7 Analytical Methods Used 32
3.7.1 Gas Chromatography GC-MS 32
3.7.2 Fourier-Transform Infrared Spectroscopy FTIR 32
3.7.3 Ultraviolet-Visible Spectroscopy UV-VIS 33
3.7.4 Fluorescence Spectroscopy 33
3.8 Biological Evaluation 33
3.8.1 Antioxidant Properties 34
3.8.2 Antimicrobial Properties 35
3.8.3 Agar Disc Diffusion Method for Conducting Anti-bacterial Assays. 35

CHAPTER IV RESULT AND DISCUSSION 37

4.1 Chemistry of *Ganoderma Lucidum* 37
4.2 Extract Yields 38
4.3 *Ganoderma*-prepared Soap Evaluation 38
4.4 Gas Chromatography GC 40
4.5 Fourier Transform Infrared Spectroscopy (FTIR) Measurements 45
4.6 Ultraviolet-Visible Spectrophotometer (UV-Vis) Measurements 59
4.7 Photoluminescence Spectrometer (PL) Measurements 70
4.8 Antioxidant Properties 74
4.8.1 Intermolecular and Chemical Bonding Interactions for *Ganoderma Lucidum* as Antioxidant Agent 88

4.9 Antimicrobial Activity 90
4.9.1 Intermolecular and Chemical Bonding Interactions for *Ganoderma Lucidum* as Antimicrobial Agent 94
CHAPTER V CONCLUSION AND RECOMMENDATIONS..... 96
REFERENCES..... 99
CURRICULUM VITAE..... 110

LIST OF TABLES

Page*

Table 2.1 A comparison of the polysaccharide and triterpenoid contents in popular *Ganoderma lucidum* products available in the market [56]. 14

Table 2.2 The categories of free radicals and their primary effects providing a systematic overview, aiding in the understanding of the distinct types and subsequent consequences of each free radical [88]. 21

Table 3.1 Bacteria strain utilized to assess the antimicrobial efficacy of *ganoderma* extracts and soap. 35

Table 4.1 Main soap made from *Ganoderma luciduim* characteristics 39

Table 4.2 Bioactive chemicals from the Soxhlet extract 42

Table 4.3 Bioactive chemicals from the sonication extract 44

Table 4.4 FT-IR results of olive oil (OO) 48

Table 4.5 FT-IR data of coconut oil (CO) 50

Table 4.6 FT-IR data of *Ganoderma lucidum* obtained by Soxhlet extraction (Gan-Sox) 53

Table 4.7 FT-IR data of soap prepared from olive oil and coconut oil (SOP) 56

Table 4.8 FT-IR data of soap prepared from olive oil, coconut oil and *Ganoderma lucidum* extract (Gan-SOP) 59

Table 4.9 UV-Vis data of *Ganoderma lucidum* extract obtained by Soxhlet extraction 62

Table 4.10 UV-Vis data of *Ganoderma lucidum* extract obtained by sonication extraction 64

Table 4.11 UV-Vis data of soap prepared from olive oil and coconut oil 66

Table 4.12 UV-Vis data of soap prepared from olive oil, coconut oil and *Ganoderma lucidum* extract 68

Table 4.13 UV-Vis data of vitamin C used as a standard 69

Table 4.14 Photoluminescence data for the *Ganoderma lucidum* extract obtained by Soxhlet extraction (a), *Ganoderma lucidum* obtained by sonication extraction (b), soap prepared from olive oil and coconut oil (c) and soap prepared from olive oil, coconut oil and *Ganoderma lucidum* (d) 73

Table 4.15 Antioxidant activity data and the linear correlation coefficients evaluated by the free radical scavenging capability of the samples 87

Table 4.16 Summary of the antimicrobial findings. The areas of inhibition were measured on the culture medium and reported as the diameter of growth inhibition in millimeters 91

Table 4.17 Areas of inhibition measured on the culture medium and reported as the diameter of growth inhibition in millimeters for both *GL* extracts and their effect on *Klebsiella pneumoniae*, *Escherichia coli*, and *Staphylococcus aureus* bacteria 93

LIST OF FIGURES

Page*

Figure 1.1 Yearly global production of cultivated edible mushrooms from 1965 to 1991 2

Figure 2.1 Pictorial representation for the medical properties of *G. lucidum* [21]..... 6

Figure 2.2 *Ganoderma lucidum* (MZKI G97) fruiting body, first obtained from a Slovenian woodland [23] 7

Figure 2.3 Patents dominating for the accelerating research on *Ganoderma* [31] 8

Figure 2.4 Beta-glucan structure [36] 9

Figure 2.5 Different isomers of GAs [50]..... 13

Figure 2.6 Compression between the cellular barriers of gram-negative and gram-positive microorganisms [78]..... 18

Figure 3.1 *Ganoderma* fruiting bodies..... 24

Figure 3.2 *Ganoderma lucidum* sample, natural form and ground form 24

Figure 3.3 visualization of sonicator machine's sound wave (Source: www.lubio.ch) 25

Figure 3.4 Experimental study plan 26

Figure 3.5 Soxhlet instrument photograph, taken from the laboratory..... 27

Figure 3.6 The sonicator instrument photograph, taken from the laboratory..... 28

Figure 3.7 Rotary evaporator instrument photograph, taken from the laboratory..... 28

Figure 3.8 Experimental plan for soap preparation 29

Figure 3.9 Weighted soap components in various beakers..... 30

Figure 3.10 Prepared soap..... 30

Figure 3.11 Diluted soap..... 31

Figure 3.12 General saponification reaction using KOH as base 31

Figure 3.13 Fluorescence spectroscopy instrument photograph, taken from the laboratory 33
Figure 3.14 Extract concentration series' and DPPH photograph, taken from the laboratory 35
Figure 4.1 *Ganoderma* growth on the tree edges 37
Figure 4.2 Diluted *ganoderma* soap observed as a yellowish-brown color 39
Figure 4.3 Soap lather upon the addition of distilled water 40
Figure 4.4 Soap pH observed as 9.5 40
Figure 4.5 GC-MS for the Soxhlet extract, with EtOH solvent 43
Figure 4.6 GC-MS for the sonication extract, with EtOH solvent 44
Figure 4.7 FT-IR spectrum of (a) olive oil (OO), (b) coconut oil (CO), (c) *Ganoderma lucidum* obtained by Soxhlet extraction (Gan-Sox), (d) *Ganoderma lucidum* obtained by sonication extraction (Gan-Son), (e) soap manufactured from olive oil and coconut oil (SOP), (f) soap prepared from olive oil, coconut oil and *Ganoderma lucidum* (Gan SOP) 46
Figure 4.8 UV-Vis spectrum of *Ganoderma lucidum* obtained by Soxhlet extraction at different concentrations; a) 166.60, b) 499.80, c) 833.00, d) 1166.20, e) 1499.40, f) 1999.20, g) 2499.00 and h) 3332.00 µg/mL 61
Figure 4.9 UV-Vis spectra of *Ganoderma lucidum* extract obtained by sonication extraction at different concentrations; a) 166.60, b) 499.80, c) 833.00, d) 1166.20, e) 1499.40, f) 1999.20, g) 2499.00 and h) 3332.00 µg/mL 63
Figure 4.10 UV-Vis spectra of soap prepared from olive oil and coconut oil at different concentrations; a) 3.33, b) 6.67, c) 10.00, d) 13.33 and e) 16.67 mg/mL 65
Figure 4.11 UV-Vis spectra of soap prepared from olive oil, coconut oil and *Ganoderma lucidum* extract at different concentrations; a) 4, b) 8, c) 12, d) 16 and e) 20 mg/mL 67
Figure 4.12 UV-Vis spectra of vitamin C as a standard at different concentrations; a) 92.61, b) 185.22, c) 277.83, d) 370.44 and e) 463.06 µg/mL 69

Figure 4.13 Photoluminescence spectra of the *Ganoderma lucidum* extract obtained by Soxhlet extraction (a), *Ganoderma lucidum* obtained by sonication extraction (b), soap prepared from olive oil and coconut oil (c) and soap prepared from olive oil, coconut oil and *Ganoderma lucidum* (d) in spectrophotometric grade methanol (CH_3OH); samples were excited at 256 nm 71

Figure 4.14 Emission spectra of *Ganoderma lucidum* extract obtained by sonication extraction (b) in spectrophotometric grade methanol (CH_3OH) (c = 3332.00 µg/mL) at different excited wavelengths 73

Figure 4.15 The antioxidant potential, as determined by the radical scavenging capacity of *Ganoderma lucidum* extract procured through Soxhlet extraction at varying concentrations, was quantified in terms of percentage activity of 166.60, 499.80, 833.00, 1166.20, 1499.40, 1999.20, 2499.00 and 3332.00 µg/mL. Results are presented as the mean ±SD from three separate trials 75

Figure 4.16 The UV-Vis spectral progress of antioxidant activity of the *Ganoderma lucidum* extract obtained by Soxhlet extraction at different concentrations of 166.60, 499.80, 833.00, 1166.20, 1499.40, 1999.20, 2499.00 and 3332.00 µg/mL. Spectrum a) represents pure DPPH solution. Spectra b-k) represent the reaction of the *Ganoderma lucidum* obtained by Soxhlet extraction at different concentrations with DPPH solution 76

Figure 4.17 Reaction of the *Ganoderma lucidum* extract obtained by Soxhlet extraction at different concentrations with DPPH solution of 166.60, 499.80, 833.00, 1166.20, 1499.40, 1999.20, 2499.00 and 3332.00 µg/mL 77

Figure 4.18 The antioxidant potential, as determined by the radical scavenging capacity of *Ganoderma lucidum* extract procured through sonication extraction at varying concentrations, was quantified in terms of percentage activity of 166.60, 499.80, 833.00, 1166.20, 1499.40, 1999.20, 2499.00 and 3332.00

µg/mL. Results are presented as the mean ±SD from three separate trials 78

Figure 4.19 The UV-Vis spectral progress of antioxidant activity of the *Ganoderma lucidum* extract obtained by sonication extraction at different concentrations of 166.60, 499.80, 833.00, 1166.20, 1499.40, 1999.20, 2499.00 and 3332.00 µg/mL. Spectrum a) represents pure DPPH solution. Spectra b-k) represents the reaction of the *Ganoderma lucidum* obtained by sonication extraction at different concentrations with DPPH solution 79

Figure 4.20 Raction of the *Ganoderma lucidum* extract obtained by sonication extraction at different concentrations with DPPH solution of 166.60, 499.80, 833.00, 1166.20, 1499.40, 1999.20, 2499.00 and 3332.00 µg/mL 80

Figure 4.21 Antioxidant potential, as determined by the radical scavenging capacity of the soap made from olive oil and coconut oil at varying concentrations, of 3.33, 6.67, 10.00, 13.33 and 16.67 mg/mL. Results are presented as the mean ±SD from three separate trials 81

Figure 4.22 The UV-Vis spectral progress of antioxidant activity of the soap prepared from olive oil and coconut oil at different concentrations of 3.33, 6.67, 10.00, 13.33 and 16.67 mg/mL. Spectrum a) represents pure DPPH solution. Spectra b-f) represents the reaction of the soap prepared from olive oil and coconut oil at different concentrations with DPPH solution 82

Figure 4.23 The antioxidant potential, as determined by the radical scavenging capacity of soap made from olive oil, coconut oil and *Ganoderma lucidum* extract at varying concentrations, was quantified in terms of percentage activity of 4, 8, 12, 16 and 20 mg/mL. Results are presented as the mean ±SD from three separate trials 83

Figure 4.24 UV-Vis spectral progress of antioxidant activity of the soap prepared from olive oil, coconut oil and *Ganoderma lucidum*

at different concentrations of 4, 8, 12, 16 and 20 mg/mL. Spectrum a) represents pure DPPH solution. Spectra b-f) represents the reaction of the soap prepared from olive oil, coconut oil and *Ganoderma lucidum* at different concentrations with DPPH solution..... 84

Figure 4.25 Antioxidant potential, as determined by the radical scavenging capacity of (vitamin C) at varying concentrations, was quantified in terms of percentage activity of 92.61, 185.22, 277.83, 370.44 and 463.06 µg/mL. Results are presented as the mean ±SD from three separate trials..... 85

Figure 4.26 UV-Vis spectral progress of antioxidant activity of the ascorbic acid (vitamin C) as a standard at different concentrations of 92.61, 185.22, 277.83, 370.44 and 463.06 µg/mL. Spectrum a) represents pure DPPH solution. Spectra b-f) represents the reaction of the ascorbic acid (vitamin C) at different concentrations with DPPH solution..... 86

Figure 4.27 Key intermolecular forces in *Ganoderma lucidum*. The diagram identifies the intermolecular forces of hydrogen bonding in *ganoderma* polysaccharides. 89

Figure 4.28 Key intermolecular forces in *Ganoderma lucidum*. The diagram identifies the intermolecular forces of nitrogen-hydrogen (N-H) bonds in *ganoderma* proteins. 90

Figure 4.29 Inhibition disc diffusion zone assays for soap samples, examined with three types of bacteria 91

Figure 4.30 Comparison of each of the *GL* extracts (extract by sonication, and extract by Soxhlet) on *Klebsiella pneumoniae*, *Escherichia coli*, and *Staphylococcus aureus* bacteria..... 93

Figure 4.31 Depiction of functional groups in *Ganoderma lucidum*-Infused soap. The diagram illustrates the functional groups—hydroxyl (1), amine (2), carbonyl (3), ether (4), and phenolic (5)—and their potential role in contributing to the antibacterial properties of the soap through dipole-dipole interactions. 95

LIST OF ABBREVIATIONS

G. Lucidum	: Ganoderma Lucidum
GA	: Ganoderic Acid
GTS	: Ganoderma Triterpenes
LZ	: Lingzhi
ROS	: Reactive Oxygen Species
FR	: Free Radicals
TCM	: Traditional Chinese Medicine
NIR	: Nondestructive Near-Infrared
HPLC	: High-Performance Liquid Chromatography
RDNA	: Recombinant DNA
LAP	: Leucine Aminopeptidase
kDa	: Kilodalton
2D	: Two-Dimensional
COSY	:Techniques Consisting of Correlated Spectroscopy
TOCSY	: Total Correlated Spectroscopy
HSQC	: Heteronuclear Single-Quantum Coherence
NOEs	: Nuclear Overhauled Effects
G. Applanatum	: Ganoderma Applanatum
G. Pfeifferi	: Ganoderma Pfeifferi
PL	: Photoluminescence
UV-Vis	: Ultraviolet-Visible
FTIR	: Fourier Transform Infrared
MeOH	: Methanol
EtOH	: Ethanol

CHAPTER I

INTRODUCTION

1.1 Description and Definition of Mushroom in Biology

Particular species of macrofungus known as mushrooms may grow above the surface (epigeous) or under it (hypogeous). It has a main stem which is big for being visible to the human eyes and can be easily collected. There are around 16,000 different Basidiomycetes species, and more than 10,000 of them are thought to produce basidiocarps with a sizeable enough structure to be taken into consideration as a potential food source. On the other hand, 10% of the mushroom genus are thought for being poisonous [1]. Approximately half of these species are believed to be edible to varying degrees.

1.2 Mushroom Existence and Importance

Mushrooms can usually be found almost everywhere. Mushroom substrates are a type of lingo-cellulosic material that aid in forming, developing, as well as fruiting mushrooms. Before spawning, however, it is recommended that the substrates be supplemented with various ingredients to increase mushroom yield. Many nutrients can be supplied to the bases to promote mushroom growth. Mycelium development and mushroom productivity are both influenced by the quantities of cellulose, hemicelluloses, and lignin in fostering growth, as well as the nitrogen concentration [2,3]. Mushrooms are important for medicine and nutrition, in a globe where food costs are rising. Mushroom production is a very successful way to mitigate food insecurity as edible mushroom growth is an increasing tendency. Many mushroom types have longstanding experience of use as medicinal and health supplements. Many of these fungi have been sourced for exploration within the context of traditional Chinese medicinal studies, and their constituents have been successful in the treatment of a variety of ailments.

Additionally, one important topic in a recent study was the investigation of substances for utilization in the treatment of many malignancies, heart problems, viral infections, and other illnesses. Consequently, because of the demand, there is an increasingly attractive relevance, with the potential to develop workplace and career opportunities in both urban and rural areas. Thus, economic benefits for societies where mushrooms are been grown can be provided. Further low-cost production as well as the disposal of crop residues can result [4,5]. Figure 1.1 shows the increasing growth of mushroom production annually [1].

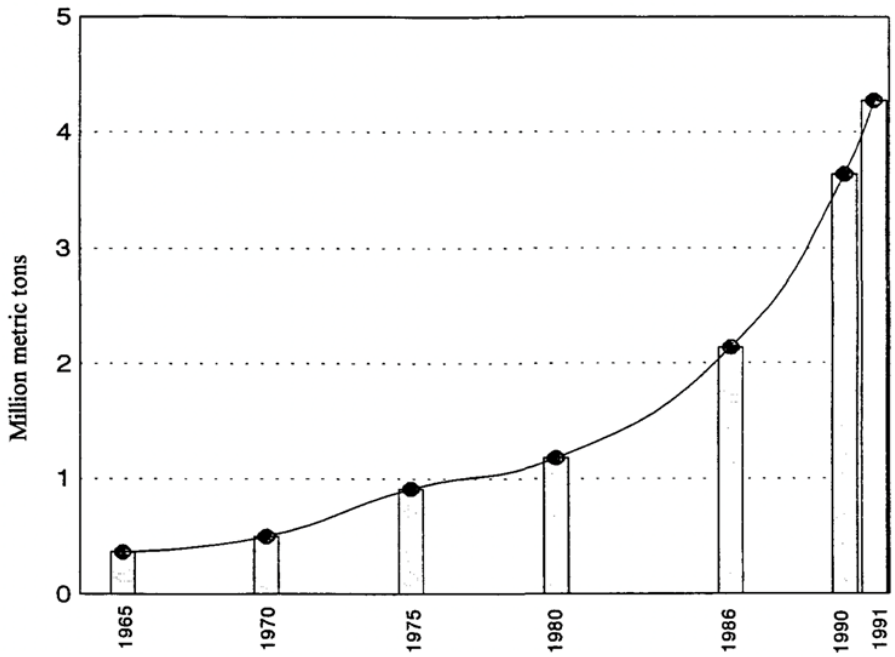

Figure 1.1 Yearly global production of cultivated edible mushrooms from 1965 to 1991

1.3 *Ganoderma Lucidum* and Studies on Progress

Chinese, Japanese, and Koreans utilized popular therapeutic mushrooms called Ganoderma fungus for centuries. Most scientific studies on the *Ganoderma lucidum* strain, and on growing laboratory tests, pharmaceutics, and clinical applications of *G. lucidum* refer to this mushroom. It is also recognized as *Reishi* in the Japanese market and *Ling Zhi* in Chinese. Traditional Chinese Medicine (TCM) has used the well-known medicinal fungus *Ganoderma lucidum* in various Asian nations as home treatments [6].

G. lucidum has been cultivated commercially employing a range of cultivating surfaces and production factors, including water content, pH, humidity, temperature, and light levels. This approach is known as conventional basidiocarp cultivation, and so it is utilized to generate a full body of the fruit [7]. While using another approach, known as submerged fermentation, involves growing mycelium in liquid culture broth to get bioactive ingredients like Ganoderic acid and polysaccharides in two or three weeks, as opposed to old methodologies, which require at least 3-5 months [8]. *G. lucidum* is sold as nutritional supplements, tonics, powder form, and specialized functional ingredients, under several nutritional names.

As a result of advances in medicine, nutrition, and cleanliness, the life expectancy of the human race has increased considerably since the beginning of the 20th century. Nonetheless, higher life expectancy is associated with a rise in the incidence of many different diseases, like cancer, and neurological problems [9]. World Health Organization (WHO) reported that more than three-quarters of the global numbers use conventional treatments to maintain optimal health *G. Lucidum*. This is a promising kind of conventional treatment for living a much healthier life [10]. In addition to being a medication, it can be considered a nutraceutical, nutritional complement, and in cosmetics [11]. Triterpenes are potent antioxidants but can also interact directly with several biological aims, notifying biological mechanisms like vasculogenic, programmed cell death, and cell lifetime [12]. The majority of such a species' polysaccharides are heteropolymers with neuroprotective and immunomodulatory effects [13]. Roy and co-workers discussed the nutrient content and chemical properties of *G lucidum*, presenting a report on the nutritional value of *Ganoderma* mushroom [14]. Both Liu et al and Shang et al explored that *G. lucidum* has a significant amount of antibiotic compounds, mostly polysaccharide molecules, that were effective against a wide range of viruses, many types of microbes, and fungi [15]. Kozarski et al. found a link between the high number of *G. lucidum* in "phenols, triterpenoids, glucans, and carbohydrate molecules" and its ability to get rid of free radicals [17]. According to Qi et al. their effectiveness depends on where they come from because the health benefits of each fungal species are different depending on where they grow [18]. Further research on the biotechnologically-derived constituents of *G. lucidum* is essential to ensure its effectiveness and safety, paving the way for increased marketing of fully functional fungi.

1.4 Motivation of Study

This research amied to isolate and characterize the beneficial constituents of *Ganoderma* mushrooms, investigating their potential biological activities for medicinal applications and harnessing their extracts for the formulation of nutrient-rich liquid soaps. Furthermore, by leveraging *Ganoderma's* properties, the study evaluated the mushroom's antibacterial and antioxidant capacities, subsequently assessing these characteristics in the soap products and drawing comparisons. Essential analyses, encompassing GC-MS, FTIR, UV-VIS, and PL, were conducted on the *Ganoderma* extracts obtained through both Soxhlet and sonication techniques, and these results were close together with the findings from the soap samples prepared by the *Ganoderma* extract. The broader implications of this study extend beyond the academic realm. By substantiating the multifaceted benefits of *Ganoderma* mushrooms, there's potential to boost their commercial cultivation, driving economic growth and fostering sustainable agricultural practices. This could position *Ganoderma* mushrooms as a cornerstone in the burgeoning nutraceutical industry, elevating its profile for both domestic markets and international trade. Beyond its economic ramifications, this research, rooted in rigorous scientific scrutiny, could bridge the gap between age-old traditional beliefs and contemporary medical science, redefining the way that perceive and utilize *Ganoderma* mushrooms in the modern era.

CHAPTER II

LITERATURE REVIEW

2.1 *Ganoderma lucidum* History

Ganoderma mushrooms can be found in many different places, which may have contributed to confusion about the genus *Ganoderma*'s precise classification. *G. lucidum* was initially applied to a species discovered in England but was later mistakenly assigned to various *Ganoderma* genus discovered and known as Chinese *Lingzhi*. Although classification uncertainty remains unresolved, *Lingzhi's* global fame has grown. This special issue on *Ganoderma* now appropriately discusses the present taxonomic position [19]. *G. lucidum* representations started showing up in literature around 1400 AD, in portraits, carvings, house furnishing, and also female makeup items and decoration. During China's Eastern Han dynasty, the treatise "Shen Nong Ben Cao Jing" was recorded, and it was devoted solely to explaining herbal substances and their medicinal advantages. (25-220 AD). This book is often called "Shen-Herbal nong's Classics" or "Classic of the Materia Medica." That was released during the second century under the term Shen-nong and described all medicinal qualities of numerous mushrooms, including *G. Lucidum* [20]. Natural *lingzhi* is in short supply, and only the privileged can afford it. Off the coast of China, according to popular belief said that the sanctified fungi were thought to grow on "three aisles of the blest" in the imperishable habitation. Evidence, cultural utilization, and traditional ethical norms are utilized to bolster various viewpoints on *G. lucidum's* therapeutic properties. Later research, on the other hand, backs up several of the historical assertions about *lingzhi's* healing properties. The many viewpoints on *G. lucidum's* health advantages are given in Figure 2.1 [21].

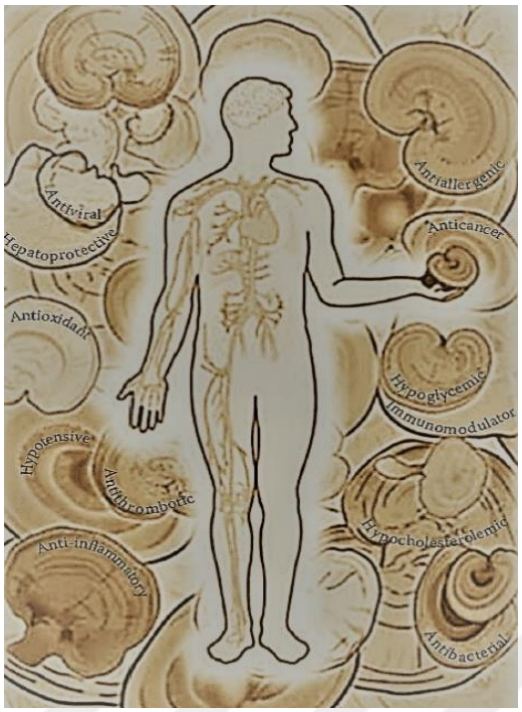

Figure 2.1 Pictorial representation for the medical properties of *G. lucidum* [21]

2.2 *G. lucidum* Taxonomy and Strains

Many attributes, for example, form and color within the mushroom's fruiting part, host specialization, and provenance are utilized in identifying specific participants of the *Ganoderma* species [22]. These characteristics have been documented in several investigations. The *Ganodermataceae* family is comprised of polypore basidiomycetous fungi that have a basidiospore that is double-walled. One of the 219 species that belong to the family *Ganoderma* is called *G. lucidum*. The genus *Ganoderma* contains all of these species. In Figure 2.2 displays the shape of the *Ganoderma* mushroom's fruiting bodies.

Figure 2.2 *Ganoderma lucidum* (MZKI G97) fruiting body, first obtained from a Slovenian woodland [23]

The existence of pilocystidia with thick walls that are embedded in an extracellular melanin structure is connected with the (bright) surface of the basidiocarps that belong to this genus [24,25]. In the taxonomy of *G. lucidum*, methods like nondestructive near-infrared (NIR) analysis linked with chemical metrics, NMR-centric metabolomics, and HPLC are deployed to form its chemical fingerprint [26,27]. One of the molecular-based procedures that can be used to determine the species of *Ganoderma* is called recombinant DNA, or rDNA, sequencing [28]. *G. lucidum* can subdivide for two categories, four types of the mushroom, each of which is determined by the shape of the fruit bodies that develop on artificial growth conditions. There was a significant amount of genetic diversity shown by the esterase, peroxidase, leucine aminopeptidase (LAP), and proteins from *Ganoderma lucidum* fruit bodies and mycelia electrophoretically arranged. The categorization of various fungus species originated from the isozyme structures of an esterase that was separated from mushroom mycelia. The different fungal strains' protein, leucine aminopeptidase, and peroxidase patterns could not indicate each sort of genetical connection [29]. The fruiting bodies of mushrooms are so hard to come by in nature, people have begun cultivating them artificially on hardwood trees and wooden chips contained within containers or pouches made of plastic. Mycelia of *G. lucidum* has become produced using biotechnology in bio apparatus, whether on fluid or hard

substances media by filled with water cultivation of fungal biomass [30]. This was done for together on hard substrates and in fluid medium. Figure 2.3 refers to the growing number of articles implying that *Ganoderma* mushroom studies are moving faster [31]. During the previous few years, patents have outnumbered non-patent publications by a wide margin.

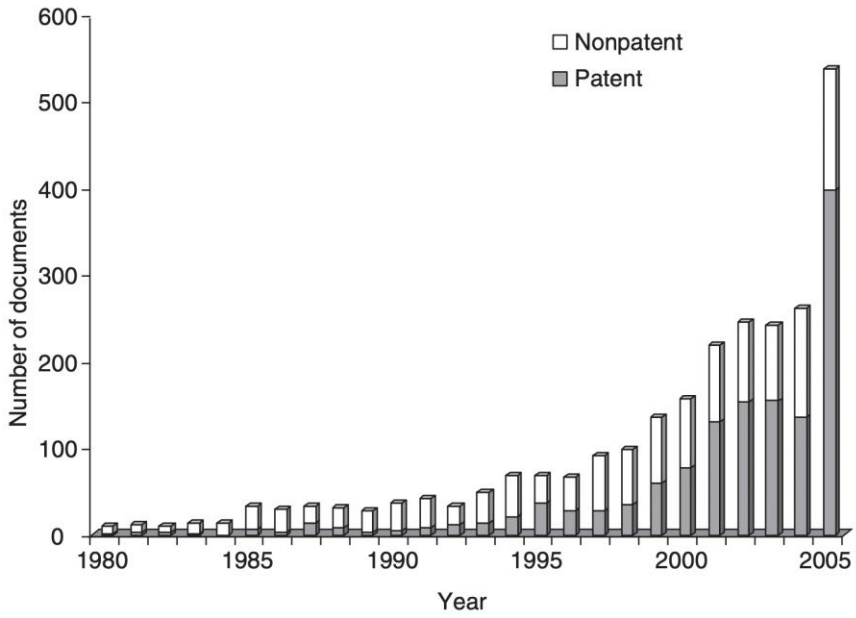

Figure 2.3 Patents dominating for the accelerating research on *Ganoderma* [31]

2.3 *G. lucidum's* Chemical Components

90% of the weight of most mushrooms is made up of water. Among the remaining 10%, there are proteins comprising 10-40% of the total; fats containing 2-8% of the total; carbohydrates containing 3-28% of the total; fabric cells comprising 3-32%; ashes comprising 8-10% of the whole; and a few minerals and vitamins containing iron, zinc, copper, selenium, calcium, phosphorus, magnesium, potassium, consisting of the majority minerals included [32]. Carbohydrates, proteoglycans, and derived products of nucleic acids are only a few of the bioactive substances found in mushrooms. Terpenoids and steroids are also found in mushrooms. proteins found in mushrooms, especially those high in leucine and lysine, include all the crucial proteins for the body. Mushrooms' high polyunsaturated lipids beside low-fat content are primarily responsible for their health advantages [33].

2.3.1 Polysaccharides and Peptidoglycans

Due to their greater structural diversity than proteins or physicochemical acids and their larger capacity for conveying biological information, *Ganoderma* polysaccharides have recently gained much scholarly interest [34]. *Ganoderma* polysaccharide "The Ganopoly" had been the focus of *Lingzhi's* studies for a long time. *Lingzhi's* fruiting bodies, spores, and mycelia added to the culture soups have been shown to contain upwards of 200 polysaccharide types [35]. Polysaccharides are present in the fungal membrane as a structural element, which is made up of two types of polysaccharides: chitin or cellulosic fibrillar, which is a mixture of glycoproteins, α-glucan, and β-glucan that resembles a matrix. The primary bioactive carbohydrates excluded from *Ganoderma* strains are the polysaccharide named Glucan, particularly the *β*-1-3 and *β*-1-6-D-glucan structures. Glucose molecules make up the vast majority of Ganopoly, with about thirty percent of carbohydrates being (1-3)-D-glucans and (1-6)-D-glucosyl side chains. These glycans comprise a linear or branched spine consist of both the- *α* or- *β* connected carbohydrate components, and some of them include edge-chains bonded at various places. The primary structure is composed of *β*-1-3 D-glucopyranose units, with every unit having 1-15 monoglucosyl *β*-1-6 branched chains attached. Figure 2.4 showcases a structure formed by a straight 1,3-glycosidic sequence of *β*-D-glucose units linked through a 1,6-glycosidic linkage [36].

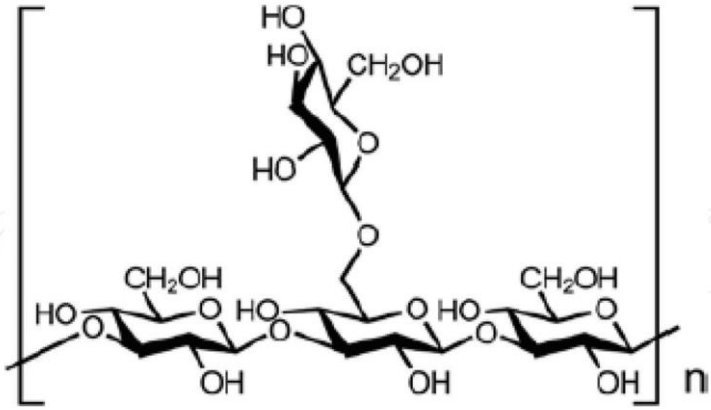

Figure 2.4 Beta-glucan structure [36]

Nevertheless, because naturally produced glycans have such a diverse range of structures, it is challenging to establish a single procedure to examine them. According to earlier research, many anti-tumor glucans were found to have

molecular mass of approximately 1,050 kDa, along with a branched glucan core featuring (1-3)-, (1-4)-, and (1-6)-connections [37]. In-depth findings on the anti-tumor components present within those fungi, particularly polysaccharides and protein-combined glucans, had also recently been carried out and findings showed that the glycopeptides and proteoglycans particularly have been recognized as additional immunomodulatory polysaccharides. Other anti-tumor polysaccharides produced by *G. lucidum* include glycoproteins, heteropolysaccharides, and a class of polysaccharides called ganoderans A, B, and C [38]. The glucose makeup and, thus, the chemical structure of the anti-tumor polysaccharides vary significantly, but one aspect they share is a relatively high molecular weight [38]. Mushrooms contain polysaccharides, which are sugar molecule polymers that may have biological benefits by protecting against germs, viruses, and parasites [39].

Cell membrane formation affects the option of extraction technique for polysaccharides. A while ago, the extraction using hot water technique was a common strategy [40]. Polysaccharides, typically separated from *Lingzhi* with the aid of water, as the solvent and alcoholic solvents extraction way, belong to a class of bioactive molecules with various structural characteristics and different physic-chemical capabilities, as a high priority has been given recently to the polysaccharides in pharmacology, particularly protein/peptide-associated polysaccharides. Research indicates that water-soluble β-1-3-D and β-1-6-D glucans, precipitated with ethyl alcohol, are present in the sediment, are the most effective immunomodulatory polysaccharides [40]. Breaking the film of the cell starting with the upper until the bottom level with moderate until severe removal circumstances is the fundamental principle of extraction both temperature and pH. Some of the naturally obtained carbohydrates from the mushrooms are attached to protein or peptide groups, while others are neutral or acidic and have various forms of glycosidic bonds [36]. NMR spectroscopy can be used as one of the best methods to determine the anomers (α or β) for very carbohydrate output. The anomeric vibration modes show characteristic conjugated double bonds with a split that is much greater in regard of β anomers in comparison with α anomers. They are visible in the spectrum. Without any help from other techniques, NMR spectroscopy is the sole technique that is regarded to have the ability to fully characterize the structure of a

polysaccharide. The comprehensive assignment of the ^{1}H and ^{13}C NMR spectrum utilizing a mixture of bi-dimensional (2D) NMR methods, and techniques consisting of correlated spectroscopy (COSY), is necessary for complete structure determination. Also total correlated spectroscopy (TOCSY), for the HSQC (heteronuclear single-quantum coherence) for ^{13}C and for ^{1}H may be necessary. Only 2D ^{1}H NMR spectroscopy is used for polysaccharides sequencing, and through-space effects (also known as nuclear overhauled effects, or NOEs) are used as a source of proof connecting locations and sequences [41,42]. The level whereby a polysaccharide's main structure has been investigated depends on the methodologies at hand. To enhance such technologies, the amalgamation of FTIR, NMR, Raman spectroscopy, GCMS, and HPLC techniques proves beneficial. These techniques are effective in pinpointing the chemical configurations of active glycans [42]. The fruiting bodies and mycelial tissue of *Ganoderma* are both grown in the culture broth and contain bioactive water-soluble polysaccharides. Several anti-tumor polysaccharides that were not water-soluble were also isolated from the culture [23]. According to a research, polyglucans having a molecular weight of between 10^{4} to 10^{-6} Daltons are typically more water-soluble and have better anti-tumor effects [39]. Polysaccharides, typically extracted from *Lingzhi* using water as the solvent and alcoholic solvents extraction method, belong to a class of bioactive molecules with various structural characteristics and different physicochemical capabilities, as a recent emphasis has been placed on polysaccharides in pharmacology, specifically protein/peptide-associated polysaccharides. Studies have shown that ethanol-precipitable water-soluble of β-1-3-D, β-1-6-D glucans rank among the foremost potent immunomodulatory polysaccharides [40]. The essential extraction principle is to fracture the cell membrane progressing from the external to the internal layer under intermediate to harsh extraction parameters like pH and temperature degree. Some of the naturally derived glycans derived from mushrooms are linked to protein or peptide groups, whilst others are neutral or acidic and contain a variety of glycosidic linkages [36]. NMR spectroscopy is one of the analytical approaches utilized for identification the anomerity for each carbohydrate residue. Anomeric vibration modes exhibit conjugated double bonds with a split significantly greater than anomeric vibration modes. They can be seen in the spectra. NMR spectroscopy is the only technique believed to characterize a polysaccharide's structure adequately.

Complete structure identification necessitates whole complete the mission of 1H and 13C NMR spectra when integrating two-dimension (2D) NMR procedures, including Techniques Consisting of Correlated Spectroscopy (COSY), and Total Correlated Spectroscopy (TOCSY) for ^{13}C and ^{1}H heteronuclear single-quantum coherence (HSQC). For polysaccharide sequencing, only two dimensional 1H NMR spectroscopy is utilized. Through-space effects (also known as nuclear overhauled effects, or NOEs) are used as a basis for validation relating to places and sequence arrangement [41,42]. The degree that a polysaccharide's main form has explored relying on the approaches obtainable. Integrating FTIR, NMR, Raman spectroscopy, GC, GC-MS, and HPLC techniques helps advance such technologies. It is possible to detect the chemical structures of functional polysaccharides using these techniques [42].

2.3.2 Triterpenes

Triterpenes are bioactive materials having isoprene C-5 units make up the ring structure. The chemical components of triterpene molecules consist of cyclic hydrophobic hydrocarbons with a lanosterol-based structure ($C_{30}H_{50}O$). This is a crucial step in the biosynthetic process that leads to the production of steroids and triterpenes in both microbes and animals [43]. Triterpenes come in a variety due to the structure's stereochemical variance. Their chemical makeup is similar to one of the components used in the manufacture of cholesterol due to the presence of oxygenated functional groups paired with stereoisomers at positions C-3 α or β, as well as C-3 or C-15 configurations and a lanosterol skeleton. Triterpenoids typically range in molecular weight from 400 to 600 kDa, and owing to their highly oxidative condition, they have much more complicated chemical structures than the group of lanostanes [44]. Due to their well-known pharmacological properties, the tasty bitterness components of *Lingzhi* called terpenes/triterpenoids have drawn a lot of interest.

According to the studies, it is still challenging to separate oxygenated triterpenoids for biological research from fruiting bodies and cultivated mycelium due to their structural similarity and compositional complexity, However, *Lingzhi's* contained more than 130 oxygenated triterpenes, the majority of which were lanostane-type triterpenes like, for example, ganoderic acid, ganoderenic, ganodermic, lucidones,

lucidenic, ganoderals, lucidic, ganolucidic, applanoxidic acids, and ganoderols [38]. Notably, there is just one primary source for these bioactive ganoderic acids *in G. lucidum*. Triterpenes, in general, are documented of having important biological properties, like anti-oxidation [45], hepatoprotection [46]. Also they prevent platelet aggregation because several enzymes, including galactosidase, angiotension-converting enzyme, and cholesterol synthase, are restricted [47], in addition to the cholesterol reduction [48].

2.3.3 Ganoderic Acids

A significant component for the creation of new medications is the ganoderic acids (GAs) obtained from *Ganoderma lucidum*, which has molecules that resemble those of steroid hormones. GAs have demonstrated exceptional therapeutic properties and medicinal benefits for several human disorders [49]. Figure 2.5 shows the different isomers of Ganoderic acid [50].

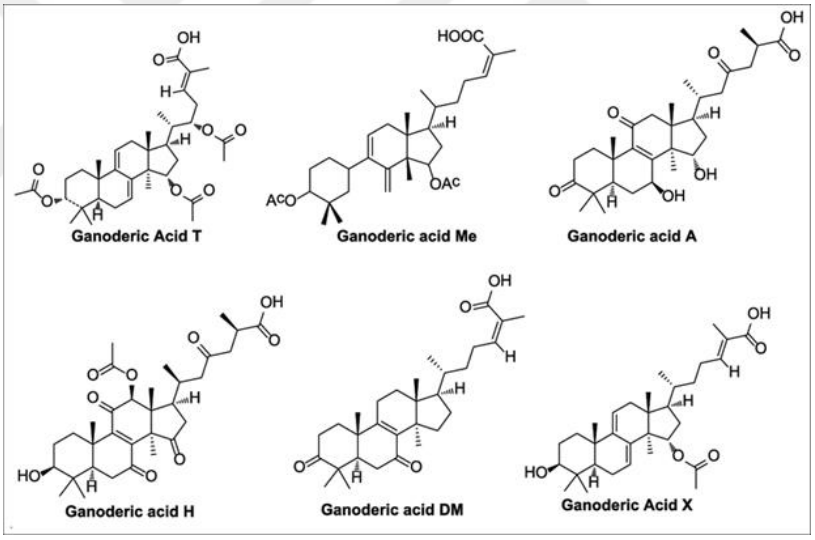

Figure 2.5 Different isomers of GAs [50]

The researchers discovered through transcribed profile analysis that the role of environmental conditions is strongly connected to the gene's expression involving in GA production. Additionally, there is a greater emphasis on outlining fresh research avenues for GAs and making an effort to gather knowledge for a deeper comprehension of GA biosynthesis and regulation [51,52]. Most of them are useful medicinally. For instance, several GAs have the capacity to prevent the creation of cholesterol [53], such as histamine discharge [54], as well as the ability to neutralize free radicals [55]. Silica gel TLC plates may be utilized for triterpenes identification,

qualitatively and semi-quantitatively. Due to the presence of carboxyl groups in many of the triterpenes isolated from *ganoderma*, solvent solutions with a little amount of acid are preferable for TLC separations. TLC has also been used to distinguish between various *ganoderma* species.

Investigators discovered that various *ganoderma* species had distinctive triterpene patterns on the TLC chromatograms [49]. A comparative analysis of several prevalent *Ganoderma lucidum* products on the market reveals differences in their polysaccharide and triterpenoid contents, as detailed in Table 2.1.

Table 2.1 A comparison of the polysaccharide and triterpenoid contents in popular *Ganoderma lucidum* products available in the market [56]

Nature of Product	Triterpenes Percentage	Polysaccharide Percentage
1	1.36	4.48
2	2.36	5.32
3	1.88	15.70
4	1.06	10.97
5	0.44	7.51
6	1.78	6.18
7	1.44	13.30
8	0.50	15.80
9	7.82	7.66
10	0.46	1.10
11	Undetectable	12.78

From 1 to 9 it is the fruit-based extraction, 10 is powdered fruit, and 11 is fungus powdered. Sterols, which are present in *ganoderma*, are closely linked to triterpenoids. Mycelium and basidiocarps both exhibit strong cytotoxic properties. Ergosterol peroxide from *G. lucidum* increases linoleic acid's ability to inhibit mammalian DNA polymerase [57]. According to studies, GS (*ganoderma sterol*) may be effective in reducing oxidative stress and inflammatory responses brought on by H/R (hypoxia/reoxygenation) [58]. The discovery of steroid compounds from the basidiocarps of *G. applanatum* with broad-spectrum activity and bactericidal capabilities, as well as antibacterial effects [59], was made. Both microorganisms

with Gram-positive and Gram-negative properties have good resistance to antimicrobial properties of ganomycins A and B produced by *Pfeiffer* [53,59]. The triterpene profiles, specifically the ganoderic acids, were isolated utilizing a mini Sep-Pak C18 cartridge, suitable for reversed-phase (RP)-HPLC chromatography, and further purified through silica gel column chromatography. The polarity of triterpenes is significantly influenced by the overall amount of acetoxy and hydroxyl units present.

Using TLC plates made of silica gel, triterpenes are identified qualitatively and semi-quantitatively. Numerous triterpenes identified from *ganoderma* contained carboxyl groups, hence chemically neutral solvent solutions generally result in band tailing. Consequently, acid-free solvent systems are preferred for TLC separations. Additionally, TLC has been used to differentiate between the many *ganoderma* species, and it was discovered that each species of ganoderma had a distinctive pattern of triterpenes on the TLC chromatograms.

2.3.4 Other Components

Proteins and lectins are a couple of the additional substances found in *G. lucidum* that may help explain its purported medical effects. Around 7-8% of dried *G. lucidum* were discovered to have protein, which is less than many other mushrooms. According to reports, *G. lucidum's* bioactive proteins, such as *LingZhi-8* which is an immunosuppressive albuminoid extracted out of the mycelia, contribute to the plant's therapeutic capabilities, featuring an acetylated amino terminus and 110 amino acid residues [60]. Lectin is another protein with a lesser sugar concentration isolated from the stems of *ganoderma*. Lectins are non-immune-derived carbohydrate-proteins, agglutinate cells, precipitate polysaccharides, or glycol-conjugates [61]. Lectins are non-catalytic proteins or glycoproteins with an affinity for carbohydrate molecules. The term lectin which roots in the Latin term Legere, that refers to seize or select. Numerous varieties of microorganisms, implants, and animals generate lectins, which serve various functions. Lectins, for instance, participate in multiple cell functions in the operation of immunological system mechanisms in animals [62]. In addition, enzymes including metalloprotease, which prolongs the clotting process, ergosterol (provitamin D2), nucleosides, and nucleotides have been extracted from *G. lucidum*, adenosine, and guanosine [63,64].

2.4 The Bacteria

Bacteria are the simplest living species, and researchers believe they strongly resemble the first organisms to emerge on earth. Bacteria, which are too small to be observed with the human eye, are the most prevalent organisms [65]. Bacteria are currently an essential tool in genetics and biotechnology research, but for the first forty years following the recent resurgence of Mendel's findings and the resuscitation of genomics, it was believed that bacteria were very easy to have genetic code, experience mutations, or procreate sexually. It is hardly remarkable, given that those microorganisms are tiny enough that it is difficult to be investigated as individual organisms. Researchers have seen significant variances in bacterial cultures but have not understood that all of these changes were driven by the process of mutating [66].

2.4.1 Bacteria Mutating

Any heritable alteration in the genetic code is known as a mutation. The phenotypic of the organism is or is not impacted by this. Hugo de Vries used a latin phrase that means "to change" to create the word mutation. Mutation is a crucial topic in modern biology that causes differences in genetics. A mutation is considered as a long-lasting change, change related to the order of nitrogen bases in a particle of DNA. Generally, a mutation causes a modification to the outcome indicated through the gene. Whether it is an industrial chemical, pesticide, food additive, or medication, testing for mutation is typically the first stage in the selection of compounds for research and a necessary step for regulatory approval and commercialization [67]. Mutations can either arise spontaneously or be caused by an environmental mutagen. Most mismatches in DNA can be attributed to internal cellular processes like tautomeric base changes, oxidative harm to DNA, loss of purines, and the deamination process. External factors, encompassing chemicals, radiation, viruses, dietary habits, and lifestyle choices, also play a significant role [68]. Missense mutations are DNA modifications that modify how proteins' amino acids are arranged, because of a mutation; one incorrect codon and one incorrect amino acid. In addition, the nonsense mutation, which is a genetic alteration that produces an endpoint codon, produces an incomplete protein since stop codons halt protein synthesis. Sometimes mutations impact essential processes, making the bacterial cell unprofitable. Thus, deadly mutations are those alterations that can kill the cell named lethal mutation

[68-70]. As a result, Various human illnesses, such as cholera, leprosy, bacterial pneumonia, whooping cough, diphtheria, etc., are brought on by bacteria. Scarlet fever, rheumatic fever, pneumonia, and other infections are associated with streptococcus bacteria. Diarrhea, severe pediatric constipation, and intestinal protozoal diseases can all be brought on by *Escherichia coli.*

2.4.2 Antibacterial Propriety in *G. lucidum*

Numerous studies have indicated that *Ganoderma lucidum* is an effective antibacterial agent. Extracts of *G. lucidum*, when prepared using water and methanol, have demonstrated inhibitory effects against a range of both gram-positive and gram-negative bacterial strains. According to studies, most times when *G. lucidum* extract and other antibiotics were combined, the effects were beneficial in vitro, active substances with broad-spectrum antibacterial action include triterpenes, ganomycein, and other aqueous extracts [20,71]. In recent years, the abuse and overuse of antibiotic medications contributed to a significant raise in the number of antimicrobial-reluctant human pathogenic microorganisms [72]. Antimicrobial drug resistance is a serious financial issue that affects doctors, patients, universal healthcare executives, the drug industry, and the general public. Pathogens caused by bacteria and fungi have also made treating infectious diseases more difficult [73]. New and potent therapeutic medicines must be created immediately, given the rise of multidrug-resistant human pathogenic bacteria. Infectious disease treatment has become more difficult as a result of bacterial and fungi pathogens.

The development of newer and promising bioactive medicines is essential given the rise in the multidrug resistance of human pathogenic bacteria [74]. For thousands of years, traditional tribal cultures, native people, and people in the eastern countries have used herbs, spices, and fungi as curative agents. In order to understand the scientific foundation for their therapeutic benefits and to find novel lead compounds for the creation of therapeutic medications, attention has recently been focused on the extracts and biologically active chemicals employed in herbal remedies [75]. Leveraging botanical extracts for their antimicrobial properties has been studied, and it has been discovered that they contain a variety of biologically active components. This has allowed scientists to identify the main classes of antimicrobial compounds present in plants as well as the crucial experimental techniques needed to identify

newer active substances. Adding to the plant outputs as producers of antibiotic chemicals, experimental studies are being conducted for mushrooms to investigate whether they can activate the humoral defense system of the body, thereby preventing illnesses caused by bacteria, viruses, or fungi that refuse treatment with standard approaches and drugs. *Penicillin* with other major antibiotic agents is produced by the fungus, but antimicrobials' presence in the basidiomycetes fungus family, also popular as ‘the mushroom,’ is not popular [76]. Early research suggested that most antibacterial properties of the basidiomycetous fungus were just effective towards the gram-positive bacteria [77], nonetheless, more Recent research has shown that these extracts also exhibit in *vitro* efficacy against gram-negative bacteria, notably *E. coli* and *P. Vulgaris* [71]. Bacteria that are gram-positive possess robust cell walls, predominantly made of peptidoglycan, in addition to their inner cellular membranes, while gram-negative bacterial microorganisms have inner cell walls, a layer of peptidoglycan, with a fatty polysaccharide complex-coated wide exterior. The external layer of gram-negative bacteria offers a higher resistance most likely because of its external cell wall that acts as a barrier against numerous external elements, comprising antibacterial medications. Figure 2.6 shows a comparison of the cellular structures of gram-negative and gram-positive microorganisms [78].

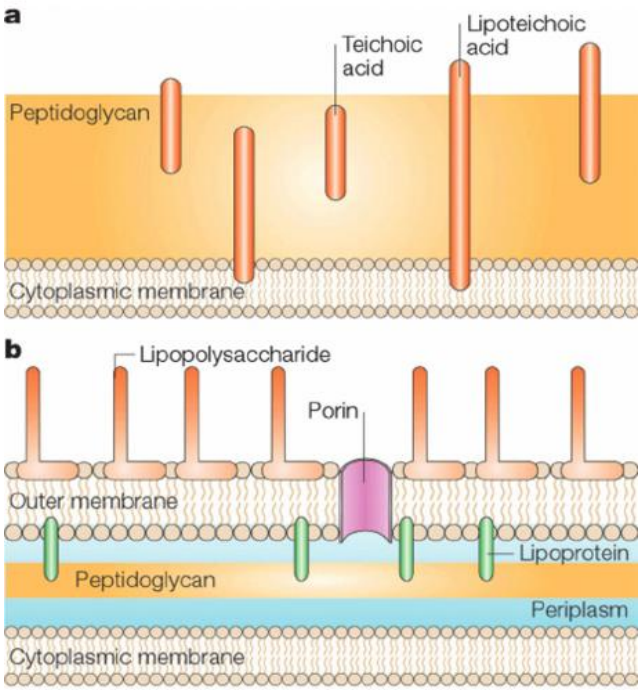

Figure 2.6 Compression between the cellular barriers of gram-negative and gram-positive microorganisms [78]

From *Ganoderma lucidum* mushroom extraction, antimicrobial properties toward gram-positive bacteria have been demonstrated [79]. It was determined that the antibacterial activity of *G. lucidum* liquid extraction increased when coupled with 4 well-known antibiotics. It is notable that relatively few investigations have been conducted on extracts of liquid-cultured mycelium using the *ganoderma* genus, while nearly all antibacterial studies were conducted on the fruit-based part [71]. The fruiting-body of *G. applanatum* was discovered to contain steroid compounds with broad-spectrum antibacterial activity and bactericidal characteristics [80]. In addition, both A and B ganomycins were isolated from the fruit-based part of *Pfeiffer* and displayed antimicrobial effectiveness towards gram-positive and gram-negative microorganisms [59]. Researchers discovered that methanolic extracts of *G. lucidum* and *G. recinaceum* mycelia and culture extracts inhibited *Staphylococcus aureus* and *B. subtilis*, respectively [79].

2.5 Oxidative Stress

The generation of oxidative stress is attributed to reactive oxygen entities like superoxide anion ($O_2{*}^-$), hydroxyl radical (OH^*), and hydrogen peroxide (H_2O_2) are what create oxidative stress, that might harm cellular walls, peptides, and nucleotides. Even more, research demonstrates the accumulated harm via oxygen radical types which plays a role in numerous diseases. A recent investigation suggests a clear connection between the damage from hypochlorous acid (HOC) and reactive nitrogen intermediates like nitric oxide (NO), peroxynitrite (HOONO), and nitroso thiols (RSNO), in conjunction with the effects of previously mentioned oxidizing agents [81]. To resist oxidative stress, cells can respond to the enzymatic detoxifying which treat the harm resulting from reactive oxgeyne species (ROS) [82]. In addition, bacteria, fungi, include mammals' cells demonstrate adaptable reactions to large concentrations of oxidative stress, showing that such organisms can detect greater amounts of ROS and translate the message as an increase in the production of defense mechanisms. *E. coli* has proven as an excellent template to clarify each fundamental and flexible in reaction to the oxidative stress that is experienced throughout typical respiratory development [83]. It has been shown that strenuous exercise might result in an increase in oxidative stress. Consequently, oxidative stress may perform a part in the situation of overtraining [84]. Free radicals

(FR) refers to particles or molecular pieces that have one or many unbound electrons located within their valence shells. Due to their propensity to transfer electrons to other molecules, FRs are extremely unstable and reactive (oxidation). They have a very brief lifespan and are created through an electron transfer that needs a lot of energy. An FR has the ability to react with other radicals or chemicals to produce new radicals [85].

2.5.1 Biological Effects of ROS

Reactive oxygen species plays a significant part in cellular communications or in the biogenesis of cells, even if most of the studies has emphasized the negative consequences of FR. This is since they can function as cell transmitters and undergo oxidation-reduction changes. Additionally, ROS has been linked to the activation of enzymes, the detoxification of drugs, and the promotion of glycogen replenishment. Additionally, ROS is crucial for muscle contraction, which are positive effects of ROS [86]. As a negative effect of ROS, healthy cells can undergo apoptosis due to ROS, which can also cause inflammation or disrupt biological processes. All these impairments contribute to pathologies that degenerate with time, including cancer, Alzheimer's disease, and Parkinson's disease, cataracts, and cell aging [87]. A clear understanding of the different types of free radicals and their main effects can be found in Table 2.2.

Table 2.2 The categories of free radicals and their primary effects providing a systematic overview, aiding in the understanding of the distinct types and subsequent consequences of each free radical [88]

FR	Constriction	Halves life	Key Outcome
ROS			
Superoxide ion	O_2^{*-}	10^{-5} s	proteins being oxidized, DNA being damaged, and lipids being oxidized and peroxidase
Ozon	O_3	steady	
Ioxygen (singlet) or dioxidene	$1O_2$	1 μs	
Hydroxyl radical	OH^*	10^{-9} s	
dihydrogen dioxide	O_2H_2	steady	
Dichlorine oxide	HOCL	steady	
Alkoxyl free radical	RO^*	10^{-6} s	
Peroxyl free radical	ROO^*	7 s	
Hydroperoxy radical	$ROOH^*$		
RNS			
Nitrogen monoxide	NO^*		proteins being oxidized, DNA being damaged, and lipids being oxidized and peroxidase
Nitrogen dioxide	NO_2^*	1^{-10} s	
peroxonitrite	$ONOO^{*-}$	0.05^{-1} s	
RSS			
Thiyl radical	RS^*		proteins being oxidized, DNA being harmed, ROS generating

2.5.2 The Antioxidant Activity *in G. lucidum*

Antioxidants are either naturally occurring or synthetic molecules that can inhibit the cell-damaging effects of free radicals. *G. lucidum* is a fungus which is frequently utilized due to its antioxidant characteristics. Antioxidants could assist in preventing tumor and many other serious diseases [88]. Antioxidants protect bio-substances from oxidative harm, hence lowering the mutations risk beside the cancer development. They also protect immune cells, keeping their immunological response and surveillance capabilities. Several *G. lucidum* components demonstrate antioxidant activity in *vitro*, particularly polysaccharides and triterpenoids [89]. *G.*

lucidum polysaccharides associated with proteins, *G. tsugae* methanolic extracts, and *G. lucidum* ethanolic extracts have all demonstrated Actions that scavenge superoxide and hydroxyl radicals [90,91]. In terms of lipid peroxidation within the liver and kidney of mice, a *G. lucidum* extract prepared using hot water exhibited antioxidative effects [92]. Additionally, the activity of protein-bound polysaccharides increases when the ratio of carbohydrates to protein decreases. As naturally occurring antioxidants, phenols have been identified as an important component of mushroom methanolic extracts [14]. Moreover, compared to other researched mushrooms, the *ganoderma* geniuses were discovered to provide greater oxidation inhibition performance, scavenging, and chelating activities. Few studies have been conducted on the antioxidant actions of triterpenes from the *ganoderma* geniuses [55].

CHAPTER III

MATERIALS AND METHODS

3.1 Materials and Methods Used Overview

An essential step in the research of physiologically active chemicals is the extraction procedure. The solvent kind that was used in the study and extraction, the extraction method used, and the components of cultivating living tissue, can all significantly affect the sort of compound that can be retrieved when removing chemicals from the fungus or other biological sources.

3.2 Chemicals/Reagents List

G. lucidum sample (fresh fruiting body), bacteria (*Escherichia coli, Klebsiella, Mesophile, Pseudomonas aeruginosa*), Mueller Hinton Agar, Paper discs filtration (6 mm in diameter), Caliper to measure the inhibition zone, Ethanol 90%, Methanol, Aceton, and distilled water. *DPPH* (2,2-diphenyl-1-picrylhydrazyl), Vitamin C (ascorbic acid).

3.3 *Ganoderma lucidum* Samples Collection and Identification

The fresh mushrooms were gathered from period March-April 2022. The mushrooms were discovered to be expanding on various species of alive and not alive trees. The *ganoderma* mushrooms had hard, woody, glossy, ear-shaped fruiting bodies that ranged in size from reddish-brown to yellow-brown, shown in Figure 3.1.

Figure 3.1 *Ganoderma* fruiting bodies

3.4 *Ganoderma lucidum* Samples Preparation

Ganoderma lucidum fruiting bodies that had been gathered were cured by air in the shadow. Then cut up every dehydrated specimen into tiny fragments, combined, ground into powder, then it was put into paper bags and kept at room temperature until extraction time in a dark, dry location. Shown in Figure 3.2.

Figure 3.2 *Ganoderma lucidum* sample, natural form and ground form

3.5 Devices Used in the Extraction

3.5.1 Soxhlet Apparatus

Modern extraction techniques such Soxhlet extraction method involve continuously running the same solvent through the extraction. It is a method for continuous extraction even if it can describe it as a series of tiny special processes. A Soxhlet

extractor can only be used with components that are very soluble in the solvent. The Soxhlet method of extraction has a loop that incorporates extraction after the solvents have vanished. This cycle can technically be repeated as frequently as required to produce the target compound with the maximum yield.

3.5.2 Sonication

The method of stirring up the particles in solutions using sound waves. The sonication method makes use of ultrasound frequencies. Dozens of microscopic vacuum bubbles are created in the fluid during the procedure due to the applied tensions. The produced bubbles burst into the solution during the cavitation procedure. The bubble will pop in the cavitation field, generating vibrations that transfer significant energy. Consequently, the structural bonds connecting the water droplets are destroyed. As even the molecular bonds weaken, the atoms begin to separate, which makes it possible for the combining reaction to take place. Figure 3.3 shows how the sound wave from the sonicator device generates sound energy to travel through the liquid, causing bubbles to form and then shatter.

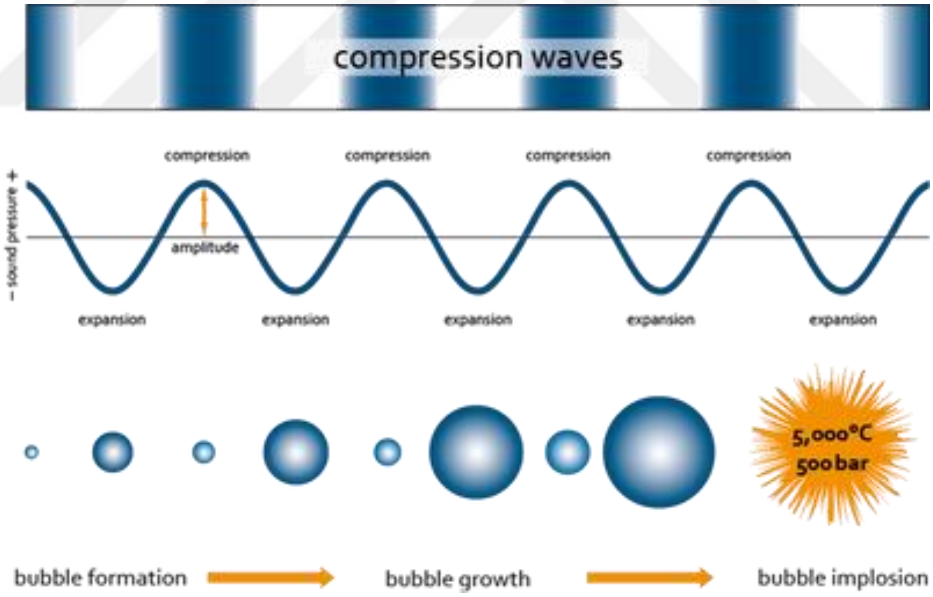

Figure 3.3 visualization of sonicator machine's sound wave (Source: www.lubio.ch)

The sonicator device is frequently used to separate body cells, obtain peptides, prepare, and disperse graphene and nanoparticles, and more. Like the process used to obtain important oils, conventional Chinese medication, or pure pigmentation.

Figure 3.4 Experimental design for the study, formulated to ensure the most accurate and comprehensive results.

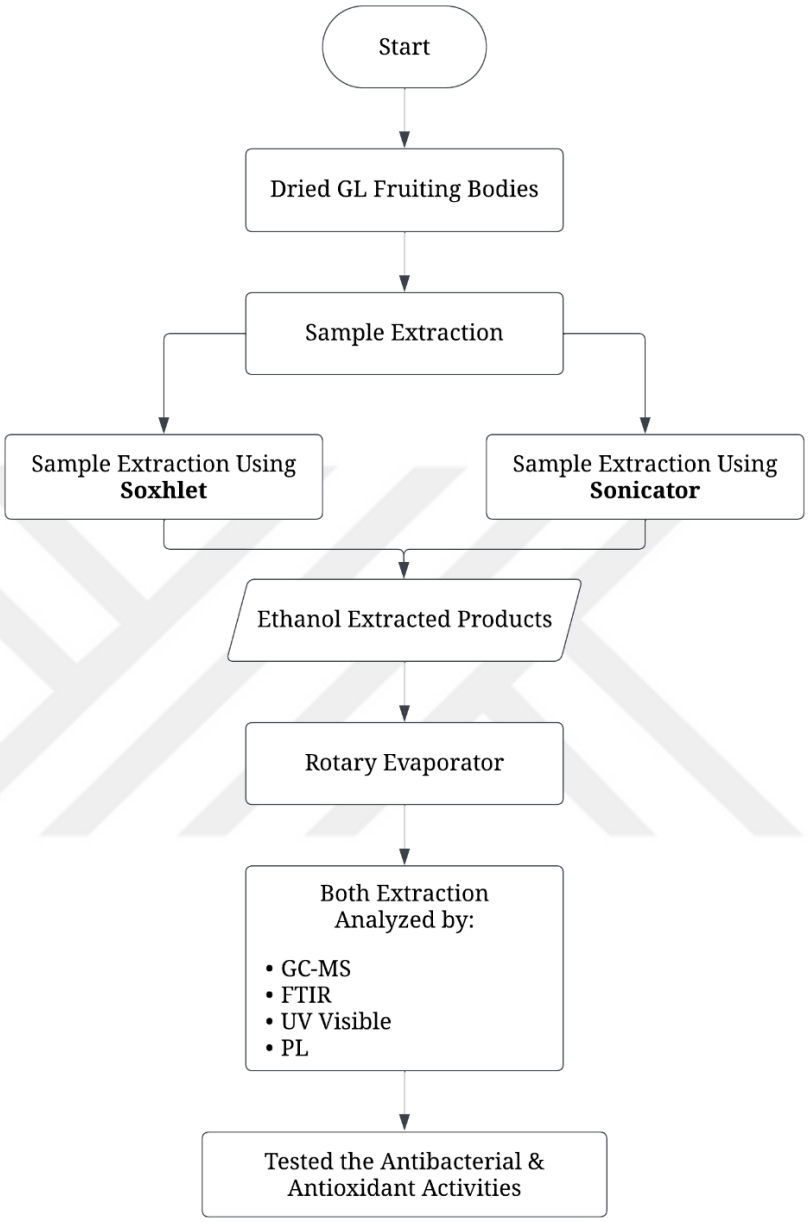

Figure 3.4 Experimental study plan

3.5.3 Extraction of *G. lucidum* Using Soxhlet Apparatus

All *ganoderma* mushroom sample material was used to extract and isolate the bioactive components. It must be noted that all pieces and equipment used in the experiment were cleaned with acetone and dried. The specified 10 g samples were processed for around 37 hours at 180 °C in a Soxhlet extractor. Adding ethanol (EtOH) gradually. Utilizing a rotary evaporator for solvent evaporation, then the

generated extracts were concentrated. The Soxhlet extraction process and the instrument is shown in Figure 3.5

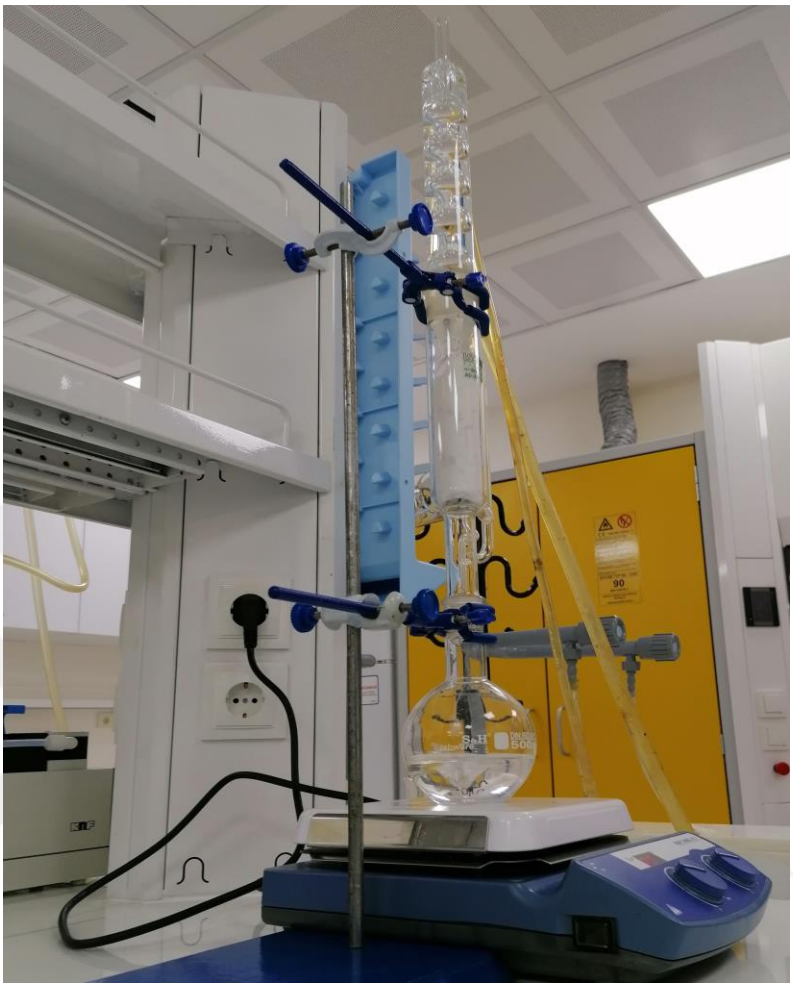

Figure 3.5 Soxhlet instrument photograph, taken from the laboratory

3.5.4 Extraction of *G. lucidum* Using Sonicator

In a flask with a flat bottom, 10 g of the desiccated specimen were mixed with 150 mL of ethanol. The mixture was then extracted for 37 hours in the sonicator device, followed by two hours of standing time. EtOH was used to separate the liquid and remove the solid (repeated three times). After the extraction, the liquids were combined, and the solvent was vaporized in a rotating process. The sonicator extraction process and the instrument is shown in Figure 3.6. Also, the rotary evaporation process and instrument used, is shown in Figure 3.7.

Figure 3.6 The sonicator instrument photograph, taken from the laboratory

Figure 3.7 Rotary evaporator instrument photograph, taken from the laboratory

3.6 Soap Preparation

In Figure 3.8, the detailed experimental plan laid out for the preparation of soap.

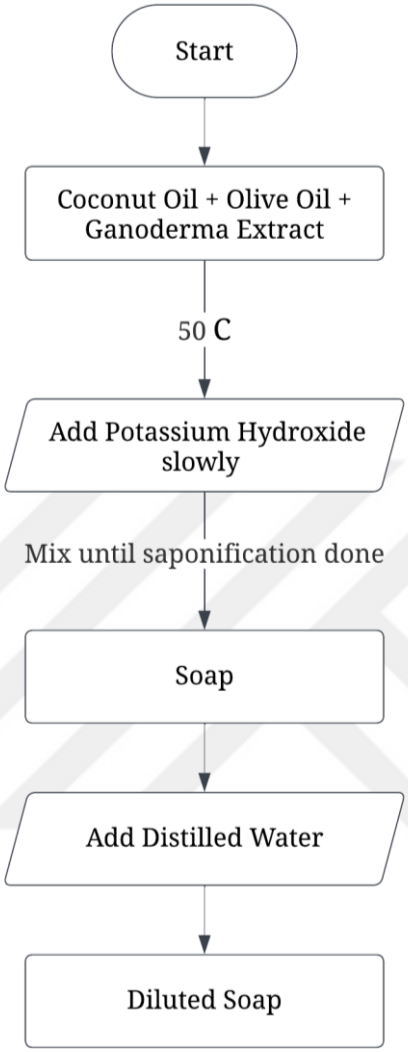

Figure 3.8 Experimental plan for soap preparation

For the preparation and testing of soap, a set of specific materials was employed. Organic virgin coconut oil and organic olive oil were chosen for their purity and quality. Potassium hydroxide, an essential ingredient for saponification, was also used in the soap-making process. Additionally, to ensure the correct alkalinity and acidity levels of the final soap product, a pH indicator was utilized for testing purposes.

Also, Figure 3.9 shows the soap components to be used in the saponification reaction

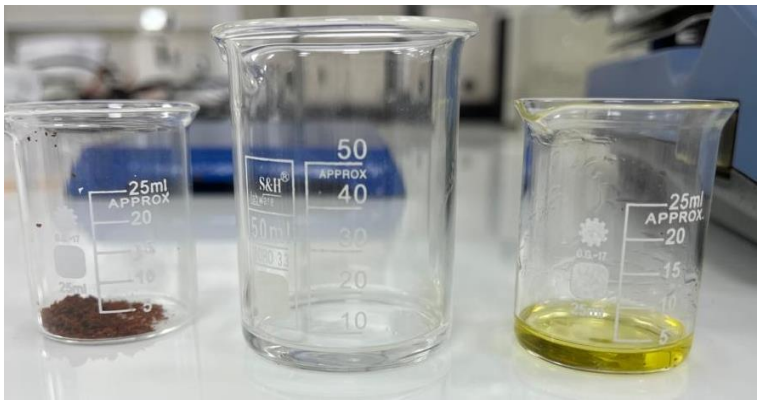

Figure 3.9 Weighted soap components in various beakers

The combined solution was warmed to a temperature ranging from 50 to 60°C, incorporating virgin coconut oil, olive oil, and *ganoderma* obtained *via* Soxhlet extraction. Potassium hydroxide was added slowly while being careful to keep the temperature below 85 °C. For a brief period, the mix was maintained around 80 and 85 °C to guarantee that the saponification reaction had fully taken place. Prepared soap shown in Figure 3.10.

Figure 3.10 Prepared soap

The production was allowed to cool and proceeded to be gently stirred before being diluted with 1:5 of the total weight of soap. Control soap was made following the same procedures without using *ganoderma* extract. Figure 3.11 shows the diluted soap.

Figure 3.11 Diluted soap

In the saponification reaction involving olive oil and coconut oil with potassium hydroxide (KOH), several important chemical transformations take place. Firstly, triglycerides, which are the primary components of oils and fats, undergo hydrolysis in the presence of the strong alkali KOH. This hydrolysis breaks down the triglycerides into their constituent fatty acids and glycerol. The chemical equations for these reactions are as follows in the **Figure 3.12** which explains the soaponsfication process.

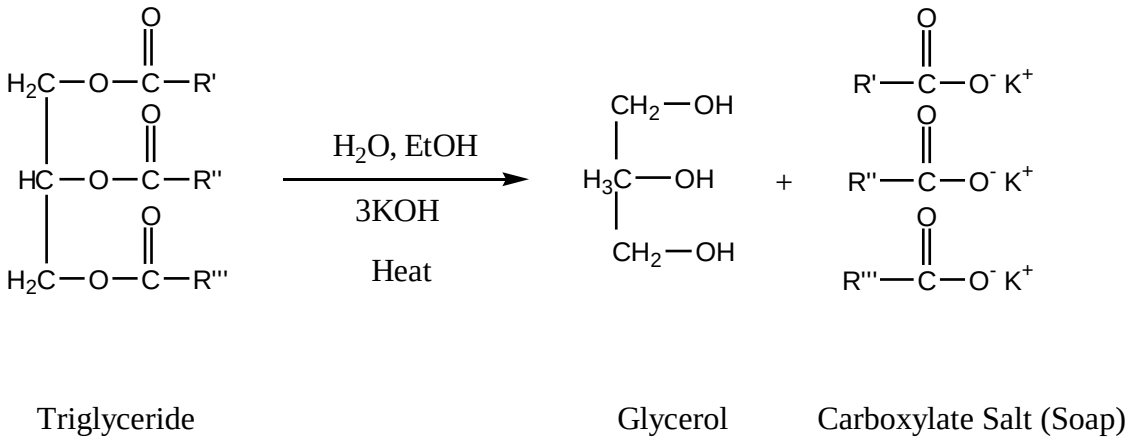

Figure 3.12 General saponification reaction using KOH as base

These equation above illustrate the conversion of the triglycerides in the oils into soap molecules and glycerol as byproducts. It's important to note that the specific

soap molecules produced depend on the fatty acid composition of each oil used. Furthermore, the inclusion of *ganoderma* extract in the soap formulation introduces additional complexity. *Ganoderma* extract is not a triglyceride, so it does not undergo the saponification process. Instead, its chemical constituents, which may include organic compounds, can potentially contribute to the overall composition and properties of the soap. The specific impact of *ganoderma* extract on the soap's characteristics, such as its scent or potential bioactive properties, will depend on its chemical composition and compatibility with the soap-making process.

3.7 Analytical Methods Used

The composition of *ganoderma* mushroom extracts is complicated, hence several analytical techniques are needed to identify specific chemicals or groups of compounds.

3.7.1 Gas Chromatography GC-MS

Gas chromatography (GC) is an analytical technique capable of analyzing gaseous, liquid, and solid samples, provided they can be vaporized by heat. This method allows for the identification and quantification of individual compounds within a mixture when processed using a GC apparatus. Heating is applied to the components inside the specimen, as well as the solvent's constituents, Subsequently, when a composite solution sample is introduced into the GC device, it is transformed into vapor. Within the GC-MS, equipped with a capillary column (30 m x 0.25 mm x 0.25 m) and utilizing helium as a carrier gas with a flow rate of 1 ml/minute and a split ratio of 1:10, 0.1 mL of each extract (obtained *via* Soxhlet and sonicator methods) was introduced. The oven was initially set to 50°C and maintained isothermally for five minutes. Subsequently, the temperature was ramped up to 280°C at a rate of 10°C per minute, where it was held for fifteen minutes. The mass spectrometer interface temperature was 230°C, and the injector port was set to 290°C.

3.7.2 Fourier-Transform Infrared Spectroscopy FTIR

This approach is employed to determine the functional groups found with carbon-containing and non-carbon-containing compounds by determining the absorption of infrared energy over a wavelength range. This procedure utilizes an interferometer

for creating an interferogram of such a specimen sign, which is then subjected to a Fourier transform to generate the FTIR spectrometer. All specimens were made without dispersion in KBr plates as well as the FTIR spectroscopy was subsequently obtained at ambient temperature using a straight ATR device. Infrared spectra were captured using a PerkinElmer 100 FTIR equipped with a Gladia ATR Sampling attachment, operating at a resolution of 1 cm^{-1} over 16 scans.

3.7.3 Ultraviolet-Visible Spectroscopy UV-VIS

PG Method Equipment Ltd. utilized the T80+ UV/VIS Spectrograph, employing dichloromethane as the solvent. An optical quartz cuvette with a length of 1 cm was to record the UV-Vis spectrum within the wavelength range of 190-1100 nm was used.

3.7.4 Fluorescence Spectroscopy

Utalizing a Perkin-Elmer LS55 Spectrum fluorophotometer, photoluminescence characteristics were examined. A cuvette made of ocular quartz measuring 1 cm in length was employed to analyze the whole samples after they had been diluted in dichloromethane. At varying concentrations, the specimens were measured at 300 nm. Using 9,10-diphenylantracene as the reference compound, photoluminescence quantum efficiencies were computed. The Fluorescence spectroscopy instrument is given in Figure 3.13.

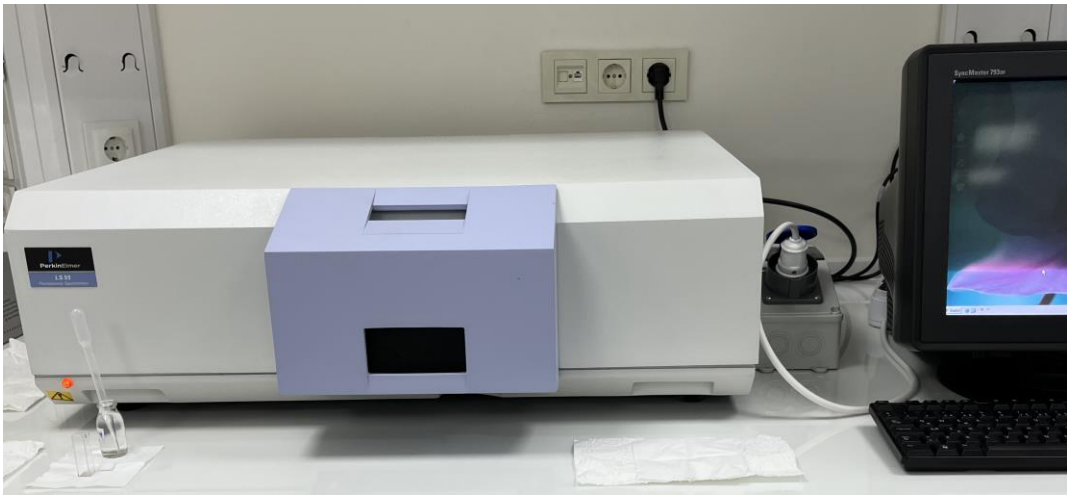

Figure 3.13 Fluorescence spectroscopy instrument photograph, taken from the laboratory

3.8 Biological Evaluation

3.8.1 Antioxidant Properties

The ability of the samples to scavenge free radicals was evaluated based on the reduction of 1,1-diphenyl-2-picrylhydrazyl (DPPH) concentration in methanol, using a UV-visible spectrophotometer. (Blois, 1958). Ascorbic acid (vitamin C) and the samples for testing were solubilized in methanol to prepare their individual solutions. To initiate the assay, 1 mL of every test solution was mixed with 9 mL of a newly prepared DPPH solution, having a concentration of 0.012 mg/mL in absolute methanol. In this setup, ascorbic acid served as a positive control, demonstrating known antioxidant activity. For the negative control, 10 mL of the 0.012 mg/mL DPPH solution prepared in pure methanol was used, which helps to establish the baseline absorbance of the DPPH solution without any antioxidant present, the samples were prepared, the contents of each preparation were thoroughly mixed, also, The Combination were kept at room temperature, away from light, to facilitate undisturbed reactions over a span of 30 minutes. This dark and stable environment is essential to avoid any photodegradation of DPPH and to ensure that any changes observed are due to the samples' antioxidant activity. After the incubation period, The absorbance of each combenation was recorded using a UV-spectrophotometer. (Specifically, the Thermo Scientific Evolution 201 Model) at a wavelength of 517 nm. This wavelength is chosen because DPPH exhibits a strong absorbance at 517 nm, which decreases when it is reduced by an antioxidant. The entire procedure was conducted in triplicate, this repetition is a standard practice to ensure that the results are reliable and not due to random chance or experimental error. The capacity of the samples to act as free radical scavengers was then quantified Utilizing the given equation, the percentage of DPPH radicals scavenged by the samples was determined:

Radical scavenging activity (%) = [(Absorbance of control − Absorbance of Sample) / Absorbance of control] × 100

This formula compares the control's absorbance measurement (DPPH solution without any antioxidant) to that of the test samples (DPPH solution with the antioxidants being tested), and expresses the reduction in absorbance as a percentage, indicating the extent to which the test sample is effective at neutralizing the DPPH

free radicals. The photograph in Figure 3.14, illustrates the series of extract concentrations and DPPH.

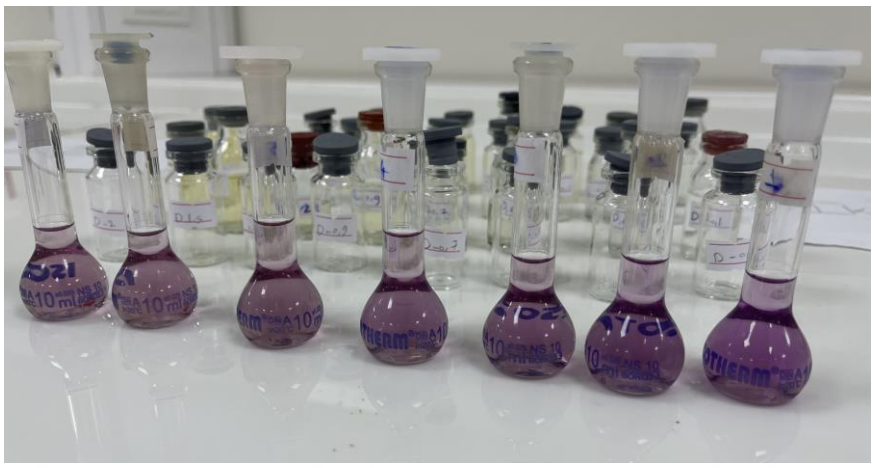

Figure 3.14 Extract concentration series' and DPPH photograph, taken from the laboratory

3.8.2 Antimicrobial Properties

The mushroom extraction samples (extracted by both sonicator and Soxhlet) and liquid soap with *ganoderma*, and liquid soap without *ganoderma* as a control, were all utilized to investigate for antibacterial properties. In this study, the antibacterial properties of *ganoderma* fungal extracts using the agar disc diffusion method were evaluated.

3.8.3 Agar Disc Diffusion Method for Conducting Anti-bacterial Assays

The sterile filter paper disk agar diffusion method was utilized to evaluate the antimicrobial activity of the specimens [93]. *Ceftriaxone*, *Gentamicin*, and *Ciprofloxacin* antibiotics were utilized as the antibacterial reference, while ETOH served as the non-reactive control, *Escherichia coli*, *Staphylococcus aureus*, and *Klebsiella pneumoniae* bacteria (as listed in Table 3.1) were used.

Table 3.1 Bacteria strain utilized to assess the antimicrobial efficacy of *ganoderma* extracts and soap

Bacteria	Strain	Gram + or Gram-
Escherichia coli	ATCC 25322	-
Staphylococcus aureus	ATCC 25923	+
Klebsiella pneumoniae	ATCC 700603	-

A bacterial inoculum, prepared to a concentration of 10^8 cells/ml according to the McFarland standard, was introduced into nutrient agar media. This served as a consistent starting point for the bacterial cultures, ensuring that each test began with the same quantity of active cells. The test solution, consisting of a compound under investigation, and EtOH as a control solution, was then samples prepared at varying concentrations: 1%, 5%, 10%, and 20%. Exact amounts of both test and control solutions were dispensed onto petri plates, and then applied to sterile filter paper disks (6 mm in diameter), under aseptic conditions. This ensures no contamination of the samples and that any observed effects are due to the test solution itself. The bacterial dishes were subsequently kept at 37°C for a 24-hour duration. This temperature was chosen to closely mimic the human body temperature, providing an environment in which human pathogens are likely to thrive. After the incubation period, the zones of inhibition around the were measured using a calibrated ruler. This measurement provides a quantitative assessment of the antimicrobial activity of the test solution: larger zones of inhibition indicate stronger antimicrobial effects. To ensure the reliability and reproducibility of the results, this entire experiment was performed three separate times, each as an independent replicate. After the completion of all replicates, the data was compiled and statistically analyzed to determine the effectiveness of the test solution in inhibiting bacterial and fungal growth compared to the control solution.

CHAPTER IV

RESULT AND DISCUSSION

4.1 Chemistry of *Ganoderma Lucidum*

The medicinal mushroom *Ganoderma lucidum*, often referred to as '*Reishi*' or '*Lingzhi*,' is a treasure trove of over 400 active biological components. Among these, polysaccharides, ganoderic acid, and *B*-glucans stand out due to their prevalent roles. These polysaccharides enhance immune functionality and present antitumor and antidiabetic properties. Ganoderic acid, a triterpene, offers liver support and plays a part in cholesterol management. *B*-glucans intensify the body's defense mechanisms against cancer cells. The proteins present in this mushroom are rich in antioxidant properties, and compounds like *Lingzhi-8* show potential anticancer benefits. Furthermore, the mushroom contains vital steroids, nucleotides essential for genetic material, beneficial fatty acids, and critical minerals such as selenium and zinc. All these elements underscore the significant medicinal value of *Ganoderma lucidum*, cementing its status as a potent natural remedy in the annals of traditional and modern medicine. The *ganoderma* growth on the tree edges given in Figure 4.1.

Figure 4.1 *Ganoderma* growth on the tree edges

4.2 Extract Yields

The extracts' yield was calculated by concluding the extracted product weight, divided by the total amount of *GL* used in the experiment. The result is multiplying by 100.

Yield of product extracted by Soxhlet = 2,350/22,567*100 =10,413%

Yield of product extracted by sonicator = 1,750/20,101*100 =8,720%

The extraction yield serves as an indicator of how efficient a particular method is in obtaining compounds from a raw material, in this case, *GL* yields were determined by taking the weight of the compounds extracted and relating it to the initial amount of *GL* used. The higher the percentage, the more efficient the method is considered. When comparing the two methods, the Soxhlet extraction yielded 10,413%, significantly outpacing the sonicator's 8,720%. This difference of nearly 1,693% suggests that the Soxhlet apparatus manages to retrieve more compounds from the same amount of *GL* than the sonicator. This could be due to the inherent working principles of each method. The Soxhlet method, which uses repeated solvent washing, might be more thorough in extracting the compounds from *GL*, thus achieving a higher yield. Conversely, the sonicator, which uses ultrasonic waves to extract compounds, might not penetrate the material as deeply or might not dislodge certain compounds as efficiently as the Soxhlet method. Additionally, the results could hint at the nature of the compounds within the *GL*. Some compounds might be more easily accessed and extracted with the thorough washing of the Soxhlet, whereas others might be more surface-bound and hence readily retrieved by the sonicator. While both methods have their merits, for those aiming to achieve the highest yield from *GL*, the Soxhlet extraction method appears to be the superior choice. It's crucial, however, to weigh this advantage against other factors like time, cost, and the specific compounds of interest before settling on a method for large-scale extraction.

4.3 *Ganoderma*-prepared Soap Evaluation

The soap made from *Ganoderma lucidum* mushroom exhibits a unique set of characteristics that contribute to its distinct appeal. It has a texture that is notably thick, the soap promises a moisturizing sensation upon use. Its yellowish-brown coloration, as seen in Figure 4.2, and earthy because it is derived from the mushroom

extract. The soap's aroma is a blend of cleanliness intertwined with herbal and woody notes, because of the *Ganoderma lucidum* mushroom's distinctive fragrance. Table 4.1 shows the main soap made from *Ganoderma luciduim* characteristics. Figure 4.3 displays the appearance of the soap lather once water is added. While, Table 4.1 indicates that the pH level of the soap stands at 9.5.

Figure 4.2 Diluted *ganoderma* soap observed as a yellowish-brown color

Table 4.1 Main soap made from *Ganoderma luciduim* characteristics

Texture	Thick and adhesive.
Color	Yellowish brown
Odor	Clean, herbal, woody, fungus – like
PH	9.5
Foaming	Moderate lather

Figure 4.3 Soap lather upon the addition of distilled water

Figure 4.4 Soap pH observed as 9.5

4.4 Gas Chromatography GC

The GC-MS displayed each compound's absorption value over the time frame. The major bioactive components found In the Soxhlet, ethanolic extract are alcohol alkanes, phenols, and fatty acids using the GC-MS method. (16) Chemicals from the GC section of the ethanolic Soxhlet extract found in the GC-MS analysis were shown. The primary and predominant active ingredient in *GL* was Ethyl linoleate, with 32,72. % and 62,02 RT a fatty acid can be produced when linoleic acid and ethanol are esterified, ethyl linoleate has numerous benefits, including its anti-inflammatory and anti-bacterial bioactivities [94], It has a positive effect on both inflammation and non-inflammatory acne, making it a successful therapy for minor to moderate acne. [95]. In *vitro* experiments have shown that ethyl linoleate inhibits the formation of cancer cells [96], also, research showed that ethyl linoleate protects the heart by lowering inflammation and oxidative damage [97]. The second biggest peak 16,98 % and 62,195 RT is the ethyl oleate while employing ethyl oleate as a

cosmetic component is quite well-known. It could effectively hydrate overall skin by strengthening the skin's membrane and halting moisture loss, according to researchers [98]. It has been found to aid in wound healing by promoting cell growth and boosting collagen production [99]. Squalene is a triterpene that is a naturally produced hydrocarbon and turns into lipids. It is a transparent, oily solution that is additionally present in certain herbs and plants, like olive trees, and in large quantities in the livers of humans and animals, such as sharks. Squalene is a product of the liver's mevalonate and functions as an intermediary in the production of cholesterol, its peak in Soxhlet extract was 16.87% and 69.348 RT, while in the sonicator extract the squalene peak was the highest among others recorded at 83,10% and 69,41 RT. Various biological features of squalene, including its antioxidants, anti-inflammatory, antitumor, and immunostimulatory effects, have already been examined. Several of these qualities include antioxidant capabilities because squalene can scavenge FR and safeguard cells from reactive oxygen species. In experiments employing both *vivo* and in *vitro*, this ability was already proven [100]. Anti-inflammatory properties have been observed, showing a reduction in pro-inflammatory compounds. [101]. And antitumor property [101]. Hexadecanoic acid, ethyl ester recorded a 10.13% peak area and 56.68 RT, this compound has antioxidant activity [102]. The bioactive chemicals, along with their preservation duration, concentration peak or area (%), name, and structure (Soxhlet extract) are included in Table 4.2.

Table 4.2 Bioactive chemicals from the Soxhlet extract

Peak	R.Time	Area	Area%	Name - Chemical	Molecular structure
1	12.044	70472	1.12	1-Pentanol, 2,2-Dimethyl-alcohol	$C_7H_{16}O$
2	12.503	86276	1.37	Pentane, 3-Ethyl-2,4-Dimethyl-alkene, pentane family	C_9H_{20}
3	19.889	252687	4.00	1,1,3-Triethoxybutane ether	$C_{10}H_{22}O_3$
4	24.165	41430	0.66	1-Tridecene terpene	$C_{13}H_{28}$
5	33.621	175862	2.79	1-Tetradecene terpene	$C_{14}H_{30}$
6	33.975	42769	0.68	Tetradecane alkene	$C_{14}H_{30}$
7	38.867	202113	3.20	Phenol, 2,4-Bis(1,1-Dimethylethyl) phenol derivative	$C_{14}H_{22}O$
8	42.099	186505	2.95	1-Heptadecene alkene	$C_{17}H_{34}$
9	49.730	141768	2.25	1-Nonadecanol Aliphatic alcohol	$C_{19}H_{40}$
10	53.325	99104	1.57	Pentadecanoic acid, fatty acid	$C_{20}H_{38}O_2$
11	54.244	65100	1.03	Ethyl 9-Hexadecenoate fatty acid ester	$C_{20}H_{38}O_2$
12	55.980	46467	0.74		
13	56.688	639221	10.13	Hexadecanoic acid, Ethyl Ester fatty acid	$C_{18}H_{34}O_2$
14	62.023	2065981	32.72	Ethyl Linoleate fatty acid	$C_{22}H_{42}O_2$
15	62.195	1072141	16.98	Ethyl Oleate fatty acid	$C_{22}H_{42}O_2$
16	62.990	60272	0.95	Octadecanoic acid, Ethyl Ester fatty acid	$C_{20}H_{38}O_2$
17	69.348	1065040	16.87	Squalene terpene	$C_{30}H_{50}$
		6313208	100.00		

Various biological substances with medicinal value, including alkaloids, polysaccharides as well as steroids, added to the essential fats, have already been

discovered to be present in *G. lucidum*. Figure 4.5 shows the GC-MS for the Soxhlet extracted sample.

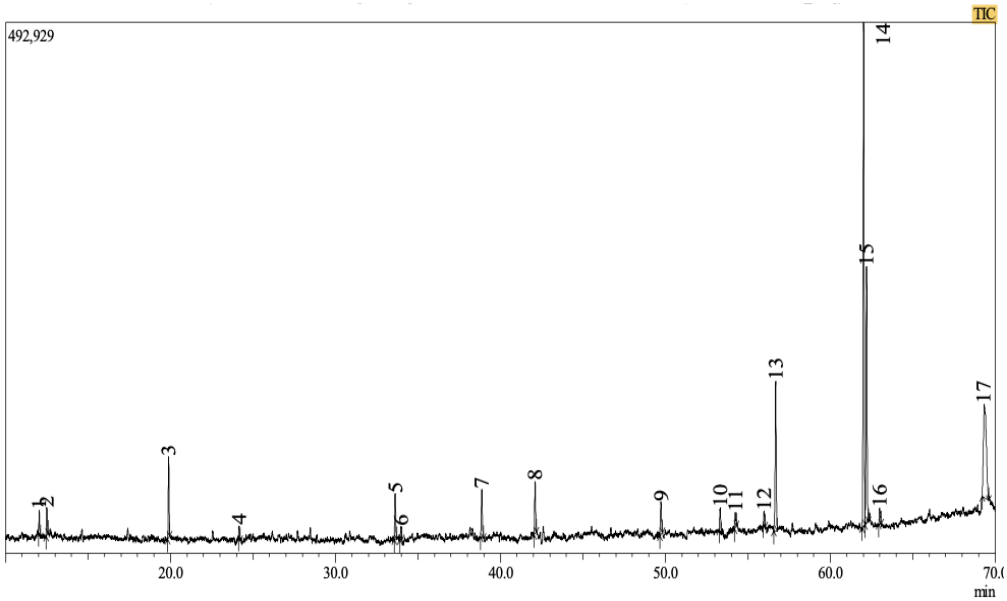

Figure 4.5 GC-MS for the Soxhlet extract, with EtOH solvent

(8) chemicals from the GC section of the ethanolic sonicator extract found in the GC-MS method. The major bioactive compounds found in the sonicator, ethanol-based extract are alcohol alkanes, phenols, and fatty acids using the GC-MS method. The bioactive chemicals, along with their preservation duration, concentration peak or area (%), name, and structure. (sonicator extract) are included in Table 4.3, as mentioned, the Squalene peak was the highest among others recorded at 83,10% and 69,41 retention time (RT).

Table 4.3 Bioactive chemicals from the sonication extract

Peak#	R.Time	Area	Area%	Name – Nature	Molecular structure
1	7.058	63464	2.00	1,1-Diethoxy-2-butene alkene	$C_8H_{14}O_2$
2	12.046	61659	1.94	1-Pentanol, 2,2-dimethyl- alcohol	$C_6H_{14}O$
3	12.509	71261	2.24	Pentane, 3-ethyl-2,4-dimethyl- (CAS) alkane	C_9H_{20}
4	19.905	107230	3.37	1,1,3-Triethoxybutane ether	$C_{10}H_{22}O_3$
5	38.869	74206	2.33	Phenol, 2,4-Bis(1,1-Dimethylethyl) phenol derivative	$C_{14}H_{22}O$
6	54.245	51437	1.62	7,9-Di-Tert-Butyl-1-Oxaspiro (4,5) Deca-6,9-Diene-2,8-Dione	$C_{17}H_{24}O_3$
7	62.022	107907	3.39	Ethyl Linoleate fatty acid ester	$C_{22}H_{42}O_2$
8	69.411	2641340	83.10	Squalene terpene	$C_{30}H_{50}$
		3178504	100.00		

Like the Soxhlet extracted sample, the sonicator extracted sample recorded squalene as the highest peak at 83,10% from total compounds and with 69,411 RT, as mentioned it is an antioxidant bioactive compound that proves the property existence in *GL*. Figure 4.6 shows the GC-MS for the Sonicator extracted sample.

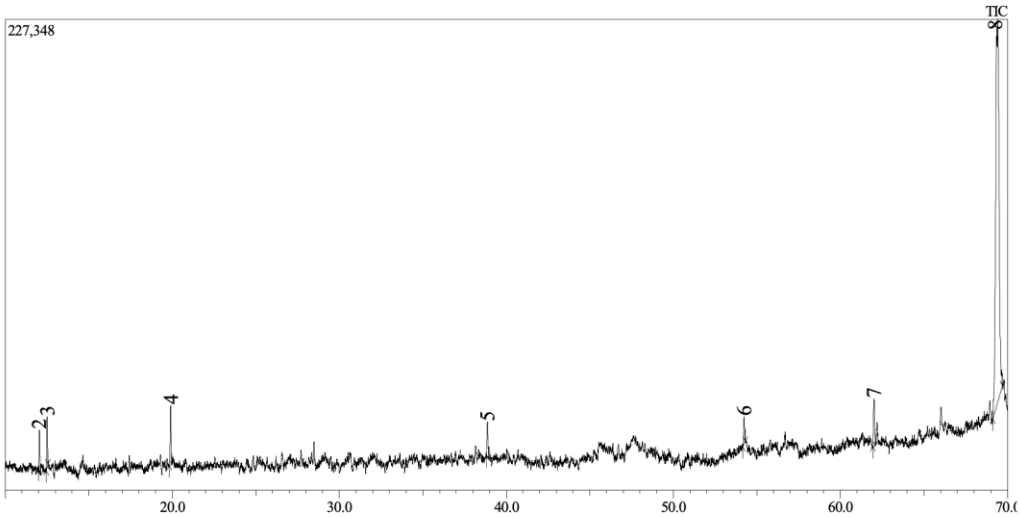

Figure 4.6 GC-MS for the sonication extract, with EtOH solvent

4.5 Fourier Transform Infrared Spectroscopy (FTIR) Measurements

This study investigates the FT-IR spectrum of various materials, including olive oil, coconut oil, and *Ganoderma lucidum* extracted through both Soxhlet and sonication methods, as well as soaps derived from these oils. Additionally, soaps containing a blend of olive oil, coconut oil, and *Ganoderma lucidum* were examined Figure 4.7 illustrates a comparative presentation of the FT-IR spectra for the above-mentioned materials. The main objectives were to elucidate the chemical structures of these substances and to analyze the distinct spectral variations resulting from saponification reactions. The spectral comparisons of these materials revealed significant alterations in peak intensities. Notably, certain peaks in the soap products exhibited heightened intensity and sharper profiles, while others demonstrated decreased intensity and broader shapes in contrast to the reference substances – olive oil, coconut oil, and *Ganoderma lucidum* extract. The saponification process resulted in the appearance of additional peaks in the spectrum of the soap products, providing clear evidence of successful saponification reactions. Initially, the FT-IR spectra of olive oil, coconut oil, and *Ganoderma lucidum* extracted through Soxhlet and sonication methods were examined. Subsequently, the focus shifted towards the spectral distinctions arising from the manufacturing of soap sourced from olive oil and coconut oil, as well as soap formulated using a combination of olive oil, coconut oil, and *Ganoderma lucidum*.

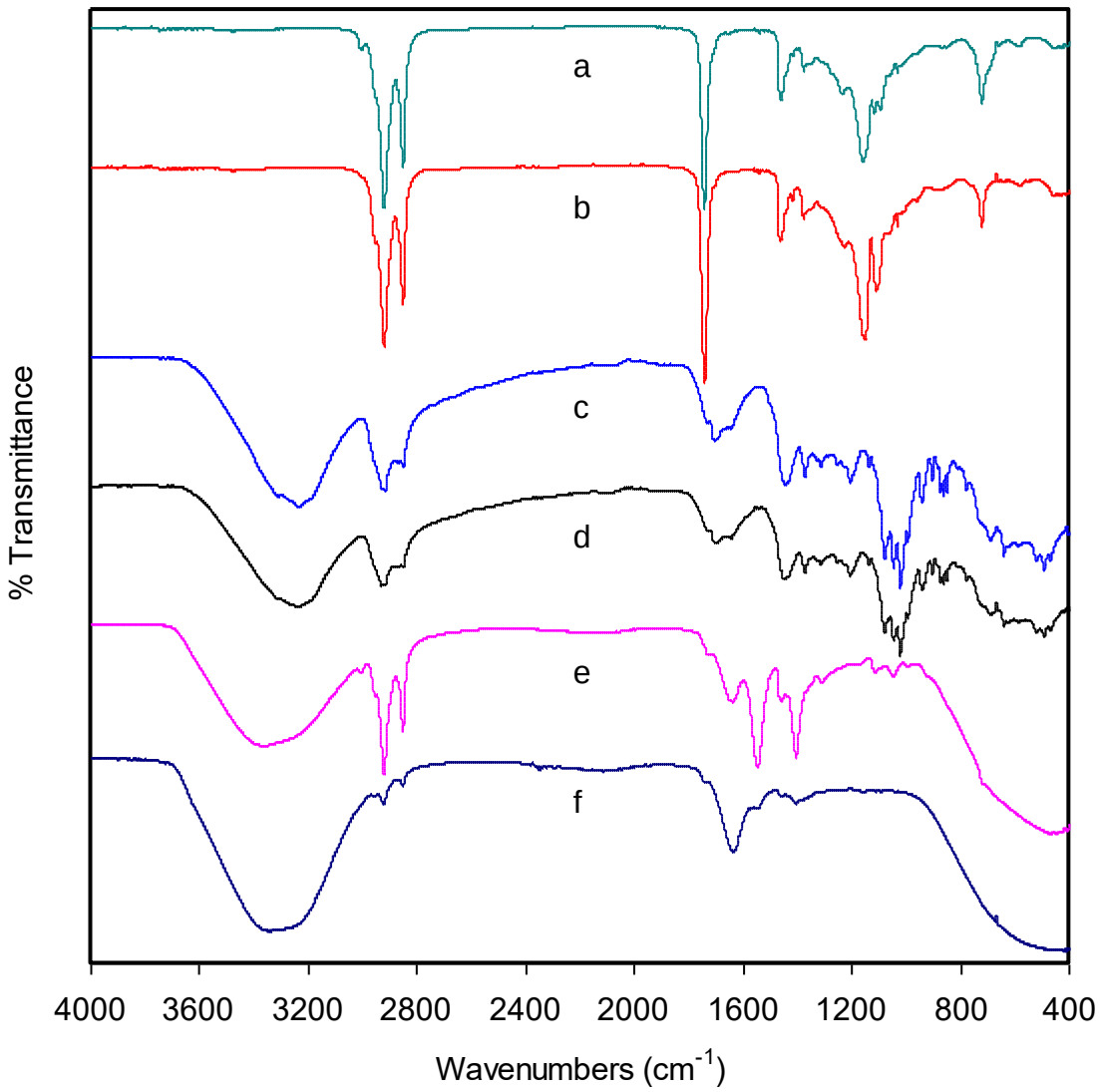

Figure 4.7 FT-IR spectrum of (a) olive oil (OO), (b) coconut oil (CO), (c) *Ganoderma lucidum* obtained by Soxhlet extraction (Gan-Sox), (d) *Ganoderma lucidum* obtained by sonication extraction (Gan-Son), (e) soap manufactured from olive oil and coconut oil (SOP), (f) soap prepared from olive oil, coconut oil and *Ganoderma lucidum* (Gan SOP)

Following the FT-IR spectra for the olive oil (Figure 4.7 (a)), the anticipated peaks were all detected based on the chemical makeup of the olive oil. These peaks can be examined to elucidate the molecular configuration of olive oil as follows. The peak of minimal intensity at 3711 cm^{-1} is ascribed to the O-H stretching in the compounds. The moderate peak at 3005 cm^{-1} is attributed to C-H vibrational stretching in aliphatic olefinic structures. The strong peaks at 2921 and 2852 cm^{-1} affiliated with the C-H stretching peak in the $-CH_2-$ aliphatic alkane chain [94,103]. The very weak

peak at 2301 cm^{-1} belongs to the C-H stretching in the aliphatic alkane chain. The distinct peak at 1743 cm^{-1} is attributed to the C=O carbonyl group's vibrational stretch of carboxylic acids [104]. The very weak peak observed at 1541 cm^{-1} corresponds to the C=C vibrational stretching in aliphatic olefinic configurations. The distinct peak at 1461 cm^{-1} is related to the C-H flexural behavior in the aliphatic alkyl or alkane sequence. The absorption indicators, of mild and intermediate intensity, at 1417 cm^{-1} and 1377 cm^{-1} likely associate with the C-H flexing mode in the $-CH_3$ section of the aliphatic alkane chain [94]. The peaks with moderate and strong intensities at 1236 cm^{-1} and 1159 cm^{-1} are linked to the O-H bending mode in compounds containing hydroxyl groups. The peaks of intermediate intensity observed at 1117, 1095, and 1033 cm^{-1} are associated with the C–O vibrational stretching [103] Carboxylic acids exhibit an asymmetric stretching vibration, highlighted by the intense and moderately intense peaks at 721, 662, and 584 cm^{-1}. These peaks refer to the out-of-plane bending in the O–H bonds. Such vibrational markers are chiefly associated with triacylglycerols and some glycerides. A synthesized overview of the FT-IR spectral data for olive oil is presented in Table 4.4.

Table 4.4 FT-IR results of olive oil (OO)

Bond (Type of compound)	Reference of Wavenumber (cm^{-1}) [105]	Observed Wavenumber (cm^{-1})	Intensity
O-H band	3750-3000 (Stretch)	3775-3530 3711	w
C-H bond (aliphatic, alkene)	3100-3000 (Stretch)	3045-2970 3005	m
C-H bond (-CH_2- aliphatic, alkane)	3100-2700 (Stretch)	3045-2759 2921, 2852	s
C-H bond (-CH- aliphatic, alkane)	2400-2100 (Stretch)	2372-2253 2301	w
C=O bond (carbonyl group)	1800-1550 (Stretch)	1776-1642 1743	s
C=C bond (aliphatic, alkene)	1680-1600 (Stretch)	1650-1500 1541	w
C-H bond (aliphatic, alkyl or alkane)	1460-1370 (Bend)	1478-1384 1461	s
-CH_3 (aliphatic, Alkane)	1450, 1375 (Bend)	1417, 1377	w,m
O-H bond	1400-1100 (Bend)	1400-1100 1236, 1159	m,s
C-O bond	1200-950 (Asymmetric stretch)	1190-930 1117, 1095, 1033	m
O-H bond	950-650 (Out-of-plane bending)	940-540 721, 662, 584	s,m

s: strong, m: medium, w: weak

The FT-IR spectrum of coconut oil can be shown in Figure 4.7 (b). All the anticipated peaks aligned with the chemical structure of coconut oil were detected. The analysis of these peaks allows for the identification of the chemical structure of CO, as outlined below. The existence of a faint peak at 3712 cm^{-1} point to the O-H stretching within the components [106]. The prominent peaks at 2921 and 2852 cm^{-1}

correspond to the C-H stretching in the aliphatic alkane sequence of $-CH_2-$ [107]. The notable absorption observed at 1742 cm^{-1} is attributed to the vibrational stretching associated with the carbonyl group present in carboxylic acids [107]. The distinct peak observed at 1462 cm^{-1} is representative of the C-H bending vibration in aliphatic alkyl or alkane structures. Absorption bands at 1417 cm^{-1} and 1377 cm^{-1}, which vary from faint to moderate intensities, likely represent the C-H bending in the $-CH_3$ segment of aliphatic alkanes. Peaks recorded at 1228 cm^{-1} and 1153 cm^{-1}, ranging from moderate to pronounced intensities, are indicative of the O-H bending vibrations in hydroxyl group-containing compounds. Meanwhile, the intermediate intensity peaks seen at 1108 cm^{-1} and 1033 cm^{-1} are characteristic of the C-O asymmetric stretch in carboxylic acid molecules [108]. The strong peak at 721 cm^{-1}, coupled with the intermediate peak at 581 cm^{-1}, is indicative of the out-of-plane bending vibrations of O–H bonds. These peaks are typically associated with compounds like lauric acid, myristic acid, palmitic acid, and other saturated fatty acids. A comprehensive summary of the peaks observed for coconut oil in the FT-IR analysis can be found in Table 4.5.

Table 4.5 FT-IR data of coconut oil (CO)

Bond (Type of compound)	Reference of Wavenumber (cm^{-1}) [105]	Observed Wavenumber (cm^{-1})	Intensity
O-H band	3750-3000 (Stretch)	3782-3532 3712	w
C-H bond (-CH_2- aliphatic, alkane)	3100-2700 (Stretch)	3038-2752 2921, 2852	s
C=O bond (carbonyl group)	1800-1550 (Stretch)	1781-1641 1742	s
C-H bond (aliphatic, alkyl or alkane)	1460-1370 (Bend)	1479-1385 1462	s
-CH_3 (aliphatic, Alkane)	1450, 1375 (Bend)	1417, 1377	w,m
O-H bond	1400-1100 (Bend)	1400-1100 1228, 1153	m,s
C-O bond	1200-950 (Asymmetric stretch)	1180-920 1108, 1033	m
O-H bond	950-650 (Out-of-plane bending)	945-545 721, 581	s,m

s: strong, m: medium, w: weak

Figure 4.7 (c) illustrates the FT-IR spectra of *Ganoderma lucidum* obtained through Soxhlet extraction. All the anticipated peaks, in line with the chemical structure of *Ganoderma lucidum*, were observed. These peaks can be interpreted to shed light on the chemical compositions within *Ganoderma lucidum* as detailed below. The compounds within *Ganoderma lucidum* present distinct significant regions in the FT-IR spectrum. The initial region spans from 3675 to 3016 cm^{-1}, representing the O-H stretching region attributed to polysaccharides like cellulose, starch, glycogen, and chitin [109]. In this region, the absorbance of *Ganoderma lucidum* is notably strong and displays a wide broadband pattern. The primary absorption peak is situated at 3244 cm^{-1}. The N-H stretching from the amide structure of protein molecules is also located in this region and overlapped with this very broad band [110]. The subsequent spectral range spans from 3032 to 2947 cm^{-1}, encompassing the

vibrational stretching of C-H bonds within aliphatic olefinic configurations present across the entirety of the compounds [111]. The absorption of *Ganoderma lucidum* in this range is very weak but it becomes evident at 2958 cm^{-1}. The subsequent segment spans from 2983 to 2787 cm^{-1}; this is the C-H stretching peak in the $-CH_2-$ aliphatic alkane chain. The strong peaks at 2923 and 2851 cm^{-1} are aligned with the C-H stretching peak in the $-CH_2-$ aliphatic alkane chain in the total compounds. The fourth region spans from 2348 to 2052 cm^{-1}; this is the C-H stretching in the aliphatic alkane chain in the total compounds. The absorption of *Ganoderma lucidum* in this region is also very weak but is observable at 2165 cm^{-1}. The fifth region spans from 1785 to 1513 cm^{-1}; this is the C=O carboxyl group vibrational stretching in carboxylic acids. The intense peak at 1699 cm^{-1} is correlated with the vibrational stretching of the C=O carbonyl group in carboxylic acids [110]. The sixth spectral range spans from 1589 to 1477 cm^{-1}, delineating the vibrational stretching characteristics of C=C bonds within aliphatic olefinic structures. Notably, a peak of moderate intensity at 1443 cm^{-1} is specifically aligned with the C=C vibrational stretching present in both triterpenes and the overall aliphatic olefinic configurations. Moving on to the seventh region, which extends from 1472 to 1393 cm^{-1}, this range encompasses the C-H bending mode observable in the aliphatic alkyl or alkane chain. Within this scope, a subtle peak at 1461 cm^{-1} is attributed to the C-H bending mode inherent to the aliphatic alkyl or alkane chain across all compounds. The eighth segment, ranging from 1460 to 1350 cm^{-1}, encapsulates the C-H bending mode within the $-CH_3$ aliphatic alkane chain. A significant robust peak at 1372 cm^{-1} is distinctly associated with the C-H bending mode of the $-CH_3$ aliphatic alkane chain. Advancing to the ninth region, spanning 1405 to 1210 cm^{-1}, the O-H bending mode is observed for compounds containing hydroxyl groups. A peak of moderate strength, positioned at 1314 cm^{-1}, corresponds well with the O-H bending mode of hydroxyl-containing compounds. Within the tenth spectral region, spanning from 1360 to 1180 cm^{-1}, the C-N stretching peak is encountered, indicative of amine and amide compounds. Notably, peaks at both 1254 and 1207 cm^{-1}, ranging from moderate to strong intensity, align with the C-N stretching peak observed in amide compounds within the complete protein molecules [110]. Moving to the eleventh spectral range, spanning from 1156 to 950 cm^{-1}, the C–O asymmetric stretching vibration can be encountered and is characteristic of carboxylic acids. Further, in this range, peaks of moderate strength, specifically at 1138, 1079, 1064, 1047, and 1022 cm^{-1}, align

distinctly with the C–O asymmetric stretching vibration within carboxylic acids. The subsequent twelfth segment, extending from 945 to 570 cm^{-1}, pertains to the out-of-plane bending of O–H bonds. Within this context, faint peaks at 942, 904, and 873 cm^{-1} can be seen, signifying the out-of-plane bending of O–H bonds. Furthermore, the peaks present at 993, 863, and 850 cm^{-1} are attributed to the alfa-configuration of OH within polysaccharides [112]. Entering the thirteenth spectral region, which spans from 899 to 560 cm^{-1}, are discernible for the N-H bending mode in 1° and 2° amines and amides. This region shows faint peaks positioned at 778 and 690 cm^{-1}, distinctly corresponding to the N-H bending mode present in 1^{*} and 2^{*} amine and amide compounds [112]. Concluding the analysis, with the final spectral range extending from 799 to 550 cm^{-1}, pertains to the stretching vibration characteristic of alkyl halides [112]. The faint peak at 641 cm^{-1} is ascribed to the alkyl halide stretching vibration encompassing all the compounds under investigation. The culmination of observed peaks from the entire FT-IR data set for *Ganoderma lucidum* is succinctly presented in Table 4.6. Figure 4.7 (d) displays the FT-IR spectrum of the *Ganoderma lucidum* obtained by sonication extraction. Similar FT-IR data of *Ganoderma lucidum* were also obtained by sonication extraction (Gan-Son).

Table 4.6 FT-IR data of *Ganoderma lucidum* obtained by Soxhlet extraction (Gan-Sox)

Bond (Type of compound)	Reference of Wavenumber (cm^{-1}) [105]	Observed Wavenumber (cm^{-1})	Intensity
O-H band	3750-3000 (Stretch)	3675-3016 3244	s
C-H bond (aliphatic, alkene)	3100-3000 (Stretch)	3032-2947 2958	w
C-H bond (-CH_2- aliphatic, alkane)	3100-2700 (Stretch)	2983-2787 2923, 2851	s
C-H bond (-CH- aliphatic, alkane)	2400-2100 (Stretch)	2348-2052 2165	w
C=O bond (carbonyl group)	1800-1550 (Stretch)	1785-1513 1699	s
C=C bond (aliphatic, alkene)	1680-1600 (Stretch)	1589-1477 1443	m
C-H bond (aliphatic, alkyl or alkane)	1460-1370 (Bend)	1472-1393 1461	w
-CH_3 (aliphatic, alkane)	1450, 1375 (Bend)	1460-1350 1372	s
O-H bond	1400-1100 (Bend)	1405-1210 1314	m
C-N bond (amine, amide)	1380-1170 (Stretch)	1360-1180 1254, 1207	m,s
C-O bond	1200-950 (Asymmetric stretch)	1156-950 1138, 1079, 1064, 1047, 1022	m
O-H bond	950-650 (Out-of-plane bending)	945-570 942, 904, 873	w
N-H bond (1° and 2° amines, amides)	900-550 (Bend)	899-560 778, 690	w
Alkyl halide	800-500 (Stretch)	799-550 641	w

s: strong, m: medium, w: weak

Figure 4.7 (e) presented the FT-IR spectra of the soap derived from both olive oil and coconut oil (SOP). All anticipated peaks align consistently with the chemical makeup of the soap originating from olive oil and coconut oil (SOP). These observed peaks can be elucidated to provide insight into the underlying chemical compositions of the soap resulting from olive oil and coconut oil (SOP). Notably, the soap product obtained from the use of olive oil and coconut oil (SOP) exhibits distinctive regions of significance within the FT-IR spectrum. Specifically, the spectral range spanning 3682-3009 cm^{-1} pertains to the O-H stretching region derived from glycerols [113]. Within this spectral range, the absorbance of soap derived from olive oil and coconut oil (SOP) was exhibited as a distinct and broad intensity. Notably, a principal absorption peak emerges at 3367 cm^{-1}. Shifting to the span of 3035-2950 cm^{-1}, the C-H vibrational stretching can be encountred, being inherent in aliphatic olefinic structures present across the entirety of the compounds. Within this scope, a peak of moderate magnitude emerged at 3007 cm^{-1} and corresponds to the C-H vibrational stretching within aliphatic olefinic structures. Progressing to the interval of 2980-2766 cm^{-1}, this region encompasses the C-H stretching peak within the $-CH_2-$ aliphatic alkane chain. It's noteworthy that robust peaks positioned at 2922 and 2852 cm^{-1} specifically align with the C-H stretching peak occurring in the $-CH_2-$ aliphatic alkane chain across all compounds [94,103]. Spanning the range of 2345-2040 cm^{-1}, the spectrum captures the C-H stretching intrinsic to the aliphatic alkane chain across all compounds. Within this spectrum, a subtle peak emerges at 2163 cm^{-1}, corresponding to the C-H stretching present within the aliphatic alkane chain. Transitioning to the region of 1745-1582 cm^{-1}, this segment is associated with the C=O carbonyl group vibrational stretching, characteristically found in carboxylic acids or carboxylates [113]. The 1739 and 1641 cm^{-1} peaks exhibit medium and strong intensities, respectively, and correspond to the C=O carbonyl group's vibrational stretching, prevalent in carboxylic acids or carboxylates. Shifting to the spectrum encompassing 1585-1490 cm^{-1}, it can be encountered the C=C vibrational stretching inherent in aliphatic olefinic structures. A prominent peak at 1546 cm^{-1}, characterized by its strong intensity, aligns directly with the C=C vibrational stretching observed across all aliphatic olefinic structures. Advancing to the range of 1473-1395 cm^{-1}, this portion of the spectrum relates to the C-H bending mode characteristic of the aliphatic alkyl or alkane chain [113]. The strong peak at 1464 cm^{-1} corresponds to the C-H bending mode within the aliphatic alkyl or alkane chain

across all compounds. Progressing to the range of 1463-1355 cm^{-1} , it can be encounterd that the C-H bending mode specific to the $-CH_3$ aliphatic alkane chain. Notably, a strong peak at 1405 cm^{-1} is attributed to the C-H bending mode inherent in the $-CH_3$ aliphatic alkane chain. Shifting to the interval of 1360-1210 cm^{-1}, this spectrum captures the O-H bending mode characteristic of hydroxyl-containing compounds. A peak of moderate strength emerges at 1312 cm^{-1}, distinctly corresponding to the O-H bending mode present within hydroxyl-containing compounds. Advancing further to the range of 1170-990 cm^{-1}, for the C–O asymmetric stretching vibration characteristic of carboxylic acids or carboxylates. Peaks of moderate strength at 1114 and 1048 cm^{-1} precisely align with the C–O asymmetric stretching vibration observed within carboxylic acids or carboxylates. Transitioning to the spectral span of 1010-750 cm^{-1}, this region pertains to the out-of-plane bending of O–H bonds. A faint peak at 996 cm^{-1} signifies the out-of-plane bending of O–H bonds. These discerned peaks collectively originate from potassium oleate and potassium laurate-based soap prepared from olive oil and coconut oil (SOP). The culmination of observed peaks from the comprehensive FT-IR dataset of soap prepared from olive oil and coconut oil (SOP) is presented concisely in Table 4.7.

Table 4.7 FT-IR data of soap prepared from olive oil and coconut oil (SOP)

Bond (Type of compound)	Reference of Wavenumber (cm^{-1}) [105]	Observed Wavenumber (cm^{-1})	Intensity
O-H band	3750-3000 (Stretch)	3682-3009 3367	s
C-H bond (aliphatic, alkene)	3100-3000 (Stretch)	3035-2950 3007	m
C-H bond (-CH_2- aliphatic, alkane)	3100-2700 (Stretch)	2980-2766 2922, 2852	s
C-H bond (-CH- aliphatic, alkane)	2400-2100 (Stretch)	2345-2040 2163	w
C=O bond (carbonyl group)	1800-1550 (Stretch)	1745-1582 1739, 1641	m,s
C=C bond (aliphatic, alkene)	1680-1600 (Stretch)	1585-1490 1546	s
C-H bond (aliphatic, alkyl or alkane)	1460-1370 (Bend)	1473-1395 1464	s
-CH_3 (aliphatic, Alkane)	1450, 1375 (Bend)	1463-1355 1405	s
O-H bond	1400-1100 (Bend)	1360-1210 1312	m
C-O bond	1200-950 (Asymmetric stretch)	1170-990 1114, 1048	m
O-H bond	950-650 (Out-of-plane bending)	1010-750 996	w

s: strong, m: medium, w: weak

Figure 4.7 (f) displaying the FT-IR spectrum of the soap resulting from olive oil, coconut oil, and *Ganoderma lucidum* (Gan-SOP). All anticipated peaks align harmoniously with the chemical composition of the soap formulated from olive oil, coconut oil, and *Ganoderma lucidum* (Gan-SOP). These observed peaks can be comprehensively interpreted to elucidate the underlying chemical structures of the

soap derived from olive oil, coconut oil, and *Ganoderma lucidum* (Gan-SOP). Notably, the soap product arising from the amalgamation of olive oil, coconut oil, and *Ganoderma lucidum* (Gan-SOP) presents distinct and pivotal regions within the FT-IR spectrum. Within the spectral range of 3696-2988 cm^{-1}, refers to the O-H stretching region originating from glycerols and all hydroxy-containing compounds. In this spectrum, the absorbance attributed to *Ganoderma lucidum* emerges with strong intensity, manifesting as a broad band. Notably, the principal absorption peak is positioned at 3323 cm^{-1}. It's important to note that the N-H stretching feature stemming from the amide structure within protein molecules of *Ganoderma lucidum* also resides within this spectral range, coinciding with the broad band absorbance [112]. Spanning the rigon of 3030-2945 cm^{-1}, the spectrum pertains to the C-H vibrational stretching occurring within aliphatic olefinic structures across the entire set of compounds. Within this scope, a faint peak emerges at 2956 cm^{-1}, corresponding to the C-H vibrational stretching present within aliphatic olefinic structures. Progressing to the range of 2960-2780 cm^{-1} , this region captures the C-H stretching peak characteristic of the $-CH_2-$ aliphatic alkane chain. Notably, strong peaks situated at 2924 and 2853 cm^{-1} distinctly align with the C-H stretching peak inherent in the $-CH_2-$ aliphatic alkane chain within all compounds. Advancing to the span of 2349-2050 cm^{-1}, this part of the spectrum corresponds to the C-H stretching observed in the aliphatic alkane chain across the entire range of compounds. A very weak peak at 2167 cm^{-1} signifies the C-H stretching within the aliphatic alkane chain. Transitioning to the region spanning 1760-1545 cm^{-1}, this spectrum represents the C=O carbonyl group's vibrational stretching, characteristic of carboxylic acids or carboxylates [113]. The modrate and robust peaks at 1742 and 1638 cm^{-1} belong to the C=O carbonile group vibrational stretching in carboxylic acids or carboxylates [110]. In the range spanning 1587-1475 cm^{-1}, the spectrum corresponds to the C=C vibrational stretching intrinsic to aliphatic olefinic structures. Positioned at 1541 cm^{-1}, a peak of moderate intensity is distinctly connected to the C=C vibrational stretching, encompassing triterpenes and the entire aliphatic olefinic structures. Advancing to the spectrum ranging from 1470-1390 cm^{-1}, we encounter the C-H bending mode characteristic of the aliphatic alkyl or alkane chain. Within this context, a very weak peak at 1460 cm^{-1}pertains to the C-H bending mode within the aliphatic alkyl or alkane chain found across all compounds. Moving to the interval of 1465-1350 cm^{-1}, we delve into the C-H bending mode specific to the $-CH_3$ aliphatic

alkane chain. Notably, a medium-intensity peak emerges at 1407 cm^{-1}, distinctly corresponding to the C-H bending mode present in the $-CH_3$ aliphatic alkane chain. Advancing further to the range of 1365-1215 cm^{-1}, this spectrum pertains to the O-H bending mode characteristic of hydroxy-containing compounds. A weak peak at 1313 cm^{-1} corresponds to the O-H bending mode within hydroxy-containing compounds. Transitioning to the spectral span of 1189-995 cm^{-1}, this region encapsulates the C–O asymmetric stretching vibration characteristic of carboxylic acids or carboxylates. Peaks of medium strength at 1158 cm^{-1}precisely align with the C–O asymmetric stretching vibration observed within carboxylic acids or carboxylates. Moving further to the range spanning 1005-755 cm^{-1}, this segment pertains to the out-of-plane bending of O–H bonds. A weak peak at 992 cm^{-1} signifies the out-of-plane bending of O–H bonds, within the spectrum of 890-545 cm^{-1}, we encounter the N-H bending mode characteristic of 1° and 2° amines and amides [112]. Within the spectrum, a weak peak at 676 cm^{-1} corresponds to the N-H bending mode characteristic of 1° and 2° amine and amide compounds. Shifting to the spectral range spanning 790-500 cm^{-1}, this region specifically pertains to the alkyl halide stretching vibration. Notably, a faint peak emerges at 524 cm^{-1}, aligning with the alkyl halide stretching vibration observed across the entirety of compounds. The culmination of observed peaks from the comprehensive FT-IR dataset of soap prepared from olive oil, coconut oil, and *Ganoderma lucidum* (Gan-SOP) is concisely presented in Table 4.8.

Table 4.8 FT-IR data of soap prepared from olive oil, coconut oil and *Ganoderma lucidum* extract (Gan-SOP)

Bond (Type of compound)	Reference of Wavenumber (cm^{-1}) [105]	Observed Wavenumber (cm^{-1})	Intensity
O-H band	3750-3000 (Stretch)	3696-2988 3323	s
C-H bond (aliphatic, alkene)	3100-3000 (Stretch)	3030-2945 2956	w
C-H bond (-CH_2- aliphatic, alkane)	3100-2700 (Stretch)	2960-2780 2924, 2853	s
C-H bond (-CH- aliphatic, alkane)	2400-2100 (Stretch)	2349-2050 2167	w
C=O bond (carbonyl group)	1800-1550 (Stretch)	1760-1545 1742, 1638	m,s
C=C bond (aliphatic, alkene)	1680-1600 (Stretch)	1587-1475 1541	m
C-H bond (aliphatic, alkyl or alkane)	1460-1370 (Bend)	1470-1390 1460	w
-CH_3 (aliphatic, Alkane)	1450, 1375 (Bend)	1465-1350 1407	m
O-H bond	1400-1100 (Bend)	1365-1215 1313	w
C-O bond	1200-950 (Asymmetric stretch)	1189-995 1158	m
O-H bond	950-650 (Out-of-plane bending)	1005-755 992	w
N-H bond (1^* and 2^* amines, amides)	900-550	890-545 676	w
Alkyl halide	800-500	790-500 524	w

s: strong, m: medium, w: weak

4.6 Ultraviolet-Visible Spectrophotometer (UV-Vis) Measurements

Within the scope of this study, the UV-Vis spectra of various samples were analyzed. The samples included *Ganoderma lucidum* obtained through both Soxhlet extraction and sonication extraction methods, as well as soaps prepared from olive oil and coconut oil. Furthermore, the study encompasses the soap synthesized from olive oil, coconut oil, and *Ganoderma lucidum*, along with vitamin C serving as a reference standard. These analyses were conducted employing spectrophotometric-grade methanol (CH_3OH) as the solvent, ensuring a rigorous and consistent experimental approach. The UV-Vis spectrum of the *Ganoderma lucidum* obtained by Soxhlet extraction at different concentrations are shown in Figure 4.8. Using methanol (CH_3OH) as the solvent, which possesses a polarity index of 5.1, a distinct absorption at 276 nm is observed for the *Ganoderma lucidum* extract procured via Soxhlet extraction. Within the spectral analysis, this specific absorption at 276 nm is attributed to a π-π^* transition inherent to the chemical constituents of the extract. In the methanol (CH_3OH) solution of *Ganoderma lucidum*, sourced through Soxhlet extraction, the presence of a singular peak suggests the existence of undiluted extract chemical structures. Furthermore, this Soxhlet-extracted *Ganoderma lucidum* displays two pronounced shoulder peaks around 294 nm and 356 nm, accompanying the principal peak at 276 nm. Examination of the spectra for this extract reveals that the intensity of the π-π^* transition peak amplifies in proportion to the increase in sample concentration, as anticipated. Moreover, a subtle redshift in the maximum absorption wavelength is observed, moving from 267 nm to 276 nm, correlating with heightened sample concentrations. As illustrated in Figure 4.8, it is evident that the sample concentrations have a minor influence on the peak absorption wavelengths of the specimen. The UV-Vis data for *Ganoderma lucidum* obtained by Soxhlet extraction are shown in Table 4.9. The molar absorptivity values for the sample diminished with rising concentrations. This decline suggests that elevated concentrations negatively impact the molar absorption potential of the specimen.

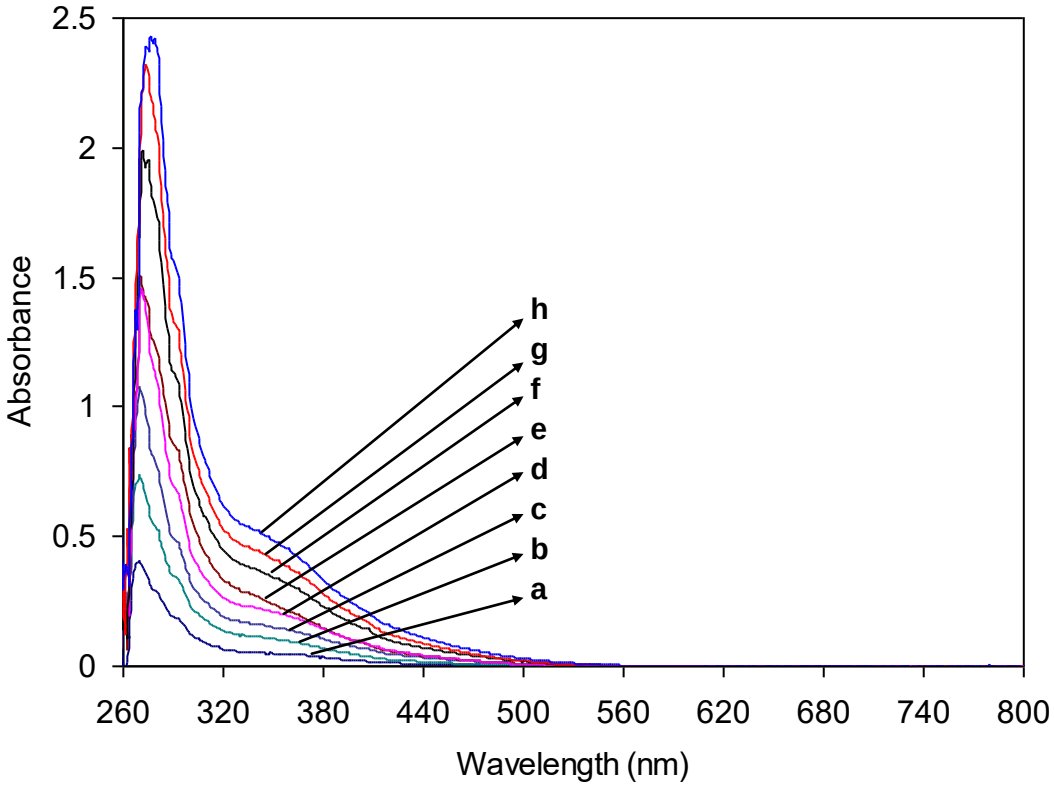

Figure 4.8 UV-Vis spectrum of *Ganoderma lucidum* obtained by Soxhlet extraction at different concentrations; a) 166.60, b) 499.80, c) 833.00, d) 1166.20, e) 1499.40, f) 1999.20, g) 2499.00 and h) 3332.00 µg/mL

Table 4.9 UV-Vis data of *Ganoderma lucidum* extract obtained by Soxhlet extraction

Concentration (µg/mL)	ε (mL µg^{-1} cm^{-1})	λ_{max} Abs (nm)	In Abs
a) 166.60	2.26x10^{-3}	267	0.376
b) 499.80	1.45x10^{-3}	268	0.727
c) 833.00	1.30x10^{-3}	269	1.082
d) 1166.20	1.17x10^{-3}	270	1.367
e) 1499.40	1.00x10^{-3}	271	1.506
f) 1999.20	9.74x10^{-4}	272	1.947
g) 2499.00	9.30x10^{-4}	273	2.323
h) 3332.00	7.26x10^{-4}	276	2.418

λ_{max} Abs: maximum absorption wavelength, In Abs: maximum absorption intensity, ε: molar absorptivity coefficient

Figure 4.9 displays the UV-Vis spectra for *Ganoderma lucidum* extracted using sonication at varying concentrations. Utilizing methanol (CH_3OH) as a solvent, with a polarity index of 5.1, a distinct absorption at 277 nm is observed for this sonicated extract. This 277 nm absorption in the spectra is attributed to the π-π* transition within the chemical constituents of the extract. The single peak in the CH_3OH solution for the sonicated *Ganoderma lucidum* suggests a chemically pure extract. Additionally, the sonication-derived extract displays two pronounced shoulder peaks around 295 nm and 358 nm, besides its primary peak at 277 nm. A notable feature in the spectra of this sonicated extract is the augmented intensity of the π-π* transition peak with rising sample concentrations. Furthermore, a subtle shift towards longer absorption wavelengths (from 268 nm to 277 nm) was observed as concentration

increased, as evident in Figure 4.9. This behavior implies a minimal concentration influence on the peak absorption wavelengths. Table 4.10 summarizes the UV-Vis data for the sonication-extracted *Ganoderma lucidum*. Interestingly, the molar absorptivity values decreased with enhanced sample concentrations. This decrement suggests that increased sample concentrations might adversely affect the molar absorption efficiency of the specimen.

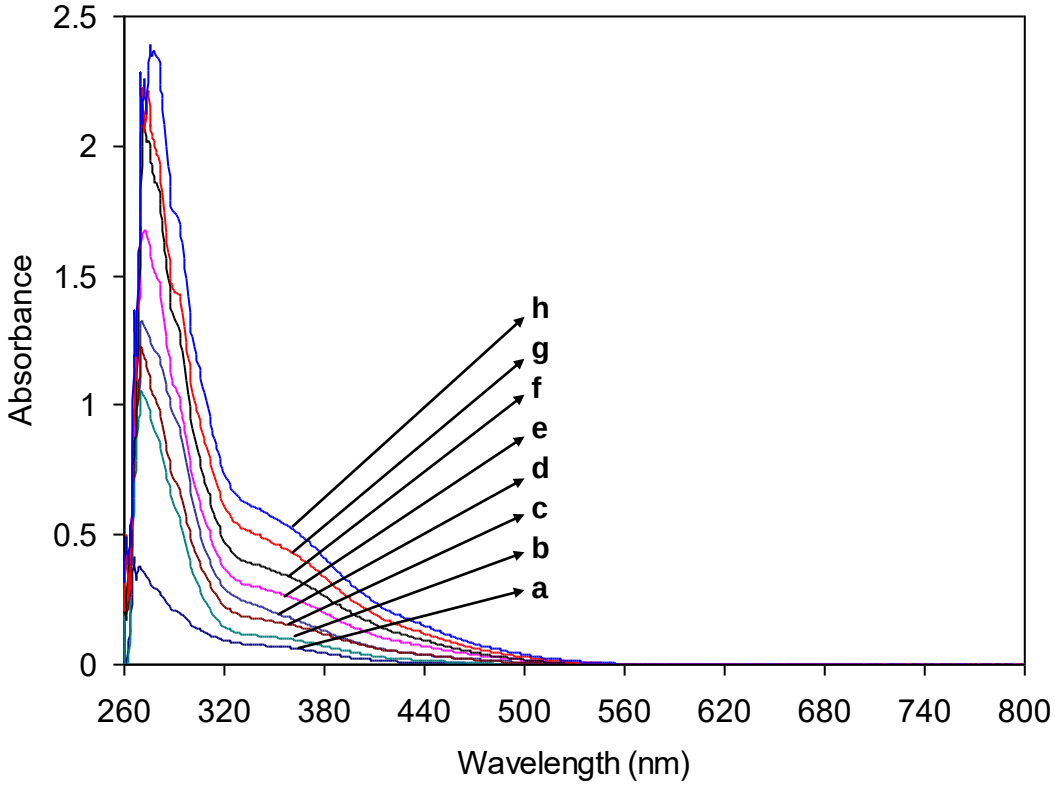

Figure 4.9 UV-Vis spectra of *Ganoderma lucidum* extract obtained by sonication extraction at different concentrations; a) 166.60, b) 499.80, c) 833.00, d) 1166.20, e) 1499.40, f) 1999.20, g) 2499.00 and h) 3332.00 µg/mL

Table 4.10 UV-Vis data of *Ganoderma lucidum* extract obtained by sonication extraction

Concentration (µg/mL)	ε (mL µg^{-1} cm^{-1})	λ_{max} Abs (nm)	In Abs
a) 166.60	2.27x10^{-3}	268	0.379
b) 499.80	2.13x10^{-3}	268	1.063
c) 833.00	1.48x10^{-3}	269	1.229
d) 1166.20	1.14x10^{-3}	269	1.334
e) 1499.40	1.12x10^{-3}	270	1.677
f) 1999.20	1.03x10^{-3}	271	2.051
g) 2499.00	8.86x10^{-4}	274	2.214
h) 3332.00	7.18x10^{-4}	277	2.393

λ_{max} Abs: maximum absorption wavelength, In Abs: maximum absorption intensity, ε: molar absorptivity coefficient

Figure 4.10 illustrates the UV-Vis spectra for the soap formulated from olive oil and coconut oil across various concentrations. Using methanol (CH_3OH) with a polarity index of 5.1, a noticeable absorption at 278 nm is evident for this combined soap. This absorption, noted at 278 nm in the spectra, is linked to the π-π* transition observed in the product's molecular constituents. The singular peak seen in the CH_3OH solution of the olive and coconut oil-based soap suggests the existence of distinct and pure product compounds. Furthermore, this soap displays an additional shoulder peak around 304 nm, accompanying its dominant peak at 278 nm. Reviewing the spectra of the soap, a consistent augmentation in the intensity of the π-π* transition peak corresponds with the escalating sample concentrations. There's also a minor transition towards extended absorption wavelengths moving from 275 nm to 278 nm correlating with the concentration increase, as visualized in Figure

4.10. These observations highlight a modest concentration-dependent impact on the peak absorption wavelengths of the product. The collected UV-Vis data for the soap derived from olive oil and coconut oil can be found in Table 4.11. As sample concentrations ascended, a decline in the molar absorptivity coefficient values was observed. This diminishing trend suggests that elevating the sample concentration might adversely influence the molar absorption potential of the product.

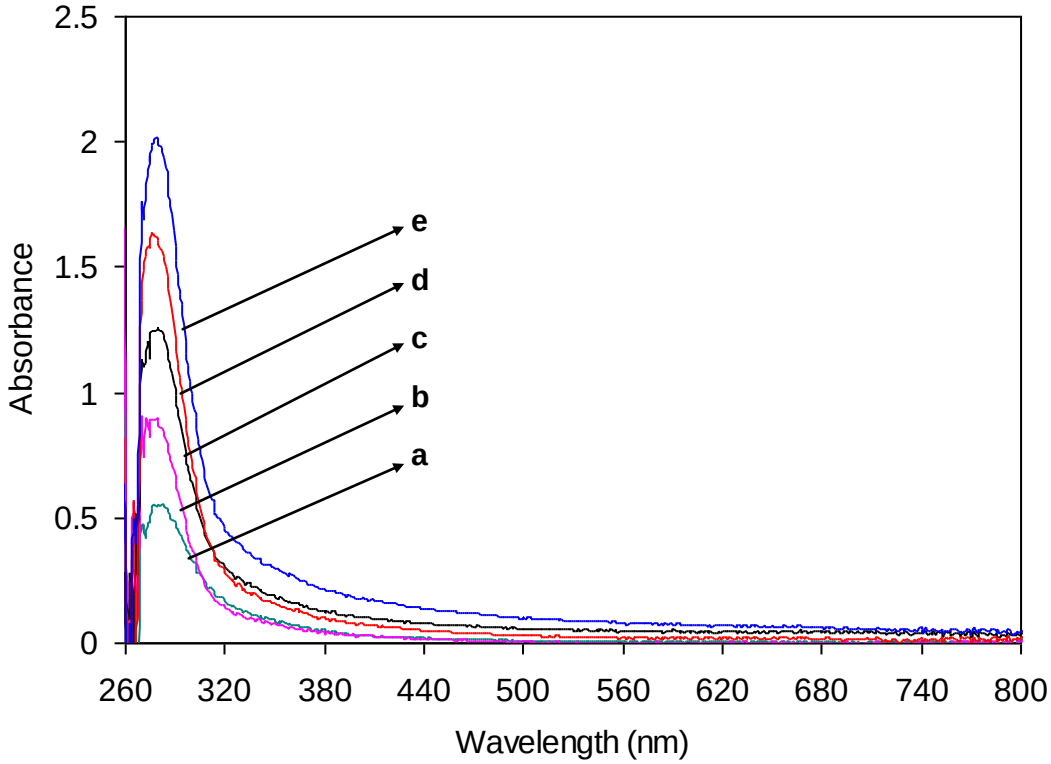

Figure 4.10 UV-Vis spectra of soap prepared from olive oil and coconut oil at different concentrations; a) 3.33, b) 6.67, c) 10.00, d) 13.33 and e) 16.67 mg/mL

Table 4.11 UV-Vis data of soap prepared from olive oil and coconut oil

Concentration (mg/mL)	ε (mL mg^{-1} cm^{-1})	λ_{max} Abs (nm)	In Abs
a) 3.33	$1.66x10^{-1}$	275	0.553
b) 6.67	$1.34x10^{-1}$	276	0.892
c) 10.00	$1.25x10^{-1}$	277	1.247
d) 13.33	$1.22x10^{-1}$	277	1.633
e) 16.67	$1.19x10^{-1}$	278	1.982

λ_{max} Abs: maximum absorption wavelength, In Abs: maximum absorption intensity, ε: molar absorptivity coefficient

The UV-Vis spectra for the soap derived from a blend of olive oil, coconut oil, and *Ganoderma lucidum* across different concentrations is depicted in Figure 4.11. Utilizing methanol (CH_3OH) as a solvent, boasting a 5.1 polarity index, an absorption peak at 281 nm is discernible for this composite soap. This 281 nm absorption in the spectra signifies the π-π* transition in the molecular structures of the product. The pronounced singular peak within the CH_3OH solution of this tri-component soap confirms the purity of its chemical composition. Moreover, the soap formulation that incorporates olive oil, coconut oil, and *Ganoderma lucidum* exhibits a pair of shoulder peaks around 296 nm and 342 nm, accompanying its primary absorption at 281 nm. Evaluating the spectra for this mixed soap formulation, an expected rise in the intensity of the π-π* transition peak aligns with the increasing concentrations of the sample. Additionally, a noteworthy shift in peak absorption wavelengths was observed, transitioning from 269 nm up to 281 nm, in tandem with increasing concentrations, as illustrated in Figure 4.11. This shift underscores the pronounced impact sample concentrations exert on the soap's peak absorption wavelengths. A comprehensive compilation of UV-Vis data pertaining to the soap synthesized from olive oil, coconut oil, and *Ganoderma lucidum* is presented in Table 4.12. A trend was observed wherein the molar absorptivity coefficients waned

as sample concentrations surged. This diminishing pattern underscores the potential adverse ramifications of heightened sample concentrations on the molar absorption efficacy of the soap.

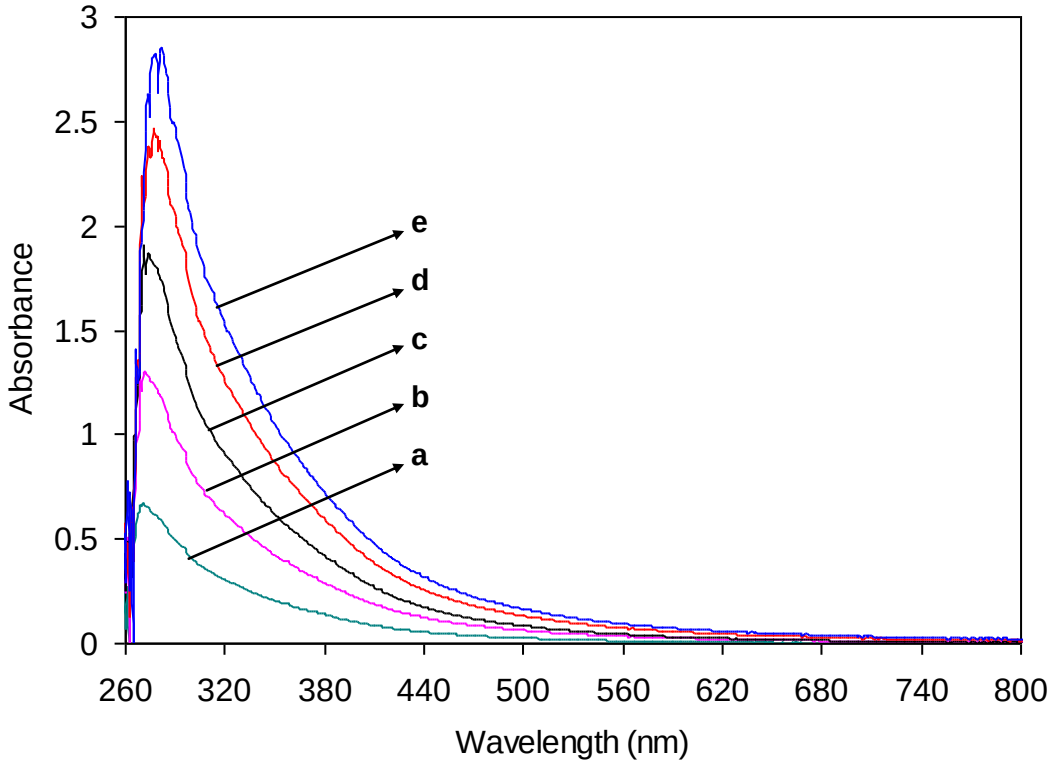

Figure 4.11 UV-Vis spectra of soap prepared from olive oil, coconut oil and *Ganoderma lucidum* extract at different concentrations; a) 4, b) 8, c) 12, d) 16 and e) 20 mg/mL

Table 4.12 UV-Vis data of soap prepared from olive oil, coconut oil and *Ganoderma lucidum* extract

Concentration (mg/mL)	**ε (mL mg^{-1} cm^{-1})**	**λ_{max} Abs (nm)**	**In Abs**
a) 4	1.66x10^{-1}	269	0.662
b) 8	1.60x10^{-1}	271	1.281
c) 12	1.56x10^{-1}	274	1.871
d) 16	1.51x10^{-1}	278	2.423
e) 20	1.41x10^{-1}	281	2.825

λ_{max} Abs: maximum absorption wavelength, In Abs: maximum absorption intensity, ε: molar absorptivity coefficient

The UV-Vis spectra of vitamin C, used as a reference standard, at various concentrations is presented in Figure 4.12. When dissolved in methanol (CH_3OH), having a polarity index of 5.1, a distinct peak emerges at 271 nm for standard Vitamin C. This absorption at 271 nm is tied to the π-π* transition found within Vitamin C's molecular framework. The singular pronounced peak in the CH_3OH solution indicates the pure and consistent composition of vitamin C. As one interprets the spectra, it's clear that as the concentration of Vitamin C increases, the intensity of the π-π* transition peak also elevates. Concurrently, there's an observable shift in the peak from an initial 268 nm to 271 nm with increasing concentration, as highlighted in Figure 4.12. Such findings suggest that the concentration has a subtle influence on the dominant absorption wavelengths. The UV-Vis analytical data for vitamin C is collated in Table 4.13. There's a noted decline in the molar absorptivity coefficient as sample concentrations rise, indicating that increased concentrations diminish the molecule's absorbance efficacy.

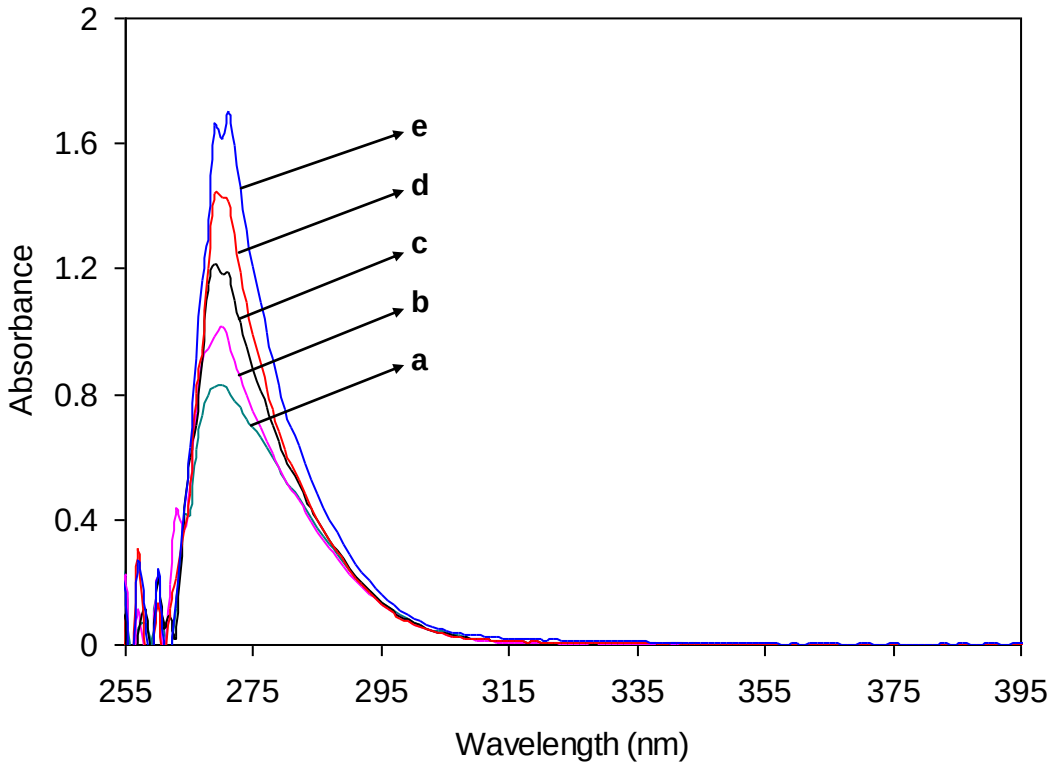

Figure 4.12 UV-Vis spectra of vitamin C as a standard at different concentrations; a) 92.61, b) 185.22, c) 277.83, d) 370.44 and e) 463.06 µg/mL

Table 4.13 UV-Vis data of vitamin C used as a standard

Concentration (µg/mL)	**ε (mL µg^{-1} cm^{-1})**	**λ_{max} Abs (nm)**	**In Abs**
a) 92.61	8.89x10^{-3}	268	0.823
b) 185.22	5.47x10^{-3}	269	1.013
c) 277.83	4.37x10^{-3}	270	1.215
d) 370.44	3.88x10^{-3}	270	1.437
e) 463.06	3.67x10^{-3}	271	1.701

λ_{max} Abs: maximum absorption wavelength, In Abs: maximum absorption intensity, ε: molar absorptivity coefficient.

4.7 Photoluminescence Spectrometer (PL) Measurements

Photoluminescence is a vital technique frequently employed in the field of medical science. The photophysical properties of the extracts and soaps produced in this study were analyzed to explore their potential applications in medical imaging and other healthcare-related uses. The absorption and photoluminescence spectral analyses were conducted for the *Ganoderma lucidum* obtained by Soxhlet extraction (a), *Ganoderma lucidum* obtained by sonication extraction (b), soap derived from olive oil and coconut oil (c) and soap prepared from olive oil, coconut oil and *Ganoderma lucidum* (d) solutions, excited at 256 nm. A notable observation in this reasearch was the extracts of *Ganoderma lucidum* exhibited strong photoluminescent emission, whereas the soap formulated from these extracts displayed weak emission when exposed to ultraviolet (UV) light. The photoluminescence spectra of the *Ganoderma lucidum* obtained by Soxhlet extraction (a), *Ganoderma lucidum* obtained by sonication extraction (b), soap manufactured from olive oil and coconut oil (c) and soap derived from olive oil, coconut oil and *Ganoderma lucidum* (d) in spectrophotometric grade methanol (CH_3OH) is represented in Figure 4.13. In the analysis of *Ganoderma lucidum* sourced through Soxhlet extraction (a), there was a distinct luminescence peak detected at 368 nm with a full width at half maximum (FWHM) of 104 nm. This extract (a) manifested a photoluminescence quantum yield of 38% and an excited-state lifetime of 3.55 ns. Conversely, when the *Ganoderma lucidum* was procured *via* sonication extraction (b), the luminescent intensity peak was notably strong at 371 nm, having an FWHM of 105 nm. This sonication-derived sample (b) registered a photoluminescence quantum yield of 39% and an excited-state duration of 3.62 ns. For the soap developed from a combination of olive oil and coconut oil, there was a muted luminescence peak at 363 nm, with an FWHM measuring 102 nm (c). This particular soap (c) displayed a subdued photoluminescence quantum yield of 11%, with its excited state duration recorded at 1.02 ns. In contrast, the soap synthesized with olive oil, coconut oil, and *Ganoderma lucidum* (d) registered a luminescence peak at 365 nm and an FWHM of 101 nm. This specialized soap (d) yielded a photoluminescence quantum efficiency of 22% and had an excited-state longevity of 2.07 ns. Comparing the two, the photoluminescence peak intensity and quantum efficiency of the soap prepared by olive oil, coconut oil, and *Ganoderma lucidum* (d) were markedly diminished

relative to the pure *Ganoderma lucidum* extracts. This decline can be attributed to the soap formation process. Additionally, the inception of the soap products prompted a diminution in the prominence of primary peaks and a shift towards reduced emission wavelengths, transitioning from 371 nm down to 365 nm. The reduction in quantum yield is due to the existence of less amount of extract as compared to the total amount of the soap product. Also, the formation of soap products and the other compounds exist in soap product caused/led photoluminescence quenching of the extracts. Therefore, the fluorescence emission intensity of the soap made from olive oil, coconut oil and *Ganoderma lucidum* (d) decreases with the formation of the soap products. This results in a reduction of the non-radiative transitions in the excited state of the soap product, subsequently causing a diminished fluorescence emission.

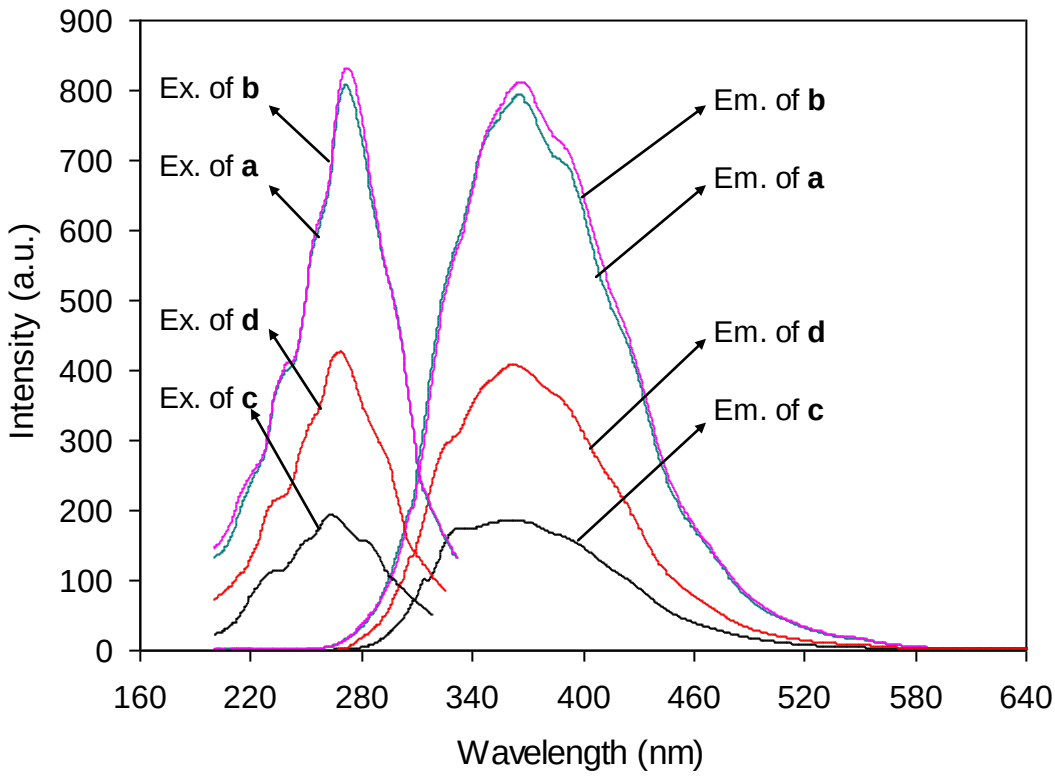

Figure 4.13 Photoluminescence spectra of the *Ganoderma lucidum* extract obtained by Soxhlet extraction (a), *Ganoderma lucidum* obtained by sonication extraction (b), soap prepared from olive oil and coconut oil (c) and soap prepared from olive oil, coconut oil and *Ganoderma lucidum* (d) in spectrophotometric grade methanol (CH_3OH); samples were excited at 256 nm

The fluorescence characteristics of *Ganoderma lucidum* extracts were investigated across various excitation wavelengths. The data revealed that the fluorescence traits

were not contingent on the excitation wavelength, confirming that the emissions originate from the lowest vibrational level of the initial electronic state, consistent with Kasha's rule of excitation wavelength independence. For instance, emission spectra for *Ganoderma lucidum* acquired through sonication extraction in methanol at diverse excitation (b) wavelengths are illustrated in Figure 4.14. The collected photoluminescence metrics for Soxhlet-extracted *Ganoderma lucidum* (a), sonication-extracted *Ganoderma lucidum* (b), and soaps made from both olive oil and coconut oil alone (c), as well as those incorporating *Ganoderma lucidum* (d), are consolidated in Table 4.14. These photophysical properties suggest a wide array of potential applications in both photophysical and medical sectors. The table also presents the Stoke's shift values (ν_{ss}) for each sample. The emission maximum (λ_{max}) for sonication-extracted *Ganoderma lucidum* (b) is at 371 nm with a corresponding Stoke's shift (ν_{ss}) of ~4128 cm^{-1} (96 nm). In contrast, the soap made from olive oil, coconut oil, and *Ganoderma lucidum* (d) registers an emission maximum λ_{max} at 365 nm, accompanied by a Stoke's shift (ν_{ss}) of ~4021 cm^{-1} (94 nm). These substantial Stoke's shift values are ascribed to the emergence of intermolecular excimers and indicate structural relaxation in the excited molecules, suggesting changes in molecular conformation upon excitation. Moreover, the Stoke's shift values across the various extracts and soap formulations were found to be notably consistent, underscoring that they are not dependent on the compound structure. Finally, the full widths at half maximum (FWHM) for the sonication-extracted *Ganoderma lucidum* (b) (105 nm) and the composite soap (d) (101 nm) were closely related [114].

Table 4.14 Photoluminescence data for the *Ganoderma lucidum* extract obtained by Soxhlet extraction (a), *Ganoderma lucidum* obtained by sonication extraction (b), soap prepared from olive oil and coconut oil (c) and soap prepared from olive oil, coconut oil and *Ganoderma lucidum* (d)

Compound	λ_{max} Ex (nm)	In Ex	λ_{max} Em (nm)	In Em	ϕ_f (%)	τ_f (ns)	ν_{ss} (cm^{-1})
a	274 (237;254;298)	796	368 (329;394;427)	787	38	3.55	4042
b	275 (238;255;299)	819	371 (330;396;428)	808	39	3.62	4128
c	266 (235;253;287)	191	363 (318;334;401)	186	11	1.02	4171
d	271 (236;255;296)	414	365 (328;390;421)	407	22	2.07	4021

λ_{max} Ex: maximum excitation wavelength; In Ex: maximum excitation intensity.
λ_{max} Em: maximum emission wavelength; In Em: maximum emission intensity.
ϕ_f : quantum yield; τ_f : excited-state lifetime; ν_{ss}: Stoke shift.

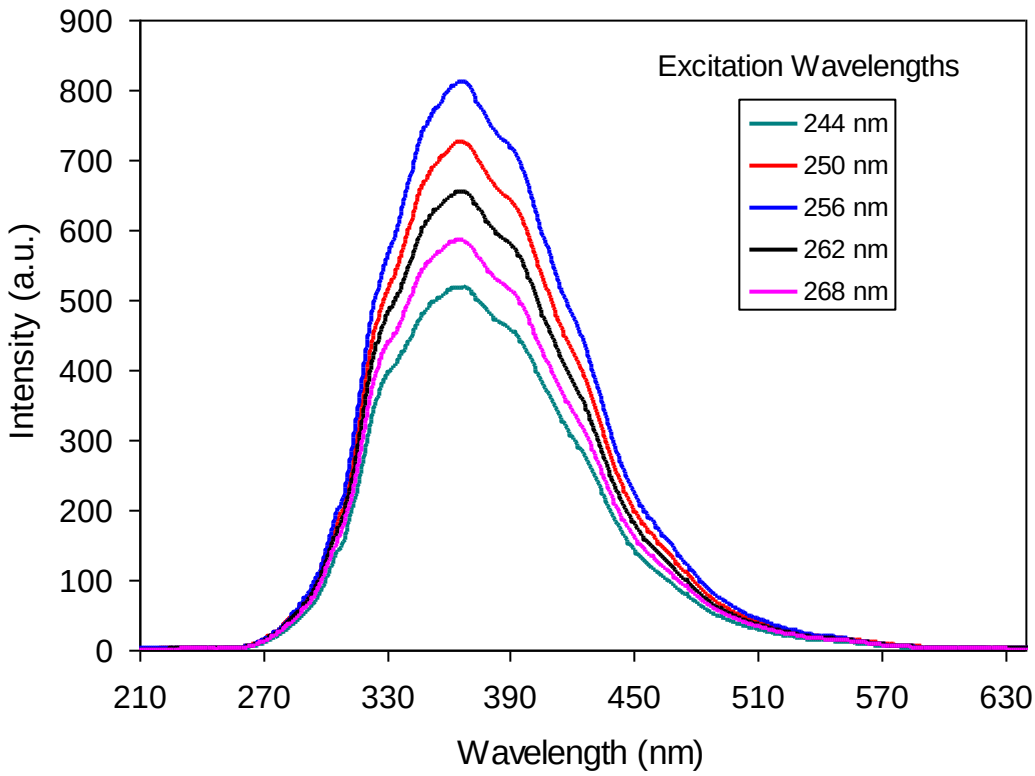

Figure 4.14 Emission spectra of *Ganoderma lucidum* extract obtained by sonication extraction (b) in spectrophotometric grade methanol (CH_3OH) (c = 3332.00 µg/mL) at different excited wavelengths

4.8 Antioxidant Properties

To determine the radical-neutralizing potential of *Ganoderma lucidum*, extracted *via* the Soxhlet method (Sample d), *Ganoderma lucidum* obtained by sonication extraction (Sample c), soap made from olive oil and coconut oil (Sample b), soap made from olive oil, coconut oil and *Ganoderma lucidum* (Sample a) and the ascorbic acid (vitamin C) as a standard, the DPPH assay was performed. In the DPPH assay, at the concentration of 166.60, 499.80, 833.00, 1166.20, 1499.40, 1999.20, 2499.00, and 3332.00 µg/mL, the *Ganoderma lucidum* obtained by Soxhlet extraction (Sample d) displayed the proportion of antioxidant effectiveness (Figure 4.15). The *Ganoderma lucidum* obtained by Soxhlet extraction (Sample d) displayed antioxidant activity ranging from 14.36 ±1.09% to 92.01 ±1.04%, which means that at the lowest concentration, Sample d neutralized approximately 14.36% of the DPPH radicals, and at the highest concentration (3332.00 µg/mL), it neutralized approximately 92.01% of the DPPH radicals. The highest antioxidant effectiveness of the *Ganoderma lucidum* obtained by Soxhlet extraction (Sample d) was detected at a concentration of 3332.00 µg/mL. The IC_{50} value [114] of the *Ganoderma lucidum* obtained by Soxhlet extraction (Sample d), obtained from regression analysis was 1390.25 ± 3.23 µg/mL (Figure 4.15).

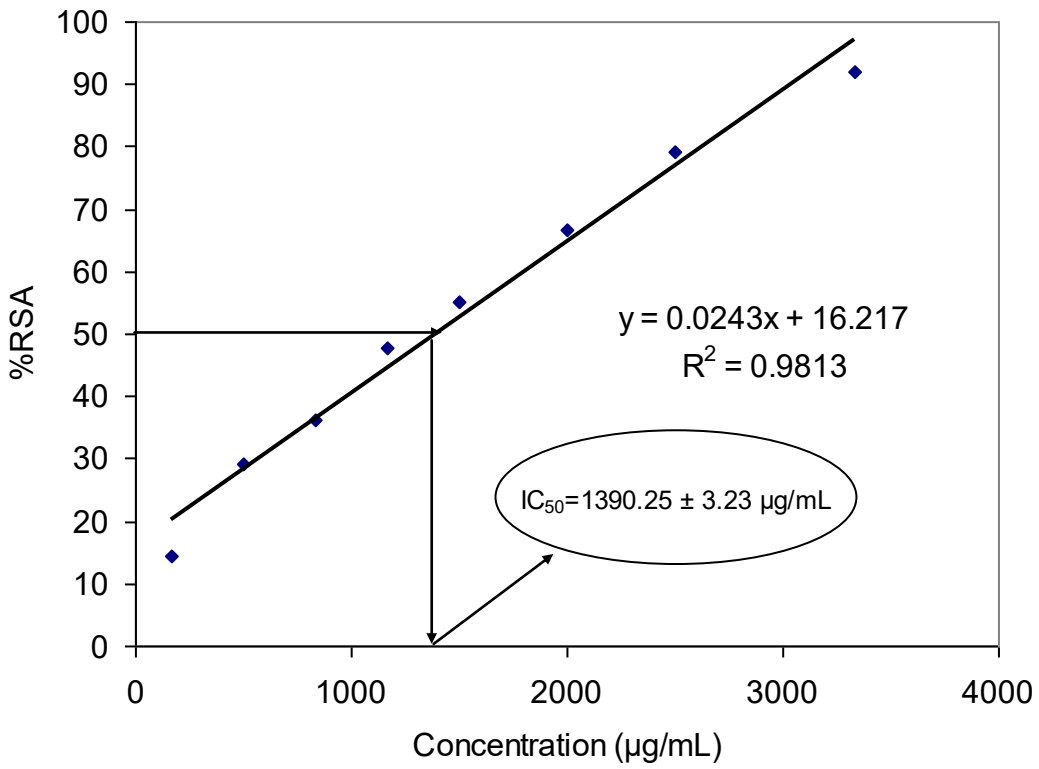

Figure 4.15 The antioxidant potential, as determined by the radical scavenging capacity of *Ganoderma lucidum* extract procured through Soxhlet extraction at varying concentrations, was quantified in terms of percentage activity of 166.60, 499.80, 833.00, 1166.20, 1499.40, 1999.20, 2499.00 and 3332.00 µg/ mL. Results are presented as the mean ±SD from three separate trials

In the present research, the evolution of antioxidant activity for *Ganoderma lucidum*, extracted using the Soxhlet method at varied concentrations, was observed using UV-Vis spectroscopy. As shown in Figure 4.16, the spectrum labeled 'a' represents the pure DPPH solution. Using a methanol (CH_3OH) solvent with a polarity index of 5.1, two distinct absorption peaks emerge at 330 nm and 516 nm for the DPPH solution. The 516 nm absorption is attributed to the stable violet DPPH (2, 2-diphenyl-1-picryl-hydrazyl) radical form, while the 330 nm absorption is associated with its yellowish reduced counterpart (DPPH/H+). Consequently, the two peaks observed in the methanolic solution of the Soxhlet-extracted *Ganoderma lucidum* suggest the coexistence of two chemically distinct oxidative structures of DPPH: the radical form and its reduced version. [115]. As illustrated in Figure 4.16, spectra b-k shows the interaction of the *Ganoderma lucidum* obtained through Soxhlet extraction at varying concentrations, with the DPPH solution. A noticeable transformation of

the stable violet DPPH (2, 2- diphenyl-1-picryl-hydrazyl) radical to its yellowish reduced variant (DPPH/H+) is evident across these spectra. Observing the DPPH solution spectra, there's an apparent decline in the intensity of the 516 nm peak coupled with an increase in the 330 nm peak's intensity as the sample concentrations elevate. Such spectral observations confirm the consistent transition of the stable violet DPPH radical to its yellowish reduced state (DPPH/H+). Additionally, a rise in the intensity of the π-π^* transition peak at 276 nm, attributed to the Soxhlet-extracted *Ganoderma lucidum*, is evident with increasing sample concentrations. Figure 4.17 shows the interaction between *Ganoderma lucidum* extracted via the Soxhlet method and the DPPH solution. This interaction is showcased across a concentration gradient, starting from 166.60 µg/mL and culminating at 3332.00 µg/mL.

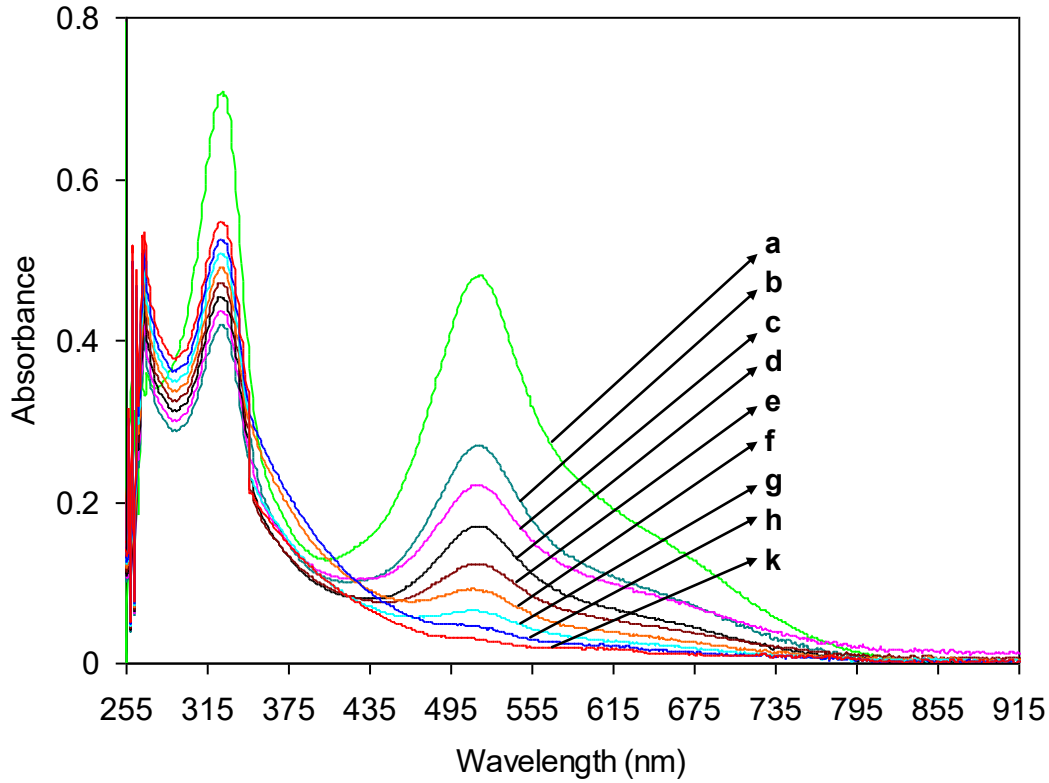

Figure 4.16 The UV-Vis spectral progress of antioxidant activity of the *Ganoderma lucidum* extract obtained by Soxhlet extraction at different concentrations of 166.60, 499.80, 833.00, 1166.20, 1499.40, 1999.20, 2499.00 and 3332.00 µg/mL. Spectrum a) represents pure DPPH solution. Spectra b-k) represent the reaction of the *Ganoderma lucidum* obtained by Soxhlet extraction at different concentrations with DPPH solution

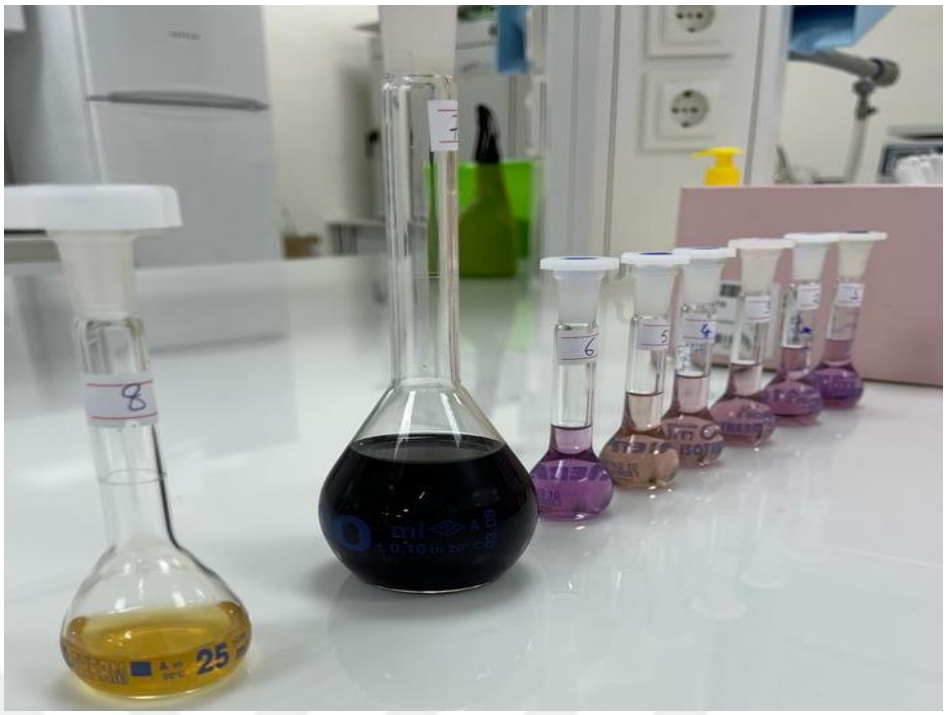

Figure 4.17 Reaction of the *Ganoderma lucidum* extract obtained by Soxhlet extraction at different concentrations with DPPH solution of 166.60, 499.80, 833.00, 1166.20, 1499.40, 1999.20, 2499.00 and 3332.00 µg/mL

To determine the ability of *Ganoderma lucidum*, extracted via sonication, to neutralize free radicals (Sample c), the DPPH assay was performed. In DPPH assay, at concentration of 166.60, 499.80, 833.00, 1166.20, 1499.40, 1999.20, 2499.00 and 3332.00 µg/mL, the *Ganoderma lucidum* obtained by sonication extraction (Sample c) indicated the proportion of antioxidant efficacy (Figure 4.18). the extract obtained by Sonication extraction (Sample c) displayed antioxidant activity ranging from 13.83 ±1.08% to 93.32 ±1.05%, which means that at the lowest concentration tested, Sample c neutralized approximately 13.83% of the DPPH radicals, and at the most elevated concentration (3332.00 µg/mL). The highest antioxidant activity of the *Ganoderma lucidum* obtained by sonication extraction (Sample c) was observed at a concentration of 3332.00 µg/mL. The IC_{50} value [93] of the *Ganoderma lucidum* obtained by sonication extraction (Sample c), obtained from regression analysis, was 1370.16 ± 3.14 µg/mL (Figure 4.18).

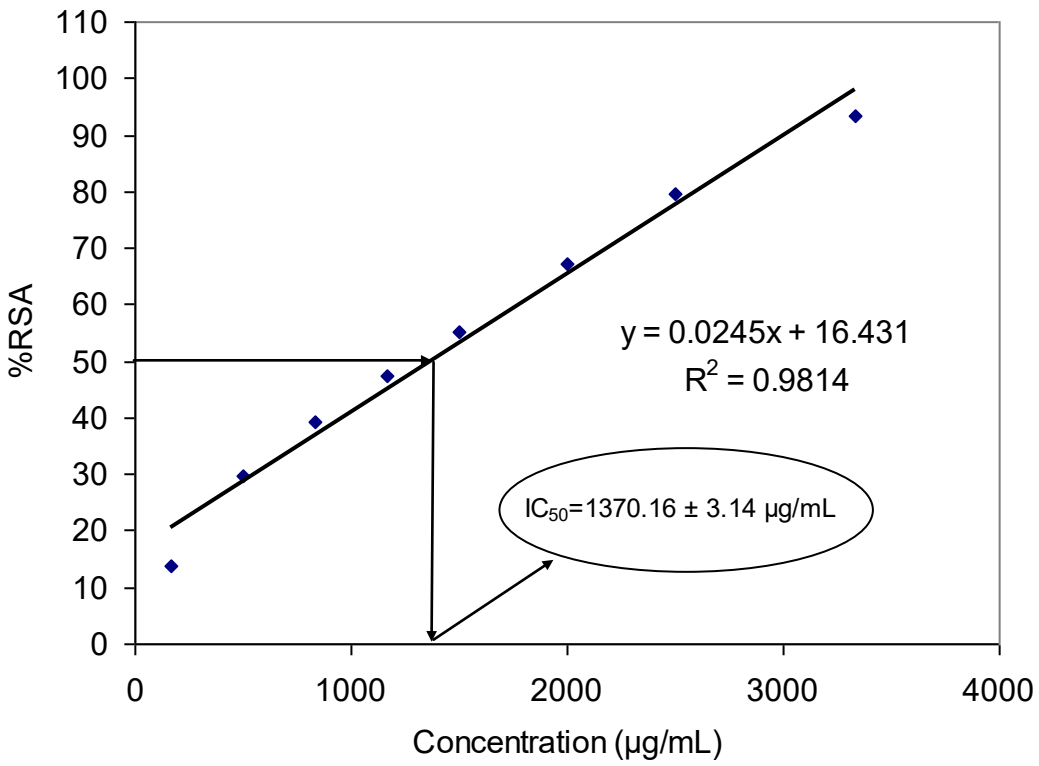

Figure 4.18 The antioxidant potential, as determined by the radical scavenging capacity of *Ganoderma lucidum* extract procured through sonication extraction at varying concentrations, was quantified in terms of percentage activity of 166.60, 499.80, 833.00, 1166.20, 1499.40, 1999.20, 2499.00 and 3332.00 µg/mL. Results are presented as the mean ±SD from three separate trials

In the current research, the evolution of antioxidant properties in *Ganoderma lucidum*, extracted *via* the Sonication method across varied concentrations, was analyzed using UV-Vis spectroscopy. Figure 4.19 illustrates the UV-Vis spectral progress of the antioxidant activity for *Ganoderma lucidum* sourced through sonication extraction at these different concentrations. In Figure 4.19, spectrum a represents pure DPPH solution, and spectra b-k represent the reaction of the *Ganoderma lucidum* obtained by sonication extraction at different concentrations with DPPH solution. The transformation of the stable violet DPPH radical to its yellowish reduced variant (DPPH/H+) was distinctly noted [115]. In the spectral analysis of the DPPH solution, a noticeable decline in the intensity of the peak at 516 nm is evident, alongside an increase in the 330 nm peak intensity, correlating with rising sample concentrations. These spectral observations suggest a pronounced transition from the stable violet DPPH radical to its yellowish reduced variant (DPPH/H+). Furthermore, the spectrum reveals that the intensity of the π-π^*

transition peak at 277 nm, attributed to *Ganoderma lucidum* acquired via sonication extraction, progressively amplified with increasing sample concentrations. In Figure 4.20, the interaction of *Ganoderma lucidum* extracted through the sonication method, with the DPPH solution is presented. The analysis spans various concentrations, from 166.60 µg/mL stretching up to 3332.00 µg/mL.

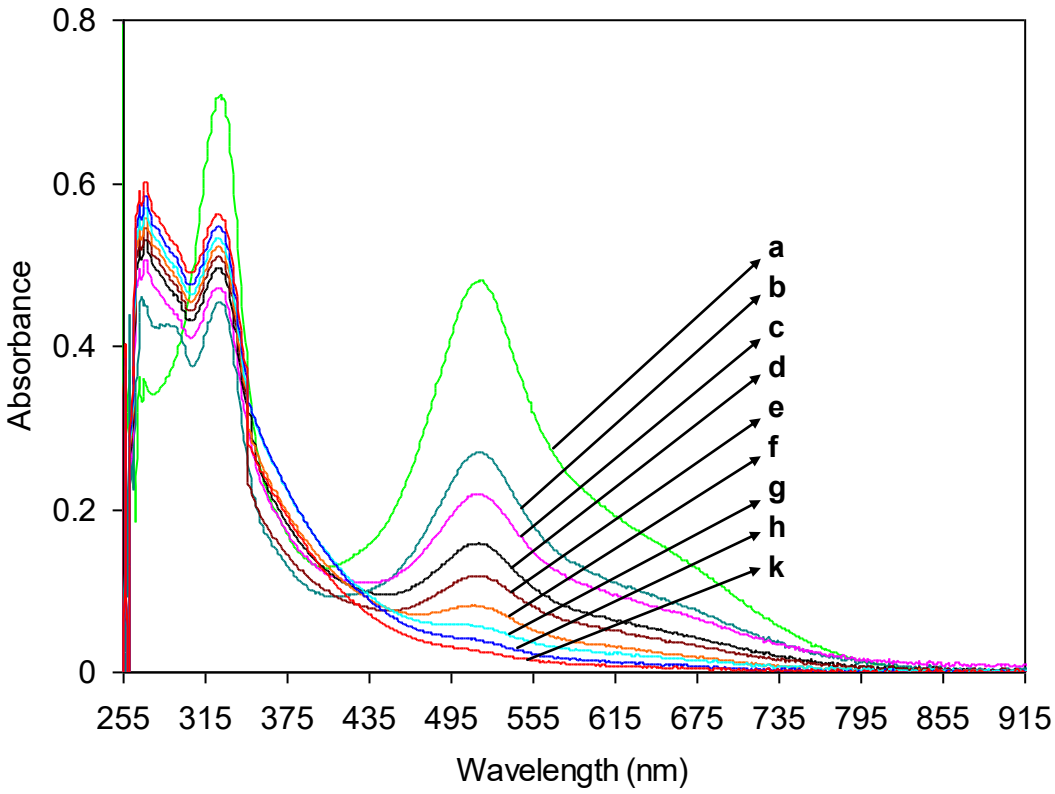

Figure 4.19 The UV-Vis spectral progress of antioxidant activity of the *Ganoderma lucidum* extract obtained by sonication extraction at different concentrations of 166.60, 499.80, 833.00, 1166.20, 1499.40, 1999.20, 2499.00 and 3332.00 µg/mL. Spectrum a) represents pure DPPH solution. Spectra b-k) represents the reaction of the *Ganoderma lucidum* obtained by sonication extraction at different concentrations with DPPH solution

Figure 4.20 Raction of the *Ganoderma lucidum* extract obtained by sonication extraction at different concentrations with DPPH solution of 166.60, 499.80, 833.00, 1166.20, 1499.40, 1999.20, 2499.00 and 3332.00 µg/mL

To determine the ability of soap made from olive oil and coconut oil , to neutralize free radicals (Sample b), the DPPH assay was performed. In the DPPH assay, at the concentration of 3.33, 6.67, 10.00, 13.33, and 16,67 mg/mL, the soap manufactured from olive oil and coconut oil (Sample b) showed a very low percentage of anti-oxidant activity (Figure 4.21). The soap made from olive oil and coconut oil (Sample b) displayed anti-oxidant activity ranging from 9.10 ±1.27% to 19.09 ±1.23%. The highest anti-oxidant activity of the Soap prepared from olive oil and coconut oil (Sample b) observed at a concentration of 16.67 mg/mL. The IC_{50} value of the soap made from olive oil and coconut oil (Sample b), obtained from regression analysis, was 59.76 ± 1.25 mg/mL (Figure 4.21).

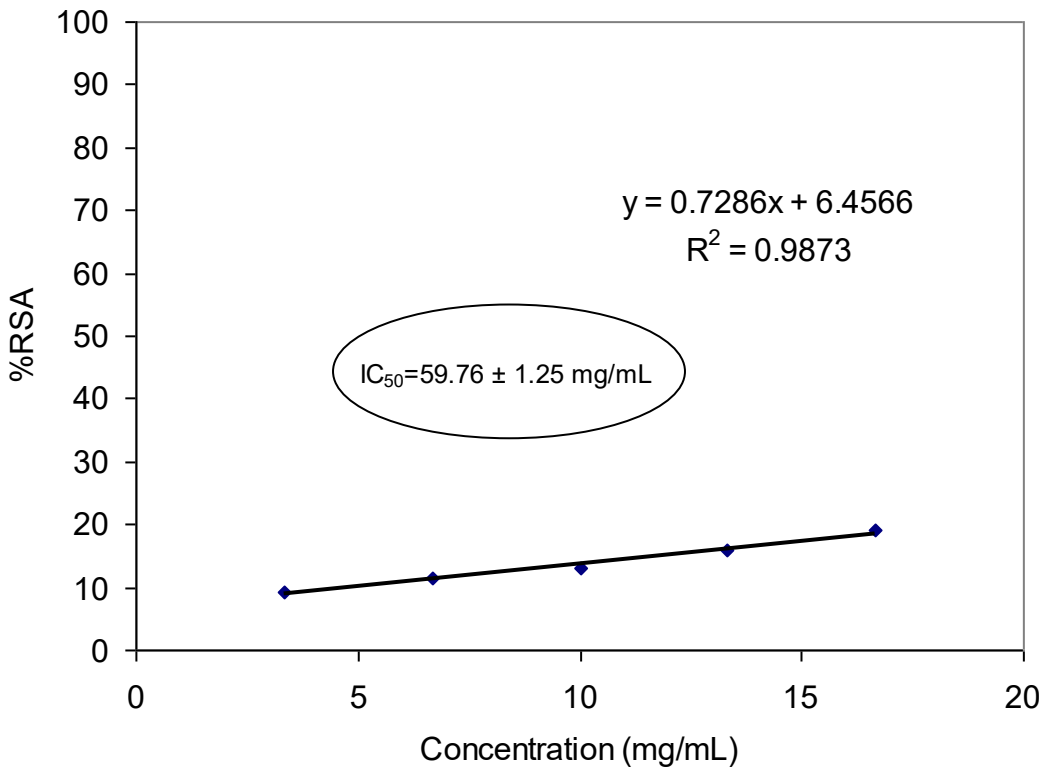

Figure 4.21 Antioxidant potential, as determined by the radical scavenging capacity of the soap made from olive oil and coconut oil at varying concentrations, of 3.33, 6.67, 10.00, 13.33 and 16.67 mg/mL. Results are presented as the mean ±SD from three separate trials

In the present research, we investigated the evolution of the antioxidant activity of soap formulated from olive oil and coconut oil across various concentrations using UV-Vis spectroscopy. The spectral data outlining this antioxidant progression for the soap can be found in Figure 4.22. Within this figure, the spectrum labeled as 'a' signifies the pure DPPH solution, while spectra b-f depict the interaction between varying concentrations of the olive and coconut oil soap and the DPPH solution. A notable transition from the stable violet DPPH radical to its yellowish reduced state (DPPH/H+) was observed. When examining the DPPH solution spectra, there's a minimal decline in the intensity of the peak at 516 nm and a slight augmentation at 330 nm as the soap concentration escalates. This implies only a minor transformation of the stable violet DPPH radical to its yellowish reduced variant (DPPH/H+). Additionally, the spectral data reveal an escalating intensity of the π-π^* transition peak at 278 nm, associated with the olive and coconut oil soap, in tandem with rising sample concentrations.

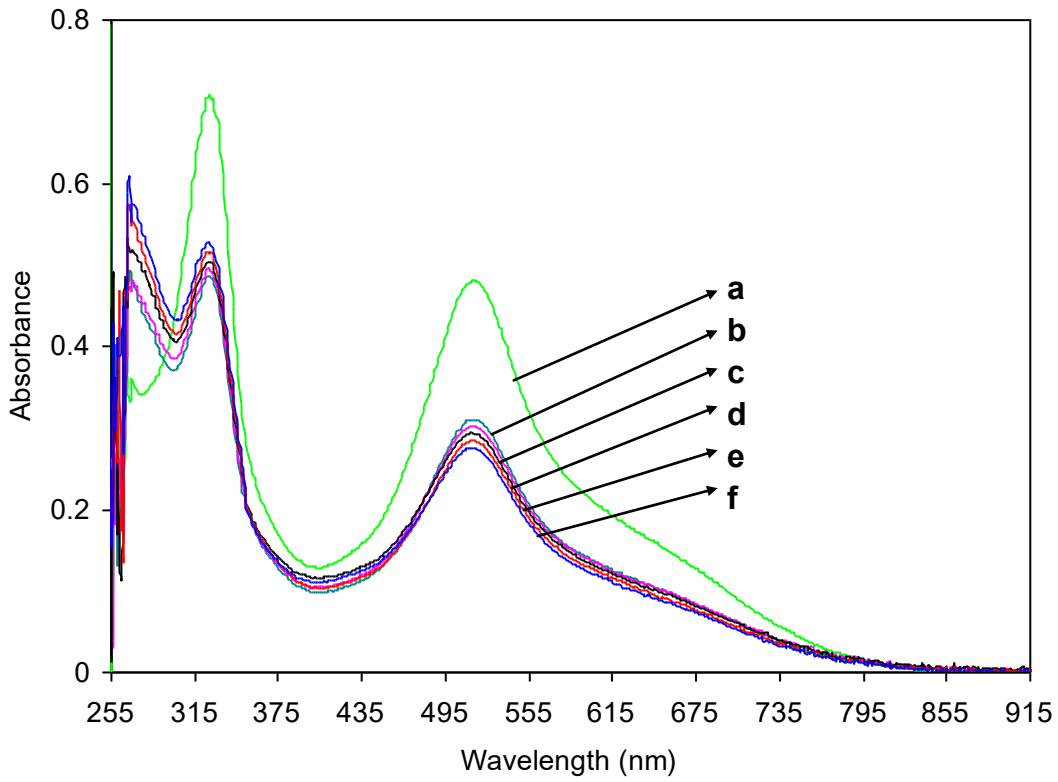

Figure 4.22 The UV-Vis spectral progress of antioxidant activity of the soap prepared from olive oil and coconut oil at different concentrations of 3.33, 6.67, 10.00, 13.33 and 16.67 mg/mL. Spectrum a) represents pure DPPH solution. Spectra b-f) represents the reaction of the soap prepared from olive oil and coconut oil at different concentrations with DPPH solution

To conclude the ability of soap made from olive oil and coconut oil and *Ganoderma lucidum*, to neutralize free radicals (Sample a), the DPPH assay was performed. In DPPH assay, at the series concentration of 4, 8, 12, 16 and 20 mg/mL, the soap made from olive oil, coconut oil, and *Ganoderma lucidum* (Sample a) indicated the proportion of antioxidant efficacy (Figure 4.23). The soap made from olive oil, coconut oil and *Ganoderma lucidum* (Sample a) displayed anti-oxidant activity ranging from 7.30 ±1.16% to 43.58 ±1.12%. The highest antioxidant activity of the soap dreived from olive oil, coconut oil and *Ganoderma lucidum* (Sample a) was observed at a concentration of 20 mg/mL. The IC_{50} value [93] of the soap manufactured from olive oil, coconut oil and *Ganoderma lucidum* (Sample a), obtained from regression analysis, was 22.73 ± 1.14 mg/mL (Figure 4.23).

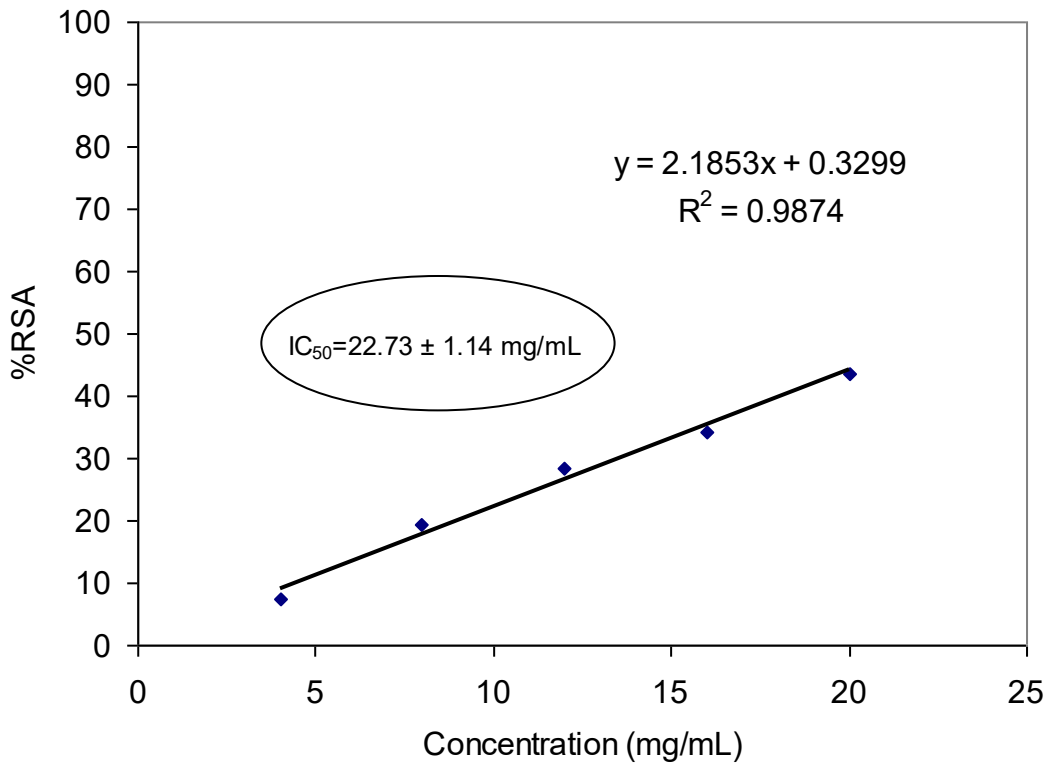

Figure 4.23 The antioxidant potential, as determined by the radical scavenging capacity of soap made from olive oil, coconut oil and *Ganoderma lucidum* extract at varying concentrations, was quantified in terms of percentage activity of 4, 8, 12, 16 and 20 mg/mL. Results are presented as the mean ±SD from three separate trials

In the current research, the antioxidant activity progression of soap formulated using olive oil, coconut oil, and *Ganoderma lucidum* at varying concentrations was assessed using UV-Vis spectroscopy. Figure 4.24 displays the UV-Vis spectral evolution associated with the antioxidant activity of this soap at different concentrations. Within Figure 4.24, the spectrum labeled 'a' corresponds to the pure DPPH solution, while spectra labeled 'b-f' depict the interaction between the soap, made from olive oil, coconut oil, and *Ganoderma lucidum* at varying concentrations, and the DPPH solution. A noticeable transformation of the violet-colored stable DPPH radical to its yellowish reduced counterpart (DPPH/H+) is evident. A close inspection of the DPPH solution spectra reveals a diminishing intensity of the peak at 516 nm coupled with a slight increase at 330 nm with rising sample concentrations. These spectral variations suggest a partial transformation of the violet DPPH radical to its yellow-reduced form (DPPH/H+). Furthermore, the spectra highlight a growing intensity of the π-π* transition peak at 281 nm, attributable to the soap formulated

from olive oil, coconut oil, and *Ganoderma lucidum*, with increasing sample concentrations.

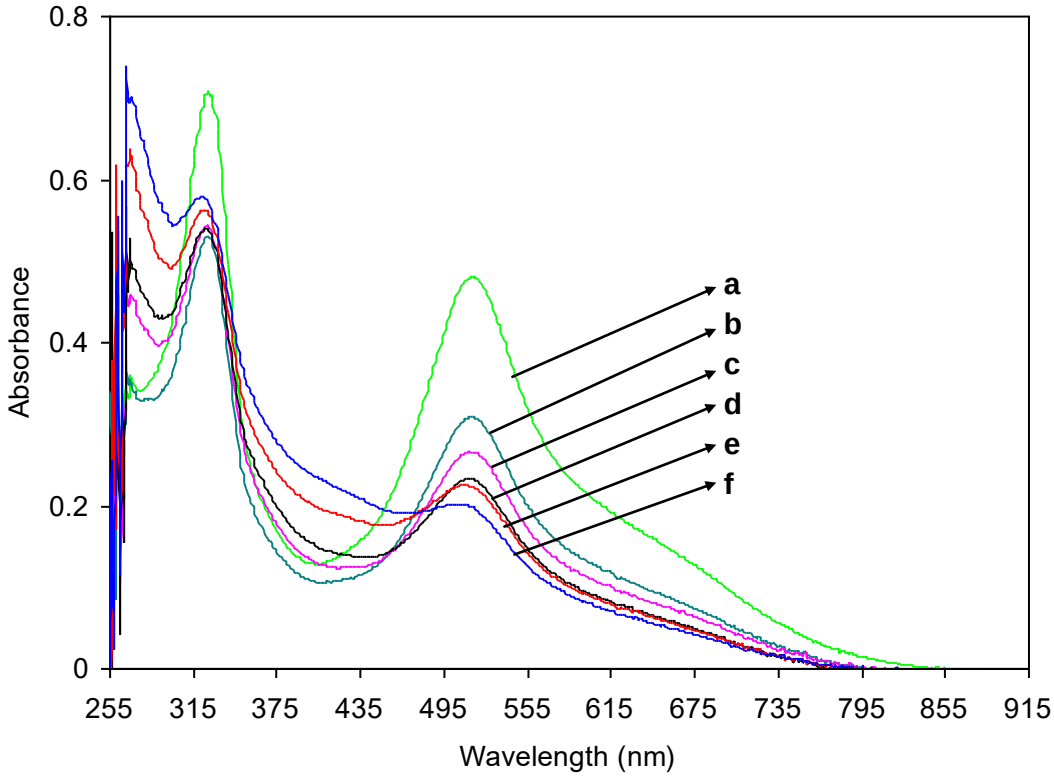

Figure 4.24 UV-Vis spectral progress of antioxidant activity of the soap prepared from olive oil, coconut oil and *Ganoderma lucidum* at different concentrations of 4, 8, 12, 16 and 20 mg/mL. Spectrum a) represents pure DPPH solution. Spectra b-f) represents the reaction of the soap prepared from olive oil, coconut oil and *Ganoderma lucidum* at different concentrations with DPPH solution

To conclude the ability of vitamin C to neutralize free radicals as a standard, the DPPH assay was performed. In the DPPH analysis, when considering the concentration of 92.61, 185.22, 277.83, 370.44, and 463.06 µg/mL, the ascorbic acid (vitamin C) showed a percentage of anti-oxidant activity at different concentrations which is shown in Figure 4.25. Ascorbic acid (vitamin C), used as a positive control (standard), displayed antioxidant activity ranging from 23.34 ±1.03% to 99.23 ±1.01%. Its peak antioxidant activity was noted at a concentration of 463.06 µg/mL. The IC_{50} value of the ascorbic acid (vitamin C), obtained from regression analysis, was 206.81 ± 1.12 µg/mL.

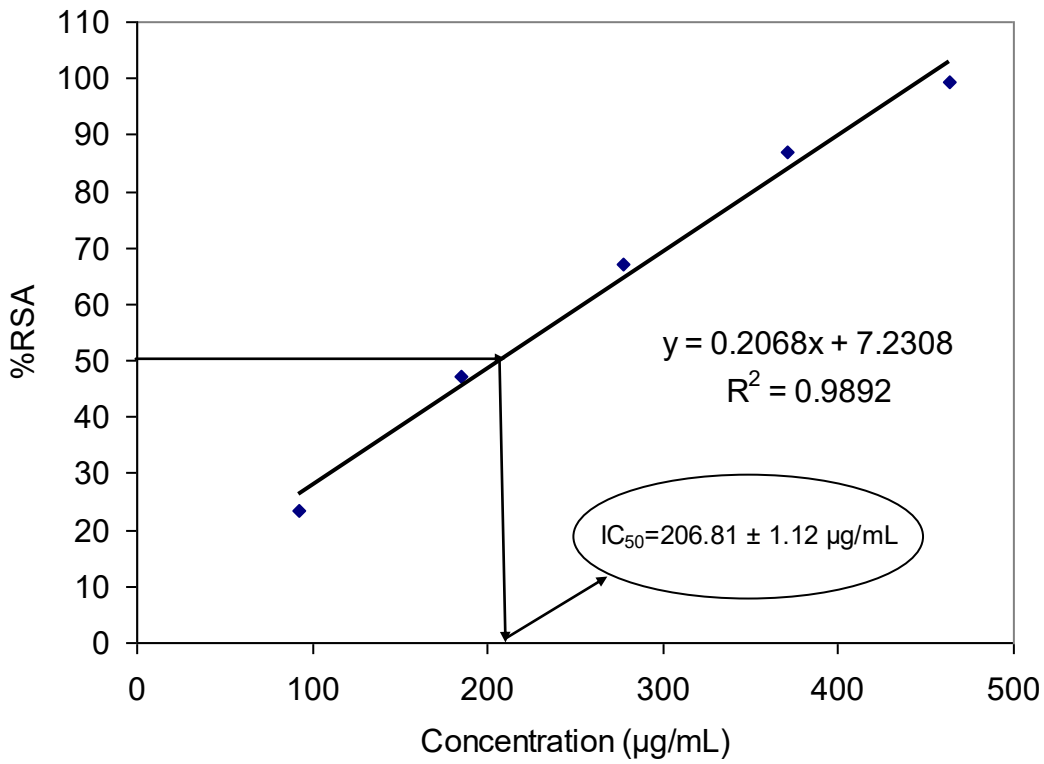

Figure 4.25 Antioxidant potential, as determined by the radical scavenging capacity of (vitamin C) at varying concentrations, was quantified in terms of percentage activity of 92.61, 185.22, 277.83, 370.44 and 463.06 µg/mL. Results are presented as the mean ±SD from three separate trials

This study utilized UV-Vis spectroscopy to monitor the antioxidant activity progression of ascorbic acid (vitamin C) at varying concentrations, with the results illustrated in Figure 4.26. Spectrum a delineates the pure DPPH solution, while spectra b-f detail the interactions between ascorbic acid at different concentrations and the DPPH solution. A notable transformation of the violet DPPH (2, 2-diphenyl-1-picryl-hydrazyl) radical into its yellowish reduced counterpart (DPPH/H+) was concurrently observed. An examination of the DPPH solution spectra revealed a decline in the peak's intensity at 516 nm, accompanied by an uptick at 330 nm as sample concentrations rose. These spectral findings confirm the evident shift of the violet DPPH radical to its yellowish reduced state (DPPH/H+). Additionally, the spectra showed a consistent increase in the intensity of the π-π* transition peak at 271 nm, attributed to ascorbic acid, corresponding with increasing sample concentrations.

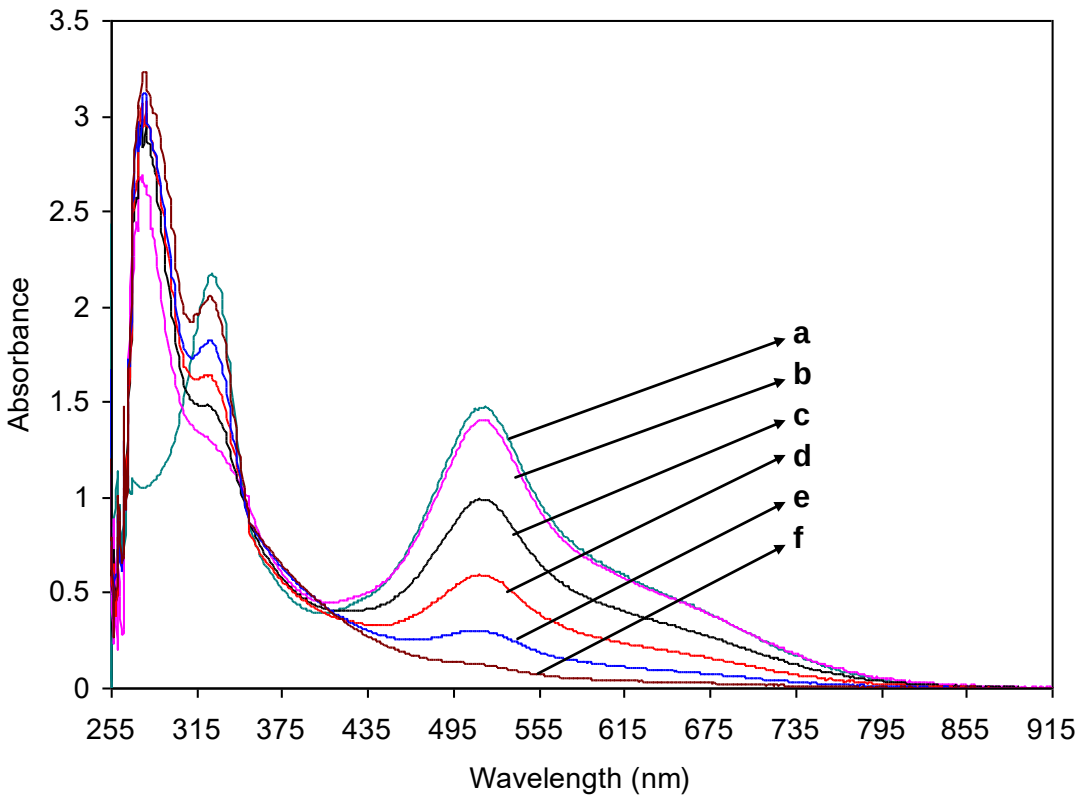

Figure 4.26 UV-Vis spectral progress of antioxidant activity of the ascorbic acid (vitamin C) as a standard at different concentrations of 92.61, 185.22, 277.83, 370.44 and 463.06 µg/mL. Spectrum a) represents pure DPPH solution. Spectra b-f) represents the reaction of the ascorbic acid (vitamin C) at different concentrations with DPPH solution

The present study evaluated the antioxidant potential of various samples using the DPPH scavenging assay. *Ganoderma lucidum* extracts, obtained through both Soxhlet (Sample d) and sonication (Sample c) methods, demonstrated high antioxidant activities, with IC_{50} values of 1390.25 ± 3.23 µg/mL and 1370.16 ± 3.14 µg/mL, and antioxidant activity percentages of 92.01 ±1.04% and 93.32 ±1.05%, respectively. A soap made from olive oil, coconut oil, and *Ganoderma lucidum* (Sample a) exhibited moderate antioxidant activity (22.73 ± 1.14 mg/mL and 43.58 ±1.12%), which is hypothesized to be due to its lower *Ganoderma lucidum* content and the introduction of new compounds during soap formation. In contrast, a soap formulated only from olive oil and coconut oil (Sample b) showed negligible antioxidant activity, which is attributed to its lack of *Ganoderma lucidum* content. The results underscore the traditional use of *Ganoderma lucidum* in Far Eastern medicine, where it has been used for treating various conditions, including cancer and immunological disorders, for thousands of years [116]. The researchers

discovered that the extract from *Ganoderma lucidum* emerged as the most efficacious antibacterial agent, outperforming the commercial strain, which displayed the least potency. Interestingly, the DPPH* scavenging activity from basidiocarps cultivated on alternative substrates surpassed that from commercially acquired basidiocarps. Notably, *Ganoderma lucidum* extracts showed enhanced cytotoxic activity relative to the commercial strain. The research also highlighted that fruiting bodies grown on wheat straw, an easily accessible and cost-effective agricultural byproduct, exhibited superior antimicrobial, antioxidant, and cytotoxic properties compared to those cultivated on the traditional oak sawdust substrate [117]. Table 4.15 provides the data on antioxidant activity, along with the linear correlation coefficients assessed based on the samples' ability to scavenge free radicals.

Table 4.15 Antioxidant activity data and the linear correlation coefficients evaluated by the free radical scavenging capability of the samples

Sample	Slope	Intercept	R^2	Antioxidant activity range	IC_{50} value
d	0.0243	16.217	0.9813	14.36 ±1.09% - 92.01 ±1.04%	1390.25 ± 3.23 µg/mL
c	0.0245	16.431	0.9814	13.83 ±1.08% - 93.32 ±1.05%	1370.16 ± 3.14 µg/mL
b	0.7286	6.4566	0.9873	9.10 ±1.27% - 19.09 ±1.23%	59.76 ± 1.25 mg/mL
a	2.1853	0.3299	0.9874	7.30 ±1.16% - 43.58 ±1.12%	22.73 ± 1.14 mg/mL
Ascorbic acid	0.2068	7.2308	0.9892	23.34 ±1.03% - 99.23 ±1.01%	206.81 ± 1.12 µg/mL

Sample d: *Ganoderma lucidum* extract obtained by Soxhlet extraction, Sample c: *Ganoderma lucidum* extract obtained by sonication extraction, Sample b: soap prepared from olive oil and coconut oil, Sample a: soap prepared from olive oil, coconut oil and Ganoderma lucidum, and ascorbic acid (vitamin C) as a standard.

4.8.1 Intermolecular and Chemical Bonding Interactions for *Ganoderma Lucidum* as Antioxidant Agent

Ganoderma lucidum's antioxidant properties are underpinned by a diverse array of interactions exhibited by its bioactive compounds. Hydrogen bonding, for instance, occurs when hydroxyl groups (-OH) in *ganoderma* polysaccharides form stabilizing bonds with free radicals like hydroxyl radicals ($OH^{\bullet}$), reducing their reactivity. Moreover, the triterpenes present in *ganoderma*, such as ganoderic acids, demonstrate electron transfer, donating electrons to neutralize free radicals like superoxide radicals ($O_2^{-\bullet}$) and peroxyl radicals ($ROO^{\bullet}$), effectively halting oxidative chain reactions. These compounds can also chelate metal ions such as iron and copper, preventing them from participating in ROS generation. *ganoderma* polyphenols, on the other hand, engage in stabilizing forces such as π-π stacking and van der Waals interactions with free radicals, reducing their reactivity. Some *ganoderma* compounds may even undergo covalent bonding with specific radicals, as seen with polyphenols forming covalent adducts with nitric oxide ($NO^{\bullet}$). Furthermore, donor-acceptor interactions are observed, with antioxidants in *ganoderma* donating or accepting electrons to neutralize radicals, exemplified by quinones interacting with lipid peroxyl radicals ($ROO^{\bullet}$). Lastly, *ganoderma's* three-dimensional compounds, including triterpenes, may physically hinder the movement and reactivity of free radicals, providing steric hindrance that protects cellular components. These diverse mechanisms collectively empower *Ganoderma lucidum* to combat oxidative stress effectively, shedding light on its potential health benefits and making it a subject of ongoing scientific exploration. The antioxidant properties of *Ganoderma lucidum* are intricately linked to a range of intermolecular forces and chemical bonding interactions between its bioactive compounds. These interactions, notably Van der Waals (VDW) forces encompassing dipole-dipole forces and London forces, play a pivotal role in shaping the physical and chemical characteristics of the mushroom. Dipole-dipole forces, occurring between polar molecules, are evident in *ganoderma* polysaccharides where hydroxyl groups engage in stabilizing bonds, exemplifying the attraction between positive and negative poles of molecules. As illustrated in **Figure 4.27** and **Figure 4.28**, the two primary intermolecular forces are highlighted to explain the stability and antioxidant efficacy of compounds found in *Ganoderma lucidum*. The hydrogen bonding present in *ganoderma* polysaccharides, shown in Figure 4.27, underlines the importance of

these intermolecular forces in maintaining the structural integrity of the bioactive compounds. This hydrogen bonding can be especially crucial for the antioxidant properties of the mushroom, providing a stabilizing network of forces that contribute to its overall effectiveness. Similarly, the nitrogen-hydrogen (N-H) bonds, designated in Figure 4.28, are also significant. These bonds are particularly prevalent in compounds containing amine functional groups. In terms of antioxidant properties, the presence of an N-H bond in a compound's structure can greatly contribute to its antioxidant activity. For instance, amino acids containing N-H bonds, commonly found in proteins, may play an essential role in the antioxidant mechanisms of *Ganoderma lucidum*. Both of these intermolecular forces, hydrogen bonding and the nitrogen-hydrogen bonds offer valuable insights into the molecular mechanisms that contribute to the antioxidant properties of *Ganoderma lucidum*. The diversity in these interactions, especially the dipole-dipole forces, is pivotal for understanding the mushroom's medicinal efficacy as an antioxidant agent [118].

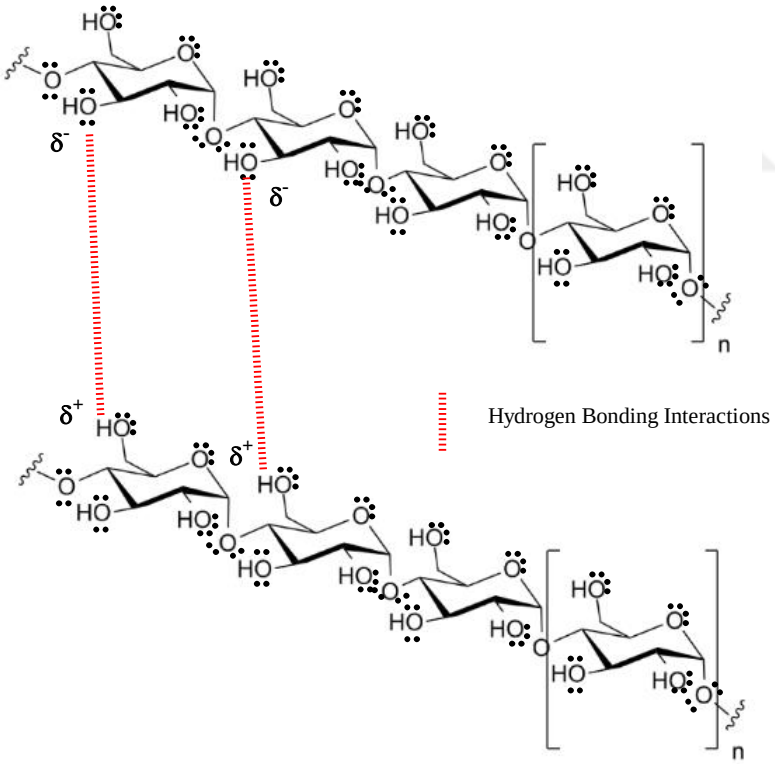

Figure 4.27 Key intermolecular forces in *Ganoderma lucidum*. The diagram identifies the intermolecular forces of hydrogen bonding in *ganoderma* polysaccharides.

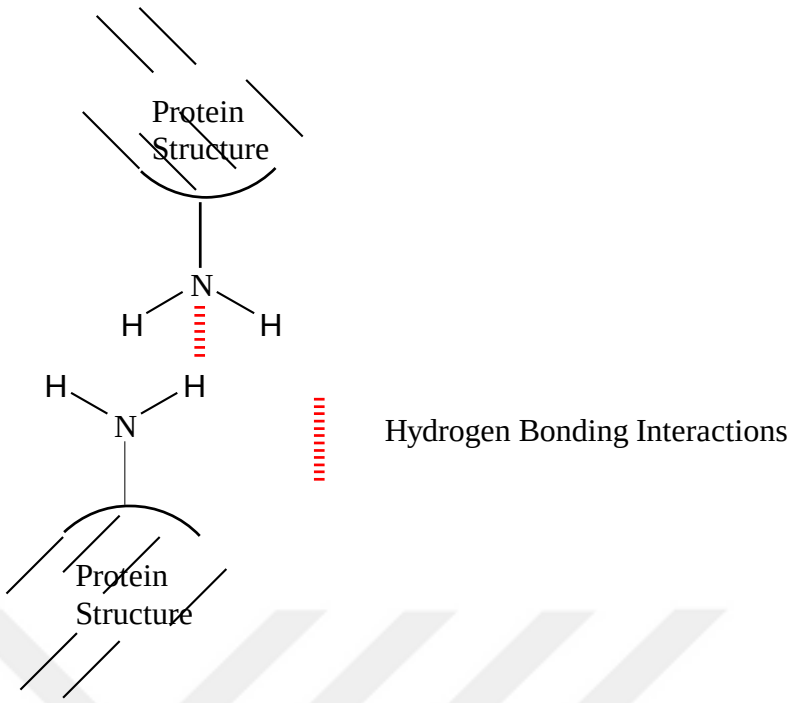

Figure 4.28 Key intermolecular forces in *Ganoderma lucidum*. The diagram identifies the intermolecular forces of nitrogen-hydrogen (N-H) bonds in *ganoderma* proteins.

4.9 Antimicrobial Activity

Investigations of the extraction' and soap's inhibitory activity across of both Gram-positive and Gram-negative microorganisms' strains were conducted. Figure 4.29 reflects the inhibition disc diffusion assay zones and quantifies the inhibition diameters in the soap samples which examined three types of bacteria by taking the concentrations of 1-5-10-20% respectively.

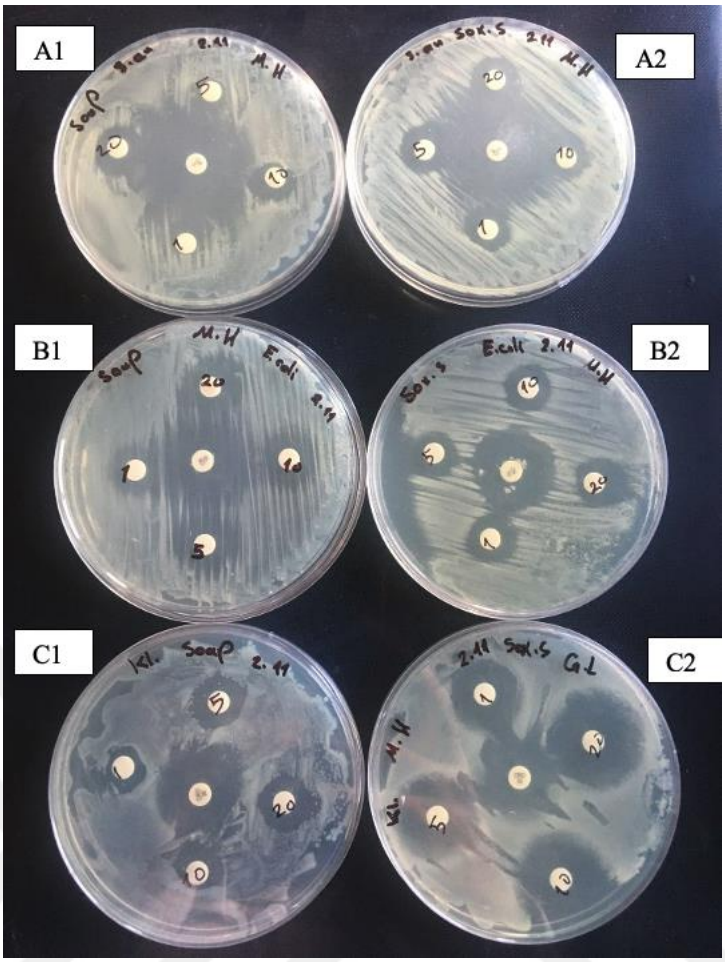

Figure 4.29 Inhibition disc diffusion zone assays for soap samples, examined with three types of bacteria

A1: soap sample examined its effect on Klebsiella pneumoniae bacteria Compared with A2: pure *ganoderma* extracted by Soxhlet which examined its effect on *Klebsiella pneumoniae* bacteria too.

B1: soap sample examined its effect on *Escherichia coli* bacteria Compared with B2: pure *ganoderma* extracted by Soxhlet which examined its effect on *Escherichia coli bacteria* too.

C1: soap sample examined its effect on *Staphylococcus aureus* bacteria Compared with C2: pure *ganoderma* extracted by Soxhlet which examined its effect on *Staphylococcus aureus* too. Table 4.16 provides a comprehensive overview of the antimicrobial results. Within this table, the inhibitory effects are quantified by measuring the diameter of growth inhibition on the culture medium, with results reported in millimeters.

Table 4.16 Summary of the antimicrobial findings. The areas of inhibition were measured on the culture medium and reported as the diameter of growth inhibition in millimeters

Microorganisim name	Sample	Cocentrations	Soap mm	SOX soap mm
Klebsiella pneumoniae ATCC 700603	Sox	1 mg/mL	10	16
		5 mg/mL	12	18
		10 mg/mL	13	22
		20 mg/mL	15	25
	Ceftriaxone		20	20
Escherichia coli ATCC 25322	Sox	1 mg/mL	13	14
		5 mg/mL	13	14
		10 mg/mL	14	14
		20 mg/mL	14	15
	Gentamicin		23	22
Staphylococcus aureus ATCC 25923	Sox	1 mg/mL	0	12
		5 mg/mL	0	13
		10 mg/mL	10	14
		20 mg/mL	13	14
	Ciprofloxacin	32	31	27

The following Figure 4.30 shows the effect of each of the *GL* extracts (extract by sonicator, and extract by Soxhlet) on *Klebsiella pneumoniae*, *Escherichia coli*, and *Staphylococcus aureus* bacteria. Table 4.17 displays the areas of inhibition, which are measured on the culture medium and reported in terms of the diameter of growth inhibition in millimeters. This data relates to the effects of *GL* extracts on bacteria strains such as *Klebsiella pneumoniae*, *Escherichia coli*, and *Staphylococcus aureus*.

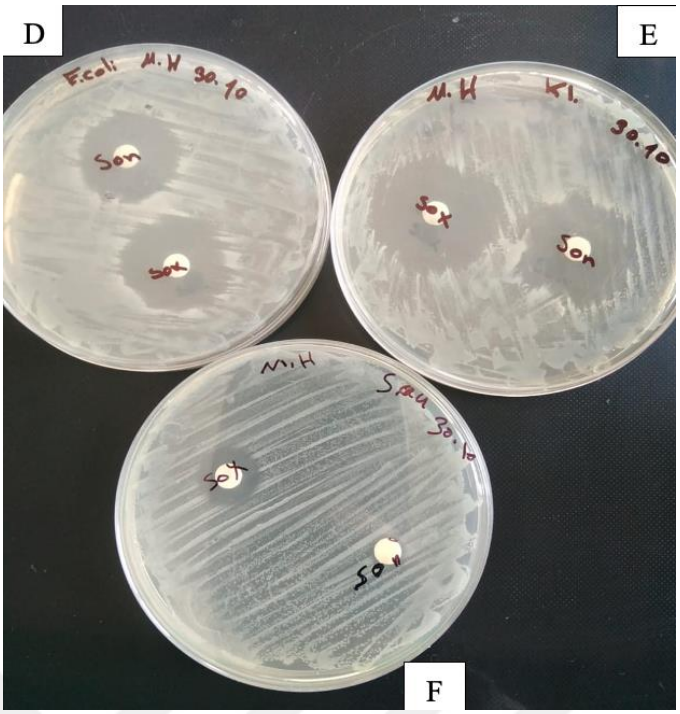

Figure 4.30 Comparison of each of the *GL* extracts (extract by sonication, and extract by Soxhlet) on *Klebsiella pneumoniae*, *Escherichia coli*, and *Staphylococcus aureus* bacteria

D: The comparison of *GL* extracts (extract by sonication, and extract by Soxhlet) on *Escherichia coli*

E: The comparison of *GL* extracts (extract by sonication, and extract by Soxhlet) on *Klebsiella pneumoniae*

F: The comparison of *GL* extracts (extract by sonication, and extract by Soxhlet) on *Staphylococcus aureus*

Table 4.17 Areas of inhibition measured on the culture medium and reported as the diameter of growth inhibition in millimeters for both *GL* extracts and their effect on *Klebsiella pneumoniae*, *Escherichia coli*, and *Staphylococcus aureus* bacteria

Microorganisim name	Sample	Concentrations	SOX mm	SONI mm
Klebsiella pneumoniae ATCC 700603	Sample	1 mg/mL	15	14
Escherichia coli ATCC 25322	Sample	1 mg/mL	10	10
Staphylococcus aureus ATCC 25923	Sample	1 mg/mL	7	0

In response to the urgent global need for new antibiotics, due to the alarming increase in bacterial and fungal resistance attributed to the misuse and overuse of existing antibiotics, *Ganoderma lucidum*, a type of macro fungus, is emerging as a promising candidate. Research indicates that *G. lucidum,* like plants, can produce valuable bioactive metabolites, including abundant triterpenoids and polysaccharides, positioning it as a potential rich source for drug development. As antibiotic resistance continues to broaden its impact across a wide variety of organisms, posing a severe public health threat, antimicrobial compounds derived from mushrooms like *G. lucidum* are garnering increasing attention. The current study indicates that extracts from *G. lucidum* could be potential candidates for creating potent antimicrobial agents, addressing diseases triggered by resistant pathogenic organisms.

4.9.1 Intermolecular and Chemical Bonding Interactions for *Ganoderma Lucidum* as Antimicrobial Agent

In the study investigating the antibacterial properties of *Ganoderma lucidum*-infused soap, several intermolecular and chemical bonding interactions were at play, contributing to the soap's observed antimicrobial efficacy. The soap's chemical formulation inherently involves chemical bonding interactions between its ingredients, including *ganoderma* extracts, allowing it to interact with bacterial cell membranes and potentially disrupt their integrity. The antibacterial efficacy of *Ganoderma lucidum* is intricately linked to a diverse array of functional groups within its bioactive constituents. In **Figure 4.31**, the various functional groups contributing to the antibacterial properties of *Ganoderma lucidum*-infused soap are elucidated. The hydroxyl group (-OH), denoted as (1) in the figure, engages in dipole-dipole interactions that are instrumental in disrupting bacterial cell membranes. Likewise, the amine group (NH2), labeled as (2), formed of nitrogen and hydrogen atoms, can also participate in dipole-dipole interactions, thereby contributing to the stability of the bioactive compounds within the soap. The carbonyl group (C=O), identified as (3) in the diagram, features a carbon-oxygen double bond. This group is also implicated in dipole-dipole interactions, playing a pivotal role in the soap's antibacterial efficacy. The ether group (R-O-R), designated as (4), consists of an oxygen atom flanked by two carbon atoms and may contribute to the overall stability of the soap's antibacterial structures via dipole-dipole interactions. Lastly, the phenolic groups (Ar-OH), marked as (5) in the figure, consist

of a hydroxyl group attached to an aromatic ring. These groups are also believed to engage in dipole-dipole interactions, thereby potentially enhancing the antibacterial activity of the soap [118].

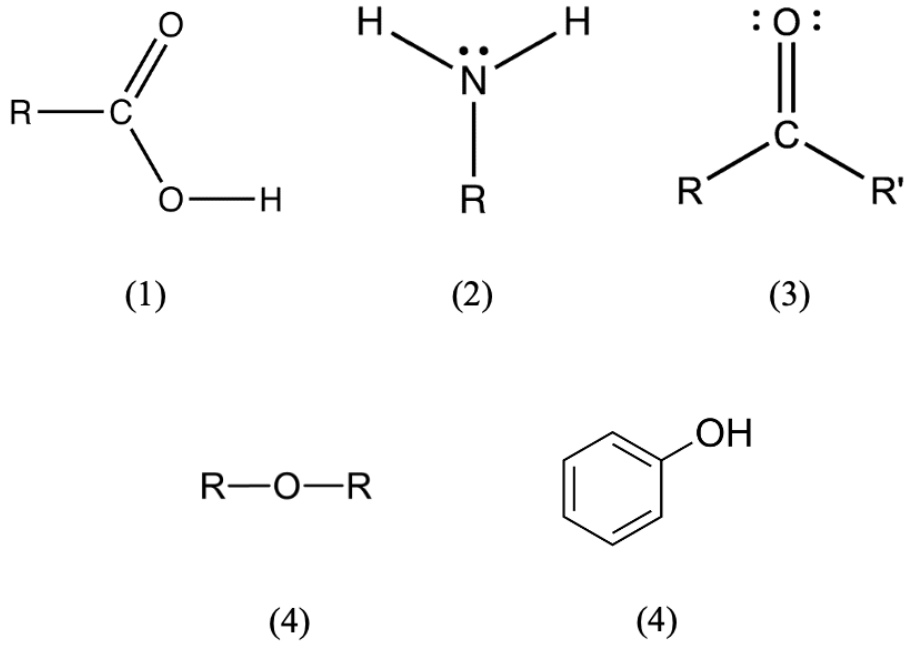

Figure 4.31 Depiction of functional groups in *Ganoderma lucidum*-Infused soap. The diagram illustrates the functional groups—hydroxyl (1), amine (2), carbonyl (3), ether (4), and phenolic (5)—and their potential role in contributing to the antibacterial properties of the soap through dipole-dipole interactions.

CHAPTER V

CONCLUSION AND RECOMMENDATIONS

All of the planned experiments in this study were carried out properly. Approaches, chemical substances, and chemical equipment, as well as antioxidant, antimicrobial, and analysis, were used. Compounds were isolated and purified using appropriate methods, and outcomes were determined and clarified.

The examination of *Ganoderma luciduim* extracted through both techniques of extraction, Soxhlet and sonication, as well as soap prepared with *Ganoderma luciduim* samples, was performed using suitable spectroscopic methods, UV-Vis, FTIR, GC-MS, and PL. These the spectral measurements' outcomes have been analyzed and provided. FTIR spectroscopy revealed that the chemical structures of *Ganoderma lucidum*, obtained via both Soxhlet and sonication extraction methods, as well as the soap formulated with *Ganoderma lucidum*, aligned with the expected compound configurations. The photophysical properties of extracts and soaps were investigated in order to determine potential applications in medical imaging and other healthcare domains. *Ganoderma lucidum* extracts obtained *via* Soxhlet and sonication extraction methods emitted strong photoluminescent emissions, whereas soaps formulated from these extracts emitted a weaker emission under ultraviolet light. The photoluminescence properties of *Ganoderma lucidum* remained consistent across various excitation wavelengths, aligning with Kasha's principle of excitation wavelength invariance. The incorporation of the extracts into soap products resulted in a decrease in photoluminescence intensity, quantum yield, and a move to lower emission wavelengths, which is attributed to the dilution of the extract in the soap and the presence of other compounds that quench the photoluminescence. The significant Stoke's shift values noted for both the extracts and soap products suggest alterations in their structure and the generation of intermolecular excimers upon excitation.

Overall, the photoluminescent properties of *Ganoderma lucidum* extracts and their derivative soap products hold promise for a variety of applications in photophysics and medicine. The study examined the antimicrobial efficacy of soap formulated using *ganoderma* extracts. A comparison was made between the *ganoderma* extracted through two distinct methods: a Soxhlet apparatus and a sonicator. The antimicrobial potential of these extracts was evaluated against three bacterial strains: *Escherichia coli*, *Staphylococcus aureus*, and *Klebsiella pneumoniae*. The efficacy was determined by measuring the diameter of the inhibition zones. The results demonstrated that the soap, which incorporated *ganoderma* in its formulation, exhibited superior antimicrobial activity against the three bacterial strains. Among these, the highest efficacy was observed against *Staphylococcus aureus*, followed by *Klebsiella pneumoniae*, and then *Escherichia coli*. In comparing the antimicrobial effectiveness of *ganoderma* extracted using the Soxhlet method versus the sonicator method, it was evident that the samples derived via the Soxhlet extraction showcased larger zones of inhibition against all three bacterial strains. This indicates that the Soxhlet extraction method potentially yields a more potent *ganoderma* extract in terms of antimicrobial activity.

The overall result underscores the potential of *G. lucidum* to produce valuable bioactive metabolites, mirroring the capabilities of plants. Specifically, *G. lucidum* is noted for its rich content of triterpenoids and polysaccharides, which may contribute to its antimicrobial properties. Regarding the antioxidant capabilities of different samples using the DPPH scavenging assay. Extracts of *Ganoderma lucidum*, procured through both Soxhlet and sonication extraction techniques, showcased potent antioxidant properties. These extracts had IC50 values of 1390.25 ± 3.23 μg/mL and 1370.16 ± 3.14 μg/mL, alongside antioxidant activity percentages of 92.01 ±1.04% and 93.32 ±1.05%, respectively. Conversely, a soap crafted from olive oil, coconut oil, and *Ganoderma lucidum* (Sample a) displayed intermediate antioxidant potential (22.73 ± 1.14 mg/mL and 43.58 ±1.12%). This reduced activity is presumed to result from its diminished *Ganoderma lucidum* concentration and the addition of other constituents during soap creation. Meanwhile, a soap composed solely of olive oil and coconut oil (Sample b) exhibited minimal antioxidant capabilities, a phenomenon ascribed to its absence of *Ganoderma lucidum*.

These findings emphasize the longstanding use of *Ganoderma lucidum* in Eastern traditional medicine, where it's been valued for its therapeutic benefits against ailments like cancer and immune-related conditions for millennia.

REFERENCES

[1] Alzand, Kutaiba & Sileman, Mansor & Bofaris, Mustafa & ugış, Abdullah. (2020). Chemical Composition and Nutritional Value Of Edible Wild Growing Mushrooms: A Review. World Journal of Pharmaceutical Research. 8. 31-46.

[2] Chang, S.T., and Miles, P.G. 1988. Edible Mushroom and their Cultivation. Crc Press, Inc. Boca Raton, Florida U.S.A. 27, Pp. 83-88.

[3] Mata, G. And Savoie, J.M. 2005. Wheat Straw. Gush R (Editors), Mushroom's Grower's Handbook 2. Mush World, Seoul.

[4] Jonathan, S.G., Okorie A.N., Garuba, E.O. Babayemi, O.J. 2012. Bioconversion of Sorghum Stalk and Rice Straw into Value Added Ruminant Feed Using Pleurotus Pulmonarius. Nature And Science. 10 (4), 10-16.

[5] Banik, S. And Nandi, R. (2004). Effect of Supplementation of Rice Straw with Biogas Residual Slurry Manure on The Yield, Protein and Mineral Contents of Oyster Mushroom. Industrial Crops and Products. 20(3): 311-319.

[6] Sliva, D. (2006). *Ganoderma Lucidum* in Cancer Research. Leukemia Research, 30(7), 767–768. Doi: 10.1016/J.Leukres.2005.12.015.

[7] Chang, S.T., Miles, P.G., 2004. Mushrooms: Cultivation, Nutritional Value Medicinal Effect and Environmental Impact. Crc Press, Boca Raton. 2nd Ed.

[8] Kapoor, P., Sharma, B.M., 2014. Studies on Different Growth Parameters of *Ganoderma Lucidum*. International Journal of Science, Environment and Technology 3, 1510–1525.

[9] R. Abdullah, I. Basak, K. S. Patil, G. Alves, J. P. Larsen, And S. G. Møller, "Parkinson's Disease and Age: The Obvious but Largely Unexplored Link," Experime Ntal Gerontology, Vol. 68, Pp. 33–38, Aug. 2015, Doi: 10.1016/J.Exger.2014.09.014.

[10] S. Huang Et Al., "Polysaccharides from *Ganoderma Lucidum* Promote Cognitive Function and Neural Progenitor Proliferation in Mouse Model of Alzheimer's Disease," Stem Cell Reports, Vol. 8, No. 1, Pp. 84–94, Jan. 2017, Doi:10.1016/J.Stemcr.2016.12.007.

[11] M.F. Ahmad, F.A. Ahmad, Z. Azad, A. Ahmad, M.I. Alam, J.A. Ansari, B.P. Panda, (2013) “Edible Mushrooms as Health Promoting Agent”, Adv. Sci. Focus. 1 (3) 189–196.

[12] I. C. F. R. Ferreira, J. A. Vaz, M. Helena Vasconcelos, And A. Martins, “Compounds from Wild Mushrooms with Antitumor Potential.”

[13] A. Mantovani and A. Sica, “Macrophages, Innate Immunity and Cancer: Balance, Tolerance, and Diversity,” Current Opinion in Immunology, Vol. 22, No. 2. Pp. 231–237, Apr. 2010. Doi: 10.1016/J. Coi.2010.01.009.

[14] Mau, J.L., Lin, H.C. & Chen, C.C. (2002). Antioxidant Properties of Several Medicinal Mushrooms. J Agric Food Chem 50, 6072-6077.

[15] Liu, D.Z.; Zhu, Y.Q.; Li, X.F.; Shan, W.G.; Gao, P.F. New triterpenoids from the fruiting bodies of *Ganoderma lucidum* and their bioactivities. Chem. Biodivers. 2014, 11, 982–986.

[16] Shang, X.; Tan, Q.; Liu, R.; Yu, K.; Li, P.; Zhao, G.-P. In *vitro* anti-Helicobacter pylori effects of medicinal mushroom extracts, with special emphasis on the Lion’s Mane mushroom, Hericium erinaceus (higher Basidiomycetes). Int. J. Med. Mushrooms 2013, 15, 165–174.

[17] Kozarski, M.; Klaus, A.; Niksic, M.; Jakovljevic, D.; Helsper, J.P.F.G.; Van Griensven, L.J.L.D. Antioxidative and immunomodulating activities of polysaccharide extracts of the medicinal mushrooms Agaricus bisporus, Agaricus brasiliensis, *Ganoderma lucidum* and Phellinus linteus. Food Chem. 2011, 129, 1667–1675.

[18] Qi, L.; Liu, H.; Li, J.; Li, T.; Wang, Y. Feature fusion of ICP-AES, UV-Vis and FTMIR for origin traceability of Boletus edulis mushrooms in combination with chemometrics. Sensors 2018, 18, 241

[19] K.S. Bishop, C.H.J. Kao, Y. Xu, M.P. Glucina, R.R.M. Paterson, L.R. Ferguson from 2000 years of *Ganoderma Lucidum* to Recent Developments in Nutraceuticals Phytochemistry, 114 (2015), Pp. 56-65.

[20] Sanodiya B. S, Thakur G. S, Baghel R. K, Prasad G. B, Bisen P. S. *Ganoderma Lucidum*: A Potent Pharmacological Macrofungus. Curr Pharm Biotechnol. 2009;10(8):717–42.

[21] John G Yuen and John Buswell and Iris Frances Forster Benzie, Chapter 9 *Ganoderma Lucidum* (*Lingzhi* or *Reishi*), 2014.

[22] Woo Y. A, Kim H. J, Cho J. H, Chung H. Discrimination of Herbal Medicines According to Geographical Origin with Near Infrared Reflectance Spectroscopy and Pattern Recognition Techniques. J Pharm Biomedanal. 1999; 21:407–13.

[23] Boh Podgornik, Bojana & Berovic, Marin & Zhang, Jingsong & Lin, Zhi-Bin. *Ganoderma Lucidum* and Its Pharmaceutically Active Compounds. Biotechnology Annual Review. 2007, 13. 265-301.

[24] Wang D-M, Wu S-H, Yao Y-J (2014) Clarification of the Concept of *Ganoderma* Orbiforme with High Morphological Plasticity. Plos One 9(5): E98733.

[25] Luangharn, T.; Karunarathna, S.C.; Dutta, A.K.; Paloi, S.; Promputtha, I.; Hyde, K.D.; Xu, J.; Mortimer, P.E. *Ganoderma* (Ganodermataceae, Basidiomycota) Species from The Greater Mekong Subregion. J. Fungi 2021, 7, 819.

[26] Chen Y, Zhu S. B, Xie M. Y, Editors. Et Al. Quality Control and Original Discrimination of Ganoderma Lucidum Based on High-Performance Liquid Chromatographic Fingerprints and Combined Chemometrics Methods. Anal Chim Acta. 2008; 623:146–56.

[27] Chen Y, Bicker W, Wu J, Xie M. Y, Lindner W. *Ganoderma* Species Discrimination by Dual-Mode Chromatographic Fingerprinting: A Study on Stationary Phase Effects in Hydrophilic Interaction Chromatography and Reduction of Sample Misclassification Rate by Additional Use of Reversed-Phase Chromatography. J Chromatogr. 2010;1217(8):1255–65

[28] Gottlieb A. M, Ferref E, Wright J. E. Rdna Analyses as An Aid to The Taxonomy of Species of Ganoderma. Mycol Res. 2000; 104:1033–45.

[29] Shin, G. C., & Seo, G. S. Classification of Strains of *Ganoderma Lucidum*. The Korean Journal of Mycology, 1988, 16(4), 235-241.

[30] Gregori, Andrej & Boh Podgornik, Bojana & Wraber, Branka & Habijanic, Jozi & Berovic, Marin & Svagelj, Mirjan & Pankl, Mojca. Cultivation of Medicinal Mushrooms Ganoderma Lucidum and Grifola Frondosa Mycelia and Polysaccharides in Bioreactors.2015, 12-16.

[31] Kaur, Hasimran & Sharma, Shivani & Khanna, P.K. & Kapoor, Shammi. Evaluation of *Ganoderma Lucidum* Strains for the Production of Bioactive

Components and Their Potential Use as Antimicrobial Agents. Journal of Applied and Natural Science.2015, 7(1):298-303.

[32] Breene Wm. Nutritional And Medicinal Values of Specialty Mushrooms, J Food Protect. 1990, 58: 883-894.

[33] Chang S. T, Buswell J. A. Safety, Quality Control and Regulation Aspects Relating to Mushroom Nutriceuticals. Proc. 6th Intl. Conf. Mushroom Biology and Mushroom Products. 2008:188–95. Gamu Gmbh, Krefeld, Germany.

[34] Lin, Z.B. Cellular and Molecular Mechanisms of Immuno-Modulation by *Ganoderma Lucidum*. J. Pharmacol. Sci. 2005, 99: 144–153.

[35] Bao, X., J.Y. Duan, X.Y. Fang and J.N. Fang. Chemical Modifications of the (1→3)-A-D-Glucan from Spores of *Ganoderma Lucidum* and Investigation of Their Physicochemical Properties and Immunological Activity. Carbohydr. Res.2001, 336: 127–140.

[36] Choong, Yew-Keong & Ellan, Kavithambigai & Chen, Xiangdong & Mohamad, Shaiful. Extraction And Fractionation of Polysaccharides from a Selected Mushroom Species, *Ganoderma Lucidum*: A Critical Review.2019, 10.5772/Intechopen.78047.

[37] Li, C., J. Yin, F. Guo, D. Zhang, and H.H. Sun. Ganoderic Acid Sz, A New Lanostanoid from The Mushroom *Ganoderma Lucidum*. Nat. Prod. Res. 2005, 19: 461–465.

[38] Khanna, P. K. Polysaccharides from Medicinal Mushrooms and Their Antitumor Activities-A Review. International Journal of Food and Fermentation Technology, 2011, 1(1), 17-37.

[39] Takashi Mizuno, Hazime Saito, Tsuyoshi Nishitoba & Hirokazu Kawagishi: Antitumor-Active Substances from Mushrooms, Food Reviews International,1995, 11:1, 23-61.

[40] Kim, B. K., Cho, H. Y., Kim, H. W., & Choi, E. C. Studies on Constituents of Higher Fungi of Korea (Lxvii). Antitumor Components of the Cultured Mycelia of *Ganoderma Lucidum*. Korean Journal of Pharmacology, 1993, 24, 203-212.

[41] Yang, L. & Zhang, L. -M. Chemical Structural and Chain Conformational Characterization of Some Bioactive Polysaccharides Isolated from Natural Sources. Carbohydrate Polymers, 2009, 76, 349-361.

[42] Zhang, M., Cui, S. W., Cheung, P. C. K., & Wang, Q. Antitumor Polysaccharides from Mushrooms: A Review on Their Isolation Process, Structural Characteristics and Antitumor Activity. Trends in Food Science and Technology, 2007, 18, 4-19.

[43] Lin, S. B., Li, C. H., Lee, S. S., & Kan, L. S. (2003). Triterpene-Enriched Extracts from *Ganoderma Lucidum* Inhibit Growth of Hepatoma Cells Via Suppressing Protein Kinase C, Activating Mitogen-Activated Protein Kinases and G2-Phase Cell Cycle. Life Sciences, 72, 2381-2390.

[44] Ip, Fanny & Zhang, Dong-Mei & Chen, Li-Xin & Zhang, Wei & Li, Yao-Lan & Ip, Nancy & Ye, Wen-Cai. Triterpenoids With Neurotrophic Activity from Ganoderma Lucidum. Natural Product Research, 2011. 25. 1607-13.

[45] Mau J. L, Lin H. C, Chen C. C. Antioxidant Properties of Several Medicinal Mushrooms. J Agric Food Chem. 2002; 50:6072–7.

[46] Kim D. H, Shim S. B, Kim N. J, Jang I. S. B-Glucuronidase-Inhibitory Activity and Hepatoprotective Effect of *Ganoderma Lucidum*. Biol Pharm Bull. 1999; 22:162–4.

[47] Y.-Z. Xie, F. Yang, W. Tan, X. Li, C. Jiao, R. Huang, B.B. Yang, The Anti-Cancer Components of *Ganoderma Lucidum* Possesses Cardiovascular Protective Effect by Regulating Circular Rna Expression, Oncoscience, 2016, 3 (7–8) 203.

[48] G.J. Wang, Y.J. Huang, D.H. Chen, Y.L. Lin, *Ganoderma Lucidum* Extract Attenuates the Proliferation of Hepatic Stellate Cells by Blocking the Pdgf Receptor, Phytother. Res, 2009, 23 (6) 833–839.

[49] Paterson, R. M. Review *Ganoderma* – A Therapeutic Fungal Biofactory. Phytochemistry,2006, 67, 1985–2001.

[50] Gill, Balraj & Gill, Navgeet & Kumar, Sanjeev. *Ganoderma Lucidum* Targeting Lung Cancer Signaling: A Mini Review. 2017, Tumor Biology.

[51] Yang M, Wang X, Guan S, Xia J, Sun J, Guo H, Guo Da. Analysis of Triterpenoids in *Ganoderma Lucidum* Using Liquid Chromatography Coupled with Electrospray Ionization Mass Spectrometry. J Am Soc Mass Spectrom, 2007. 18:927–939.

[52] Yang M, Wang X, Guan S, Xia J, Sun J, Guo H, Guo Da. Analysis of Triterpenoids in *Ganoderma Lucidum* Using Liquid Chromatography Coupled

with Electrospray Ionization Mass Spectrometry. J Am Soc Mass Spectrom, 2007. 18:927–939.

[53] Komoda Y, Shimizu M, Sonoda Y, Sato Y Ganoderic Acid and Its Derivatives as Cholesterol Synthesis Inhibitors. Chem Pharm Bull (Tokyo), 1989, 37:531–533.

[54] Kohda H, Tokumoto W, Sakamoto K, Fujii M, Hirai Y, Yamasaki K, Komoda Y, Nakamura H, Ishihara S, Uchida M, The Biologically Active Constituents of *Ganoderma Lucidum* (Fr.) Karst. Histamine Release-Inhibitory Triterpenes. Chem Pharm Bull (Tokyo),1985, 33:1367–1374.

[55] Zhu M, Chang Q, Wong Lk, Chong Fs, Li Rc. Triterpene Antioxidants from *Ganoderma Lucidum*. Phytother Res, 1999, 13:529–531.

[56] Chang S. T, Buswell J. A. Safety, Quality Control and Regulation Aspects Relating to Mushroom Nutriceuticals. Proc. 6th Intl. Conf. Mushroom Biology and Mushroom Products. 2008:188–95. Gamu Gmbh, Krefeld, Germany.

[57] Mizushina, Y., Watanabe, I., Togashi, H., Hanashima, L., Takemura, M., Ohta, K., Sugawara, F., Koshino, H., Esumi, Y., Uzawa, J., Matsukage, A., Yoshida, S., Sakaguchi, K., An Ergosterol Peroxide, A Natural Product That Selectively Enhances the Inhibitory Effect of Linoleic Acid on Dna Polymerase Beta. Biol. Pharm. Bull.1998, 21, 444–448.

[58] Zhao, H.-B., Wang, S.-Z., He, Q.-H., Yuan, L., Chen, A.F., Lin, Z.-B., *Ganoderma* Total Sterol (Gs) And Gs1 Protect Rat Cerebral Cortical Neurons from Hypoxia/Reoxygenation Injury. Life Sci. 2005, 76, 1027–1037.

[59] Mothana, R.A., Jansen, R., Julich, W.D., Lindequist, U, Ganomycins A And B, New Antimicrobial Farnesyl Hydroquinones from The Basidiomycete *Ganoderma* Pfeifferi. J. Nat. Prod.2000, 63, 416–418.

[60] Chang St, Buswell Ja. Mushroom Nutriceuticals. World J Microbiol Biotechnol. 1996 Sep;12(5):473-6.

[61] Kawagishi H, Mitsunaga S, Yamawaki M, Ido M, Shimada A, Kinoshita T, Murata T, Usui T, Kimura A, Chiba S. A Lectin from Mycelia of the Fungus *Ganoderma Lucidum*. Phytochemistry. 1997 Jan;44(1):7-10.

[62] Wang H, Ng T. B, Ooi V. E. C. Lectins from Mushrooms. Mycol Res. 1998; 102:897–906.

[63] Paterson R. R. *Ganoderma*-A Therapeutic Fungal Biofactory. Phytochemistry. 2006;67(18):1985–2001

[64] Kim S. D, Nho H. J. Isolation and Characterization of Alpha-Glucosidase Inhibitor from the Fungus *Ganoderma Lucidum*. J Microbiol. 2004; 42:223–7.

[65] Al-Mohanna, Moshtaq. Bacterial Introduction, Solation, Characterization and Identification of Bacteria from Organic Waste, 2016.

[66] Shapiro, J. A. Thinking About Bacterial Populations as Multicellular Organisms. Annual Review of Microbiology, 1998, 52(1), 81-1.

[67] Ames Bn, Lee Fd, Durston We. An Improved Bacterial Test System for The Detection and Classifi Cation of Mutagens and Carcinogens. Proc Natl Acad Sci Usa, 1973, 70:782–786.

[68] Ralph Kirby, Fundamentals of Biochemistry, Cell Biology and Biophysics. 2003, Vol. 2, Prokaryote Genetics.

[69] Gordo, I., Sousa, A., Mutation, Selection and Genetic Interactions in Bacteria. Encyclopedia Of Life Sciences (Els)2010.

[70] Kinde, I., Wu, J., Papadopoulos, N., Kinzler, Kw., Vogelstein, B., Detection and Quantification of Rare Mutations with Massively Parallel Sequencing. Proc Natl Acad Sci Usa, 2011, 108:9530–9535.

[71] Yoon Sy, Eo Sk, Kim Ys, Lee Ck, Han Ss. Antimicrobial Activity of G. Lucidum Extract Alone and in Combination with Some Antibiotics. Arch Pharm Res, 1994, 17:438–442.

[72] Monroe, S. & Polk, R. Antimicrobial Use and Bacterial Resistance. Curr Microbiol, 2000, 3, 496-501.

[73] Mcgowan, J.E.J. Economic Impact of Antimicrobial Resistance. Emerg Infect Dis, 2001, 7, 286-292.

[74] Baratta, M.T., Dorman, H.J.D., Deans, S.G., Figueiredo, A.C., Barroso, J.G. & Ruberto, G. Antimicrobial and Antioxidant Properties of Some Commercial Essential Oils. Flav Frag J, 1998. 13, 235-244.

[75] Cragg, G.M., Newman, D.J. & Snader, K.M. Natural Products in Drug Discovery and Development. J Nat Prod, 1997, 60, 52-60.

[76] Wasser, S.P. & Weis, A.L. Therapeutic Effects of Substances Occurring in Higher Basidiomycetes Mushrooms: A Modern Perspective. Crit Rev Immunol, 1999, 19, 65-96.

[77] Robbins, W.J., Kavanagh, F. & Hervey, A. Antibiotic Substances from Basidiomycetes 1. Pleurotus. Proc Nat Acad Sci, 1947, 33, 171-176.

[78] Miller, Kristen & Wang, Lei & Benicewicz, Brian & Decho, Alan. Inorganic Nanoparticles Engineered to Attack Bacteria. Chemical Society Reviews.2015, 46. 10.1039.

[79] Gupte, Arpita & Pol, Reshma. Antimicrobial Activity of *Ganoderma Lucidum* Mycelia. Journal of Pure and Applied Microbiology. 2011, 5. 983-986.

[80] Ofodile, Nwanneka & Uma, N & Kokubun, T & Grayer, Renée & Ogundipe, Oluwatoyin & Simmonds, M. Antimicrobial Activity of Some *Ganoderma* Species from Nigeria. Phytotherapy Research. 2005, 19. 310-313.

[81] Cooper Ce, Vollaard Nbj, Choueiri T, Et Al. Exercise, Free Radicals and Oxidative Stress. Biochem Soc Trans 2002; 30 (2) 280-5.

[82] Pizzino G, Irrera N, Cucinotta M, Pallio G, Mannino F, Arcoraci V, Squadrito F, Altavilla D, Bitto A. Oxidative Stress: Harms and Benefits for Human Health. Oxid Med Cell Longev. 2017; 2017:8416763.

[83] Lushchak Vi. Adaptive Response to Oxidative Stress: Bacteria, Fungi, Plants and Animals. Comp Biochem Physiol C Toxicol Pharmacol. 2011;153(2):175-90.

[84] Petibois C, Cazorla G, Poortmans Jr, Et Al. Biochemical Aspects of Overtraining in Endurance Sports. Sports Med 2002; 32 (13): 867-78.

[85] Rimbach G, Hohler D, Fischer A, Et Al. Methods to Assess Free Radicals and Oxidative Stress in Biological Systems. Arch Tierand Ernahr 1999; 52 (3): 203-22.

[86] Thompson-Gorman Sl, Zweier Jl. Evaluation of the Role of Xanthine Oxidase in Myocardial Reperfusion Injury. J Biol Chem 1990; 265 (12): 6656-63.

[87] Golden Tr, Hinerfeld Da, Melov S. Oxidative Stress and Aging Beyond Correlation. Aging Cell 2002; 1: 117-23.

[88] Finaud, J., Lac, G. & Filaire, E. Oxidative Stress. Sports Med 36, 327–358 (2006).

[89] Benzie Iff, Wachtel-Galor S (2009) Biomarkers of Long-Term Vegetarian Diets. Adv Clin Chem 47:172–175.

[90] Lee J. M, Kwon H, Jeong H, Editors. Et Al. Inhibition of Lipid Peroxidation and Oxidative Dna Damage by *Ganoderma Lucidum*. Phytother Res. 2001; 15:245–9.

[91] Yen, G.C. & Wu, J.Y. (1999). Antioxidant and Radical Scavenging Properties of Extracts from *Ganoderma* Tsugae. Food Chem 65, 375-379.

[92] Shieh, Y.H., Liu, C.F., Huang, Y.K., Yang, J.Y., Wu, I.L., Lin, C.H. & Li, S.C. Evaluation of the Hepatic and Renal-Protective Effects of *Ganoderma Lucidum* in Mice. Am J Chin Med, 2001, 29, 501-507.

[93] Perez, C., Pauli, M. and Bazerque, P. (1990) An Antibiotic Assay by Agar Well Diffusion Method. Acta Biologiae et Medicinae Experimentalis, 15, 113-115.

[94] Ko, Gyeong & Cho, Somi. (2018). Ethyl linoleate inhibits α-MSH-induced melanogenesis through Akt/GSK3β/β-catenin signal pathway. The Korean Journal of Physiology & Pharmacology. 22. 53. 10.4196/kjpp.2018.22.1.53.

[95] Charakida A., Charakida M., Chu A.-C. Double-blind, randomized, placebo-controlled study of a lotion containing triethyl citrate and ethyl linoleate in the treatment of acne vulgaris. Br. J. Dermatol. 2007;157:569–574.

[96] Kim, S. Y., Kim, J. H., Kim, S. H., Kim, J. M., Kim, J. H., Kim, J. Y., ... & Kim, H. J. (2010). Ethyl linoleate suppresses proliferation and induces apoptosis in human breast cancer cells. Journal of medicinal food, 13(5), 1235-1242.

[97] Kim, J. H., Kim, S. Y., Kim, J. H., Kim, J. M., Kim, J. H., Kim, J. Y., ... & Kim, H. J. (2010). Ethyl linoleate protects H9c2 cardiac muscle cells from hydrogen peroxide-induced oxidative stress. Journal of medicinal food, 13(5), 1243-1250.

[98] Pape-Jakobsen, J., & Jakobsen, J. (2000). Ethyl oleate as a moisturizer: properties and use in a leave-on emulsion. International journal of pharmaceutics, 205(1-2), 67-75.

[99] Kim, S. Y., Kim, J. H., Kim, S. H., Kim, J. M., Kim, J. H., Kim, J. Y., ... & Kim, H. J. (2010). Ethyl oleate promotes wound healing by increasing the rate of cell proliferation and collagen synthesis. Journal of medicinal food, 13(5), 1267-1274

[100] Sánchez-Quesada, J. L., & Fernández-Arroyo, S. (2002). Squalene and its antioxidant properties. Journal of Lipid Research, 43(10), 1697-1705).

[101] Ochiai, T., & Nakamura, Y. (2005). Squalene: a natural anticancer agent with the potential for chemotherapy. Cancer Letters, 225(2), 329-334).

[102] Rueda, C. M., & Pérez-Vizcaíno, F. (2010). Antioxidant activity of fatty acids and their derivatives. Food Chemistry, 122(4), 929-937.)

[103] Vlachos, N., Skopelitis, Y., Psaroudaki, M., Konstantinidou, V., Chatzilazarou, A., & Tegou, E. (2006). Applications of Fourier transform-infrared spectroscopy to edible oils. Analytica chimica acta, 573, 459-465.

[104] Caetano, S., Üstün, B., Hennessy, S., Smeyers-Verbeke, J., Melssen, W., Downey, G., ... & Heyden, Y. V. (2007). Geographical classification of olive oils by the application of CART and SVM to their FT-IR. Journal of Chemometrics: A Journal of the Chemometrics Society, 21(7-9), 324-334.

[105] Gary M.L., Donald L., Pavia, George S.K., James R.V. (2008). Spectroscopy 4th Edition.

[106] J.M. Fang, P.A. Fowler, J. Tomkinson, C.A.S. Hill, Carbohydr. Polym. 47 (2002) 245–252.

[107] Rajan, A., Prasad, V. S., & Abraham, T. E. (2006). Enzymatic esterification of starch using recovered coconut oil. International journal of biological macromolecules, 39(4-5), 265-272.

[108] M. Marcazzan, F. Vianello, M. Scarpa, A. Rigo, J. Biochem. Biophs. Meth. 38 (1999) 191–202.

[109] Carey, P.R., 1992. Biochemical Application of Raman and Resonance Raman Spectroscopies. New York, Academic Press

[110] Sangeetha, B., Krishnamoorthy, A. S., Amirtham, D., Sundara Sharmila, D. J., Renukadevi, P., & G Malathi, V. (2020). FT-IR spectroscopic characteristics of *Ganoderma lucidum* secondary metabolites. Current Journal of Applied Science and Technology, 38(6), 1-8.

[111] Kan Y, Chen T, Wu Y, Wu J. Antioxidant activity of polysaccharide extracted from *Ganoderma lucidum* using response surface methodology. International Journal of Biological Macromolecules. 2015;72: 151-7.

[112] Garuba, T., Olahan, G. S., Lateef, A. A., Alaya, R. O., Awolowo, M., & Sulyman, A. (2020). Proximate composition and chemical profiles of Reishi mushroom (*Ganoderma lucidum* (Curt: Fr.) Karst). Journal of Scientific Research, 12(1), 103-110.

[113] El-Sheikh, M. A., & El-Sharary, A. (2022). Preparation, characterization, and antibacterial efficacy of green aromatic soap. Egyptian Journal of Chemistry, 65(11), 385-393.

[114] Muñoz-Castiblanco, T., Peña-Cañón, R., Mejía-Giraldo, J. C., León, I. E., & Puertas-Mejía, M. Á. (2022). Anticancer and Antioxidant Activity of Water-

Soluble Polysaccharides from *Ganoderma* aff. Australe against Human Osteosarcoma Cells. International Journal of Molecular Sciences, 23(23).

[115] Kedare, S. B., & Singh, R. P. (2011). Genesis and development of DPPH method of antioxidant assay. Journal of Food Science and Technology, 48(4), 412-422.

[116] Jasmina Ćilerdžić, Jelena Vukojević, Mirjana Stajić, Tatjana Stanojković, Jasmina Glamočlija. Biological activityof *Ganoderma lucidum* basidiocarps cultivated on alternative and commercial substrate. Journal of Ethnopharmacology, 155, (2014), 312–319.

[117] Ćilerdžić, J., Vukojević, J., Stajić, M., Stanojković, T., & Glamočlija, J. (2014). Biological activity of *Ganoderma lucidum* basidiocarps cultivated on alternative and commercial substrate. Journal of Ethnopharmacology, 155(1), 312-319.

[118] Patrick, G. L. (2009). An Introduction to Medicinal Chemistry (4th ed.). Oxford University Press. 1-14.

CURRICULUM VITAE

Name and Surname: İkram ELMUSTAFA

EDUCATIONAL BACKGROUND

	Graduated School	Graduation Year
Undergraduate (B.Sc.)	Aleppo University	2017

INTERNATIONAL CONFERENCES AND PROCEEDINGS

Gülay Zengin, **İkram Elmustafa**, Huseyin Zengin "Analysis of the Composition of *Ganoderma* Mushroom Extracts and their Nourishing Liquid Soap Preparation" EurasianBioChem 2021 Conference, Ankara, 24-26 November 2021.